The olfactory system of the red flour beetle *Tribolium castaneum*, Herbst: morphology, development, and plasticty

Dissertation

zur Erlangung des Grades eines
Doktor der Naturwissenschaften
(Dr. rer. nat.)
des Fachbereichs Biologie
der Philipps-Universität Marburg

vorgelegt von
Björn Trebels, M.Sc.
aus Iserlohn

Marburg, Dezember 2021

Die Untersuchungen zu dieser Dissertation wurde zwischen August 2014 und Februar 2020 in der Arbeitsgruppe von Prof. Dr. Joachim Schachtner, Tierphysiologie - Neurobiologie/Ethologie am Fachbereich Biologie durchgeführt.

Vom Fachbereich Biologie der Philipps-Universität Marburg (Hochschulkennziffer 1180)
als Dissertation angenommen am 3. März 2022.

Erstgutachter: Prof. Dr. Joachim Schachtner
Zweitgutachter: Prof. Dr. Uwe Homberg

Tag der Disputation: 1. April 2022

It is the struggle itself that is most important.
We must strive to be more than we are.
It does not matter that we will not reach our ultimate goal.
The effort itself yields its own reward.

- Gene Roddenberry -

Contents

Eidesstattliche Versicherung

Ich versichere, dass ich meine vorliegende Dissertation mit dem Titel

The olfactory system of the red flour beetle
(*Tribolium castaneum*, Herbst):
morphology, development, and plasticity

selbstständig ohne unerlaubte Hilfe angefertigt und mich dabei keiner anderen als der von mir ausdrücklich bezeichneten Quellen und Hilfsmittel bedient habe.

Diese Dissertation wurde in der jetzigen oder einer ähnlichen Form noch bei keiner anderen Hochschule eingereicht und hat noch keinen sonstigen Prüfungszwecken gedient.

Marburg, 13.12.2021 Björn Trebels, M.Sc.

Erklärung über eigene Beiträge und veröffentlichte Teile der Arbeit

Meine eigenen Beiträge zu den gemeinsam verfassten Veröffentlichungen/Manuskripten des kumulativen Teils meiner Dissertation (Kapitel 3 bis 5) werden im Folgenden aufgeführt.

Chapter 3: Adult neurogenesis in the mushroom bodies

Kapitel 3: Adultneurogenese in den den Pilzkörpern

Veröffentlicht als:

Trebels B, Dippel S, Schaaf M, Balakrishnan K, Wimmer EA, Schachtner J. 2020. Adult neurogenesis in the mushroom bodies of red flour beetles (*Tribolium castaneum*, Herbst) is influenced by the olfactory environment. Sci Rep 10:1–11. DOI: 10.1038/s41598-020-57639-x

Eigene Beiträge:

- Konzeption der Studie in Zusammenarbeit mit Prof. Dr. Joachim Schachtner
- Entwicklung der Methode für die Neurogeneseexperimente, sowie Entwicklung und Aufbau des Injektions-Setups
- Durchführung von mehr als zwei Dritteln der Neurogeneseexperimente inkl. der histologischen Aufarbeitung, konfokaler Laserscan-Mikroskopie und Bestimmung der Zellzahlen
- Betreuung, Anleitung und teilweise praktische Unterstützung der Studentin Magdalina Schaaf, die im Rahmen ihrer Bacherlorarbeit einen Teil der Präparate zu den Neurogeneseexperimente unter Stimulation mit DMD anfertigte und histologisch aufarbeitete; in Kooperation mit Prof. Dr. Joachim Schachtner
- Entwicklung der Python-Skripte, für die statistische Auswertung der Neurogeneseexperimente und der EAG Daten
- Finale Auswertung und Interpretation der Neurogeneseexperimente
- Finale Auswertung und Interpretation der EAG-Daten in Kooperation mit Dr. Stefan Dippel

- Anfertigung aller Abbildungen
- Verfassen des Manuskripttextes in Kooperation (Korrektur) mit Prof. Dr. Joachim Schachtner und Dr. Stefan Dippel

Chapter 4: Metamorphic development of the olfactory system

Kapitel 4: Metamorphe Entwicklung des olfaktorischen Systems

Veröffentlicht als:

Trebels B[*], Dippel S[*], Goetz B, Graebner M, Hofmann C, Hofmann F, Schmid F-R, Uhl M, Vuong M-P, Weber V, Schachtner J. 2021. Metamorphic development of the olfactory system in the red flour beetle (*Tribolium castaneum*, Herbst). BMC Biol 19:155. DOI: 10.1186/s12915-021-01055-8 [* equal contribution]

Eigene Beiträge:

- Konzeption der Studie in Zusammenarbeit mit Prof. Dr. Joachim Schachtner und Dr. Stefan Dippel
- Sichtung und Evaluierung bereits bestehender konfokaler Bilddatenstapel und histochemischer Präparate, sowie teilweise Anfertigung neuer konfokaler Bilddatenstapel Letzterer
- Durchführung aller Neurogeneseexperimente inkl. der histologischen Aufarbeitung und konfokaler Laserscan-Mikroskopie
- Durchführung des Großteils der Experimente zur Entwicklung der Antennen, inkl. histologischer Ausarbeitung und Anfertigung lichtmikroskopischer Aufnahmen bzw. konfokaler Bilddatenstapel
- Durchführung und Auswertung der Spezifitätstests der genutzten GAD-Antiseren mittels Western Blot
- Betreuung, Anleitung und teilweise praktische Unterstützung der Studentin Minh-Phung Vuong, die im Rahmen ihrer Bachelorarbeit die GAD-Färbungen des Antennallobus erstellte und teilweise auswertete; in Kooperation mit Prof. Dr. Joachim Schachtner

- Betreuung, Anleitung und teilweise praktische Unterstützung der Studentin Vanessa Weber, die im Rahmen ihres Bachelor-Vertiefungsmoduls einen Teil der Präparate zur Entwicklung des GOC während der Metamorphose anfertigte und histologisch aufarbeitete; in Kooperation mit Prof. Dr. Joachim Schachtner
- Betreuung, Anleitung und teilweise praktische Unterstützung der Studiereden Florian Hofmann, Freya-Rebecca Schmid und Mara Uhl, die im Rahmen ihrer Bachelorarbeiten den Großteil der RNAi-Experimente zur Rolle von Orco durchführten; in Kooperation mit Dr. Stefan Dippel und Prof. Dr. Joachim Schachtner
- Betreuung, Anleitung und teilweise praktische Unterstützung der Studentin Carolin Hofmann, die im Rahmen ihrer Masterarbeit etwa ein Viertel der Präparate zur Entwicklung der Antenne anfertigte, histologisch aufarbeitete und lichtmikroskopische Aufnahmen bzw. konfokale Bilddatenstapel davon erstellte; in Kooperation mit Dr. Stefan Dippel und Prof. Dr. Joachim Schachtner
- Finale Auswertung und Interpretation der Daten
- Anfertigung aller Abbildungen mit Ausnahme von "Supplemental Figure S8: Staging of wild-type beetles during metamorphosis"
- Verfassen des Manuskripttextes in Kooperation (Korrektur) mit Prof. Dr. Joachim Schachtner und Dr. Stefan Dippel

Chapter 5: The palpal olfactory pathway

Kapitel 5: Die palpale Riechbahn

Die Veröffentlichung dieses Manuskriptes ist vorgesehen, jedoch zum Zeitpunkt der Einreichung noch nicht erfolgt.

Trebels B[*], Dippel S[*], Ernst C, Goetz B, Keyser T, Anders J, Rexer K-H, Wimmer EA, Schachtner J. The palpal olfactory pathway of red flour beetles (Tribolium castaneum, Herbst). [* equal contribution]

Eigene Beiträge:

- Konzeption der Studie in Zusammenarbeit mit Prof. Dr. Joachim Schachtner und Dr. Stefan Dippel
- Sichtung und Evaluierung bereits bestehende konfokaler Bilddatenstapel und histochemischer Präparate, sowie teilweise Anfertigung neuer konfokaler Bilddatenstapel letzterer
- Anfertigung von Präparaten der Mundwerkzeuge der transgenen Linien, sowie Erstellung konfokaler Bilddatenstapel bzw. lichtmikroskopischer Aufnahmen
- Betreuung, Anleitung und teilweise praktische Unterstützung der Studierenden Janet Anders und Tim Keyser, die im Rahmen ihrer Bachelorarbeiten einen Teil der immunhistologischen Färbungen des GOC durchführten und 3D-Rekonstruktionen des GOC anfertigten; in Kooperation mit Dr. Stefan Dippel and Prof. Dr. Joachim Schachtner
- Betreuung, Anleitung und teilweise praktische Unterstützung der Studentin Clara Ernst, die im Rahmen ihrer Bachelorarbeiten einen Teil der immunhistologischen Färbungen des GOC anfertigte; in Kooperation mit Dr. Stefan Dippel and Prof. Dr. Joachim Schachtner
- Anfertigung der Präparate für die Rasterelektronenmikroskopischen Aufnahmen, sowie Anfertigung der Aufnahmen in Kooperation mit Dr. Karl-Heinz Rexer
- Finale Auswertung und Interpretation der Daten
- Anfertigung aller Abbildungen
- Verfassen des Manuskripttextes in Kooperation (Korrektur) mit Prof. Dr. Joachim Schachtner und Dr. Stefan Dippel

Aim of the study

For insects, as for every other animal, orientation in and interaction with the environment is crucial for their survival. To achieve those tasks, many insects rely heavily on the chemical senses, namely their gustatory and olfactory systems. These systems are precisely tuned and need to be able to adapt to changing environmental conditions and living parameters. This adaption might be due to various processes, including the remodeling of existing synaptic networks, but also neurogenesis.

Based on *Tribolium castaneum* as a model, this study aimed to provide more insight into 1) adult plasticity of the insect brain, 2) metamorphic development of the olfactory system, and 3) anatomy of the palpal olfactory pathway. These goals are addressed in the three subprojects (chapters 3 to 5) of this thesis:

1. Prior to this thesis, it was already known that intrinsic cells of the mushroom bodies retain their potential to undergo mitotic divisions in the adult. This sub-project aimed to provide an in-depth analysis of the ongoing neurogenesis and its possible causes.
2. The adult olfactory system was already well described. This subproject aimed to describe the transition of the larval olfactory system into the adult one. Further, the role of Orco on the development of the adult olfactory system should be investigated.
3. The third subprojects scope was an in-depth description of the recently discovered pathway for palpal derived olfactory information.

This should be achieved via:

- (immuno-)histochemical staining
- reporter expression analysis
- neurogenesis detection
- manipulations of the olfactory system, including odor stimulation and deprivation, as well as an RNAi-mediated knock-down of the odorant receptor co-receptor (Orco)

Summary

Chapter 3: Adult neurogenesis in the mushroom bodies

The ground pattern of the central nervous system is genetically encoded. However, following development, when the first sensory contact with environmental stimuli occurs, adaptation to actual conditions and stimuli is essential for survival. Therefore, the genetically predetermined neuronal wiring scheme must be adaptable. This adaptability is also called plasticity and is typically limited to specific time windows of increased receptivity to sensory stimuli, called critical periods or sensitive phases. Primarily, plasticity is achieved by changes in the synaptic connections of existing neurons, biochemical changes at synapses, and the addition and removal of neurons.

Research on critical periods has long focused on vertebrates, where such occur during the postnatal development of the visual system or during song learning in birds. However, several studies have shown the existence of critical phases in insects as well - primarily in the olfactory system.

The sense of smell is used by insects for a variety of tasks, such as finding food sources, reproductive partners, or suitable habitats. In holometabolous insects, like *Tribolium castaneum*, the first contact of the adult olfactory system with the environment occurs following the pupal phase at the time of adult eclosion. Based on the already known existence of adult neurogenesis in the mushroom bodies of *T. castaneum*, this subproject investigates to what extent this depends on olfactory input during the first days as an imago and whether there is a time limit.

Reliable labeling of the newborn daughter cells of the mushroom body neuroblasts in the adult animal provided the basis for the study and allowed the determination of the number of newborn Kenyon cells under different olfactory conditions.

Within the first week after adult eclosion, the emergence of new Kenyon cells can be divided into at least two phases. In the first three days, the genesis of Kenyon cells is not dependent on olfactory stimuli and is therefore probably due to genetic programming and represents a continuation of the developmental processes from metamorphosis (nature). Directly afterward, however, the genesis of Kenyon cells probably mainly depends on the olfactory environment (nurture).

Given the role of the mushroom bodies as centers for learning and memory, neurogenesis is most likely an important component in remodeling the neuronal network, ultimately leading to environmental adaptation and behavioral optimization.

Chapter 4: Metamorphic development of the olfactory system

For insects, the olfactory sense is essential for survival. Olfactory signals are processed and ultimately translated into behavior by a rather complex system. The nervous system - and thus the olfactory system - of holometabolous insects, like *Tribolium castaneum*, is typically subject to major remodeling during metamorphosis. These changes are necessary because the lifestyle of imagines of holometabolous insects is typically very different from that of their larvae.

Larvae of holometabolous insects already possess olfactory processing centers and sensory appendages, although their complexity differs among species. In *T. castaneum*, as well as its close relative *Tenebrio molitor*, already the larvae possess an elaborate antenna consisting of three distinguishable segments (scape, pedicel, flagellum). The larval antenna of the tobacco hawkmoth *Manduca sexta* has a similar structure, while flies have only functionally equivalent dorsal organs. The current scientific picture sees the larval and adult antennae/olfactory sensory appendages as independent structures. The primary processing centers are already glomerularly organized in the mealworm beetle *T. molitor* and in *Drosophila melanogaster*, while this is not the case, for example, in the tobacco hawkmoth *M. sexta* or the western honeybee *Apis mellifera*.

Previous studies suggest that olfactory sensory neurons are necessary for the correct formation of glomeruli in adult antennal lobes. De-antennation in *M. sexta* leads to non-glomerular antennal lobes and in the ant *Ooceraea biroi* to a reduction in the number of glomeruli. In the ant, the same effect could also be achieved by knocking out the co-receptor Orco, which forms a functional unit together with a specific odorant receptor. However, it should be noted that the authors of the study attributed this to the resulting absence of olfactory sensory neurons. Furthermore, studies in *D. melanogaster* could detect Orco only after the formation of the glomeruli. Thus, in the fly, Orco cannot affect glomeruli formation.

In this subproject, the metamorphic development of the olfactory system of the beetle *T. castaneum* was studied. It could be shown that for the adult antenna, structures of the larval antennae are reused. This contradicts the previous scientific picture that they are independent structures. The same is true for the larval antennal lobes as primary olfactory processing centers, which are transformed into their adult counterparts during metamorphosis. This is supported by the fact that olfactory sensory neurons can be detected in the antennal structures and the antennal lobes throughout metamorphosis. Furthermore, it could be shown that the co-receptor Orco is not necessary for the initial formation of the glomerular structure of the antennal lobes - but is necessary for the later differentiation of the glomeruli in the early

imagines. The formation of the glomeruli of the antennal lobes occurs about midway through metamorphosis, as in all holometabolous insects studied to date. The same is true for the glomeruli of the gnathal olfactory center first described in *T. castaneum*.

Chapter 5: The palpal olfactory pathway

In the current scientific picture of the olfactory system of holometabolous insects, the paired antennal lobes are the sole primary processing centers. Accordingly, these receive input from the sensory neurons of the antennae and mouthparts. In hemimetabolous insects, however, the olfactory signals, which are received by the sensory neurons of the mouthparts, are processed separately. This is also true for the holometabolous beetle *Tribolium castaneum*, where the signals from the mouthparts are processed in the glomerular lobes (LG), previously known only from hemimetabolous insects, and the gnathal olfactory center (GOC), first described in the beetle.

This subproject focuses on a detailed description of the GOC, LGs, and their sensory inputs. Using scanning electron microscopy and comparison with confocal microscopy images of the mouthparts in a transgenic line labeling the olfactory sensory neurons, the olfactory sensilla on the mouthparts containing the dendrites of the olfactory sensory neurons innervating the GOC and LGs were identified. This revealed that at least two of the three sensilla types have an olfactory identity, which contrasts previous findings from *Drosophila melanogaster*, where only one sensilla type on the mouthparts is olfactory.

Using 3D reconstructions based on various histological stains, the anatomical description of the GOC was made more precise. The GOC consists of approximately 30 glomeruli. Thus, the number of glomeruli is at the lower end of the previously suspected range. This number of glomeruli also matches the 28 specific odorant receptors that are significantly enriched in the mouthparts compared to the body, as determined by RNA sequencing.

For the first time, the neuromediators repertoire of the GOC and LGs is investigated. For this purpose, ones that are also found in the antennal lobes were exemplarily investigated. Underlining the role of the GOC and LGs as primary olfactory processing centers, all investigated neuromediators were also found in the GOC and LGs, albeit with differences in the pattern of innervation. Therefore, it might be concluded that the neuromediator repertoire is rather not correlated with the complexity of the processing centers, but rather a necessity to ensure fine-tuning and initial evaluation of incoming signals.

Zusammenfassung

Chapter 3: Adult neurogenesis in the mushroom bodies

Kapitel 3: Adultneurogenese in den den Pilzkörpern

Die Grundstruktur des zentralen Nervensystems ist genetisch kodiert. Im Anschluss an die vorprogrammierte Entwicklung, wenn der erste sensorische Kontakt mit Umweltreizen stattfindet, ist die Anpassung an die aktuellen Bedingungen und Reize jedoch überlebenswichtig. Daher muss das genetisch vorgegebene neuronale Verschaltungsmuster anpassbar sein. Diese Anpassungsfähigkeit wird auch als Plastizität bezeichnet und wird in erster Linie durch Veränderungen der synaptischen Verbindungen bestehender Neuronen, durch biochemische Veränderungen an den Synapsen und durch das Hinzufügen und Entfernen von Neuronen erreicht. Sie ist oft auf bestimmte Zeitfenster mit erhöhter Empfänglichkeit für externe Reize beschränkt, die als kritische Perioden oder sensible Phasen bezeichnet werden. Die Erforschung kritischer Perioden hat sich lange Zeit auf Wirbeltiere konzentriert. Bei diesen wurde, kritische Perioden in der postnatalen Entwicklung des visuellen Systems oder beim Gesangslernen bei Vögeln nachgewiesen. Mehrere Studien haben jedoch gezeigt, dass kritische Perioden auch bei Insekten existieren. Bisher scheint dies vor allem im Geruchssystem der Fall zu sein.

Der Geruchssinn wird von Insekten für vielfältige Aufgaben, wie z.B. Auffindung von Nahrungsquellen, Fortpflanzungspartnern oder geeigneten Lebensräumen, genutzt. Bei holometabolen Insekten, wie *Tribolium castaneum* findet der erste Kontakt des adulten Geruchssystems mit der Umwelt im Anschluss an die Puppenphase zum Zeitpunkt des Schlüpfens aus der Puppe statt. Dieses Teilprojekt untersucht, ausgehend von der bereits bekannten Existenz der adulten Neurogenese in den Pilzkörpern von *T. castaneum*, inwieweit diese in den ersten Tagen als Imago von olfaktorischem Input abhängt und ob es eine zeitliche Begrenzung gibt.

Die zuverlässige Markierung der neugeborenen Tochterzellen der Pilzkörper-Neuroblasten im erwachsenen Tier bildete die Grundlage für die Studie und ermöglichte die Bestimmung der Anzahl der neugeborenen Kenyon-Zellen unter verschiedenen Geruchsbedingungen. Es wurde festgestellt, dass sich die Entstehung neuer Kenyon-Zellen innerhalb der ersten Woche nach dem Schlüpfen der erwachsenen Tiere in mindestens zwei Phasen unterteilen lässt. In den ersten drei Tagen ist die Entstehung von Kenyon-Zellen nicht von olfaktorischen Reizen abhängig und ist daher wahrscheinlich auf eine genetische Programmierung zurückzuführen und stellt eine Fortsetzung der Entwicklung aus der Metamorphose dar. Unmittelbar danach ist die Entstehung der Kenyon-Zellen jedoch wahrscheinlich hauptsächlich von der olfaktorischen Umgebung abhängig.

Angesichts der Rolle der Pilzkörper als Lern- und Gedächtniszentren ist die Neurogenese höchstwahrscheinlich eine wichtige Komponente bei der Neumodellierung des neuronalen Netzwerks, die letztlich zur Anpassung an die Umwelt und zur Optimierung des Verhaltens führt.

Chapter 4: Metamorphic development of the olfactory system
Kapitel 4: Metamorphe Entwicklung des olfaktorischen Systems

Für Insekten ist der olfaktorische Sinn überlebenswichtig. Die Geruchssignale werden durch ein komplexes System verarbeitet und ultimativ in Verhalten übersetzt. Das Nervensystem - und damit auch das Geruchssystem - holometaboler Insekten, wie *Tribolium castaneum*, ist während der Metamorphose typischerweise starken Veränderungen unterworfen. Diese Veränderungen sind notwendig, da sich die Lebensweise der Imagines holometaboler Insekten typischerweise stark von der der Larven unterscheidet.

Bereits die Larven der holometabolen Insekten besitzen olfaktorische Verarbeitungszentren und Sinnesanhänge, wobei sich die Komplexität zwischen den einzelnen Spezies unterscheidet. Für *T. castaneum*, wie auch seinem nahen Verwandten *Tenebrio molitor* gilt, dass bereits die Larven eine ausgefeilte Antenne aus drei unterscheidbaren Segmenten (Scapus, Pedicellus, Flagellum) besitzen. Eine ähnliche Struktur hat auch die larvale Antenne des Tabakschwärmers *Manduca sexta*, während Fliegen nur funktional äquivalente Dorsalorgane besitzen. Das bisherige Bild der Wissenschaft sieht die larvalen und adulten Antennen/olfaktorischen Sinnesanhänge als unabhängigen Strukturen. Die primären Verarbeitungszentren, sind im Mehlkäfer *T. molitor* und in *Drosophila melanogaster* bereits glomerulär organisiert, während dies beispielsweise im Tabakschwärmer *M. sexta* oder der westlichen Honigbiene *Apis mellifera* nicht der Fall ist.

Bisherige Studien legen Nahe das die olfaktorischen sensorischen Neurone für die korrekte Ausbildung der Glomeruli in den adulten Antennalloben notwendig sind. So führt ein Kappen der Antennen in *M. sexta* zu a-glomerulären Antennalloben und in der Ameise *Ooceraea biroi* zu einer Reduktion in der Glomerulianzahl. In der Ameise konnte der gleiche Effekt auch durch Ausschalten des Co-Rezeptors Orco, der zusammen mit einem spezifischen Odorantrezeptor eine funktionale Einheit bildet, erreicht werden. Zu beachten ist jedoch, dass die Autoren der Studie dies auf das resultierende Fehlen der olfaktorischen sensorischen Neurone zurückführen. Weiterhin konnten Studien in *D. melanogaster* Orco erst nach Bildung der Glomeruli nachweisen. Hier kann Orco also keinen Einfluss auf die Glomerulibildung haben.

In diesem Teilprojekt wurde die metamorphe Entwicklung des olfaktorischen Systems des Käfers *T. castaneum* untersucht. Es konnte gezeigt werden, dass für die adulte Antenne, Strukturen der larvalen Antennen wiederverwendet werden. Dies widerspricht dem bisherigen

wissenschaftlichem Bild, dass es sich um unabhängige Strukturen handelt. Das Gleiche gilt für die larvalen Antennalloben als primäre Geruchsverarbeitungszentren, die während der Metamorphose in ihre adulten Gegenstücke umgewandelt werden. Beides wird durch die Tatsache gestützt, dass olfaktorische sensorische Neurone in den Antennenstrukturen und Antennalloben während der gesamten Metamorphose nachgewiesen werden können. Weiterhin konnte gezeigt werden, der Co-Rezeptor Orco für die anfängliche Bildung der glomerulären Struktur der Antennalloben nicht notwendig ist - wohl für die spätere Differenzierung der Glomeruli in den frühen Imagines notwendig ist. Die Bildung der Glomeruli der Antennalloben findet wie in allen bisher untersuchten holometabolen Insekten etwa in der Mitte der Metamorphose statt. Gleiches gilt für das in *T. castaneum* erstbeschriebene gnathale olfaktorische Zentrum.

Chapter 5: The palpal olfactory pathway
Kapitel 5: Die palpale Riechbahn

Im aktuellen Bild der Wissenschaft des olfaktorischen Systems der holometabolen Insekten sind die paarigen Antennalloben die alleinigen primärem Verarbeitungszentren. Diese erhalten demnach Eingang von den sensorischen Neuronen der Antennen und Mundwerkzeuge. In holometabolen Insekten hingegen werden die olfaktorischen Signale, welche über die sensorischen Neurone der Mundwerkzeuge aufgenommen werden, separat verarbeitet. Dies gilt auch für den holometabolen Käfer *Tribolium castaneum*, bei dem die Signale der Mundwerkzeuge in den bisher nur von hemimetabolen Insekten bekannten glomerulären Loben (LG), sowie dem im Käfer erstbeschriebenen gnathalen olfaktorischem Zentrum (GOC) erstverarbeitet werden.

Dieses Teilprojekt konzentriert sich auf eine detaillierte Beschreibung des GOC, der LGs und deren sensorischen Inputs. Durch rasterelektronenmikroskopische Untersuchungen und Vergleiche mit konfokalmikroskopischen Aufnahmen an den Mundwerkzeugen einer, die olfaktorischen sensorischen Neurone markierenden transgenen Linie, wurden die Geruchssensillen an den Mundwerkzeugen identifiziert, welche die Dendriten der sensorischen Neurone enthalten die GOC und LGs innervieren. Dabei stellte sich heraus das mindestens 2 der 3 Sensillentypen eine olfaktorische Identität besitzen, was im Gegensatz zu bisherigen Erkenntnissen aus *Drosophila melanogaster* steht, wo nur ein Sensillentyp auf den Mundwerkzeugen olfaktorisch ist.

Mit 3D-Rekonstruktionen, die auf verschiedenen histologischen Färbungen basieren, wurde die anatomische Beschreibung des GOC präzisiert. Demnach besteht das GOC aus etwa 30 Glomeruli. Die Glomerulianzahl liegt damit am unteren Ende des bisher vermuteten Bereichs. Diese Anzahl an Glomeruli passt auch zu den 28 Duftstoffrezeptoren, die, wie durch RNA-Sequenzierung ermittelt, in den Mundwerkzeugen im Vergleich zum Körper signifikant angereichert sind.

Erstmals untersucht wird das Repertoire von GOC und LGs an Neuromediatoren. Dazu wurden exemplarisch solche untersucht, die auch in den Antennalloben vorgefunden werden. Die Rolle von GOC und LGs als primäre olfaktorische Verarbeitungszentren unterstreichend, wurden alle untersuchten Neuromediatoren, wenn auch mit Unterschieden im Innervationsmuster auch in GOC und LGs gefunden. Daraus lässt sich folgern, dass das Neuromediatorrepertoire eher nicht mit der Komplexität der Verarbeitungszentren korreliert, sondern eher eine Notwendigkeit darstellt, um Feineinstellung und initiale Evaluation der eingehenden Signale sicherzustellen.

Part I

General Introduction

1 | Insects

Insects are an astonishing group of animals, residing on earth for at least 400 million years. With about one million described species, insects are by far the largest and most species-rich as well as the most successful animal class [1] (Fig. 1.1A). They adapted to nearly all terrestrial ecological niches [2]. However, their economic, as well as ecological impact is often underestimated, while they indeed play a crucial role as pollinators or destruents, but also as the base of most terrestrial food chains [3, 4]. Further, many insects are harmful pests and disease vectors [5, 6]. Of all those described insect species Coleopterans represent about one-third and therefore are by far the largest and most species-rich insect order [2, 7, 8] (Fig. 1.1B).

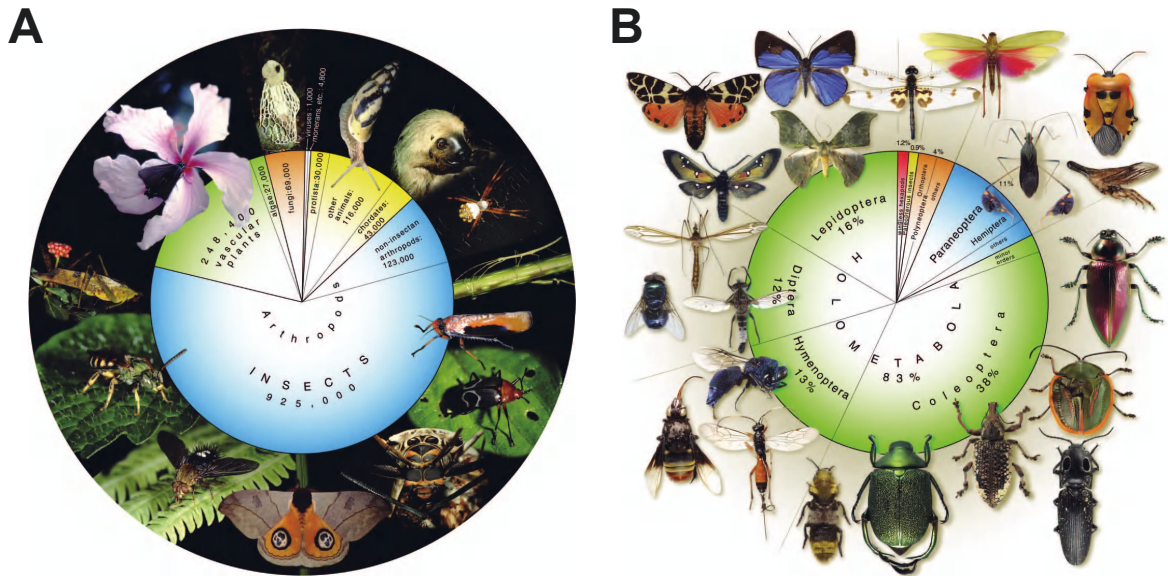

Fig. 1.1: A Insects are by far the most species rich class in the animal kingdom [2]. **B** Beetles account for about one third of insect species [2].

1.1 The red flour beetle *Tribolium castaneum*

The red flour beetle *Tribolium castaneum* Herbst (Fig. 1.2) is the main model used in this thesis. It is a representative of the largest insect order of Coleoptera (beetles) and therein belongs to the family of Tenebrionidae (darkling beetles). Together with its close relative *T. confusum*, it is today likely the most common global secondary pest for stored agricultural products [9, 10]. While its origins are uncertain, field observations indicate living under the bark of trees, in deadwood, or hymenopteran hives ad natural habitats [11]. Further, African origins are suggested based on archeological records from Egyptian tombs [12].

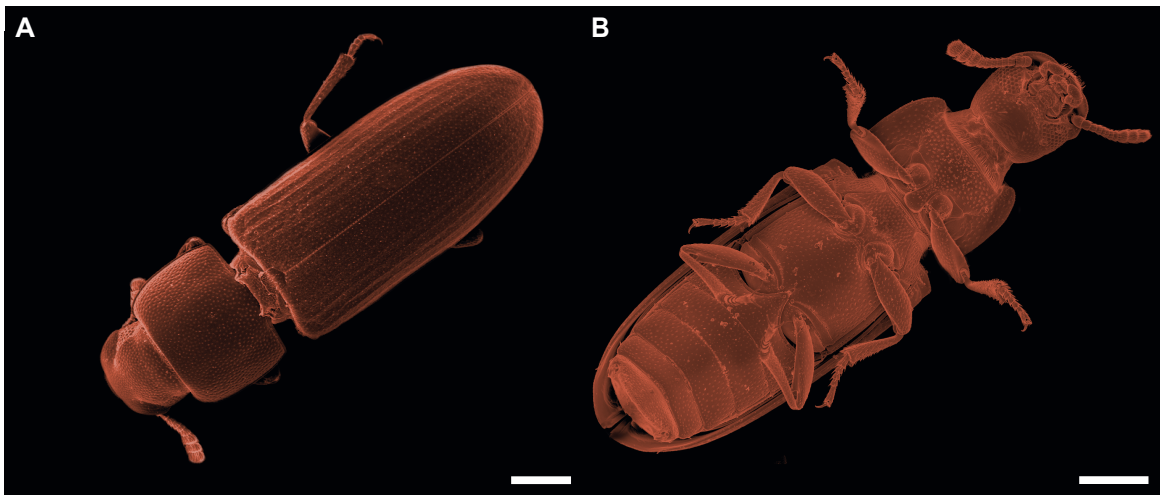

Fig. 1.2: Colorized scanning electron micrographs image of a female *T. castaneum* (A) dorsal and (B) ventral view. Scale bars 500 µm.)

The genome sequence of the red flour beetle is now well-annotated [13–17] and the genetic toolbox is since expanding [18–20], among others including strong systemic RNA interference (RNAi) [21–23].

Being easy to maintain in the lab, with low food and space requirements, as well as its short generation time of about one month and its relative longevity of about two years [24, 25] *T. castaneum*, which was first used to study population genetics in the second half of the last century, has emerged as a popular insect model organism in neurobiological research and is considered the current best-established coleopteran model organism [9].

2 | Olfaction in insects

For insects, as for every other animal, orientation in and interaction with the environment is crucial for their survival. Insects are found in most ecological niches with some environmental cues being more important than others.

To find hosts, conspecifics and mates, oviposition sites, and food sources, as wells as to avoid predators, toxins, and parasites, and also for intra- and interspecies communication, insects most often depend on their precisely tuned olfactory sense [26–37].

2.1 Perception and primary olfactory processing

Peripheral perception

The perception of olfactory stimuli occurs within the chemosensory sensilla of the antennae and mouthparts [13, 38, 39]. Filled with aqueous sensilla lymph, the sensilla house the dendrites of the olfactory sensory neurons (OSNs), which themselves present the olfactory receptors on their membrane. The receptors can be classified into two categories: the odorant receptors (ORs) and the ionotropic glutamate-like receptors (IRs) [13, 40–44]. The OSNs then relay the olfactory signals via their axons into the respective primary processing centers.

Primary processing

For the antennal OSNs, primary processing takes place in the antennal lobes (AL), while processing of information by the palpal OSNs differs among species. In hemimetabolous insects, olfactory information of the palpal OSNs is processed in the glomerular lobes (LGs) [45]. In holometabolous insects, where the LGs are thought to be fused into the ALs, the palpal signals are also processed in the ALs [46–50] This is not the case for *T. castaneum*. In the beetle the palpal OSNs project into the paired LGs and the unpaired gnathal olfactory center (GOC), which is a glomerularly organized neuropil within the gnathal ganglion [13].

The AL typically consist of somewhat spherical substructures called olfactory glomeruli, whose counts differ among insect species [45] - reaching from about 40 to 90, like in the ensiferan Orthoptera, Coleoptera, Diptera, and Lepidoptera [13, 51–55], but as in some Hymenopterans and especially in some ant species may rise to about 500 [45, 56, 57]. Furthermore, the ALs of the caeliferan Orthoptera consist of about 2000 to 3000 microglomeruli [58], while members of some other insect orders like Odonata and Ephemeroptera, but also single beetle species lack a glomerular organized AL [45].

The ALs receive input from the OSNs, with axons of OSNs expressing the same specific OR typically converging in the same glomerulus [50].

Within the AL, local neurons (LNs) connecting two or more glomeruli provide a first processing and integration layer [45, 59–63]. Most LNs use the inhibitory transmitter GABA [64]. In addition, they contain various neuropeptides [65–67].

Projection neurons (PNs) then further relay the olfactory information to higher integration centers [13, 68–70]. In holometabolous insects, the PNs typically form three distinct fiber bundles, the antennal lobe tracts, connecting the ALs with the mushroom bodies and lateral horns [13, 69]. Based on their innervation pattern within the ALs, the PNs may be divided into two classes: uniglomerular and multiglomerular PNs. While the uniglomerular PNs often send excitatory (cholinergic) signals into the mushroom bodies, the multiglomerular PNs relay inhibitory (GABAergic) signals exclusively into the lateral horns. [68].

2.2 Higher integration

Mushroom body

The paired mushroom bodies are formed by their intrinsic neurons (Kenyon cells). They consist of a dendritic input region called calyx and the peduncle and lobes, which are both formed by the Kenyon cells axon bundles (Fig. 2). Within the lobes, afferent input is conveyed from extrinsic neurons to Kenyon cells, and efferent output is conveyed from Kenyon cells to extrinsic neurons [7, 71].

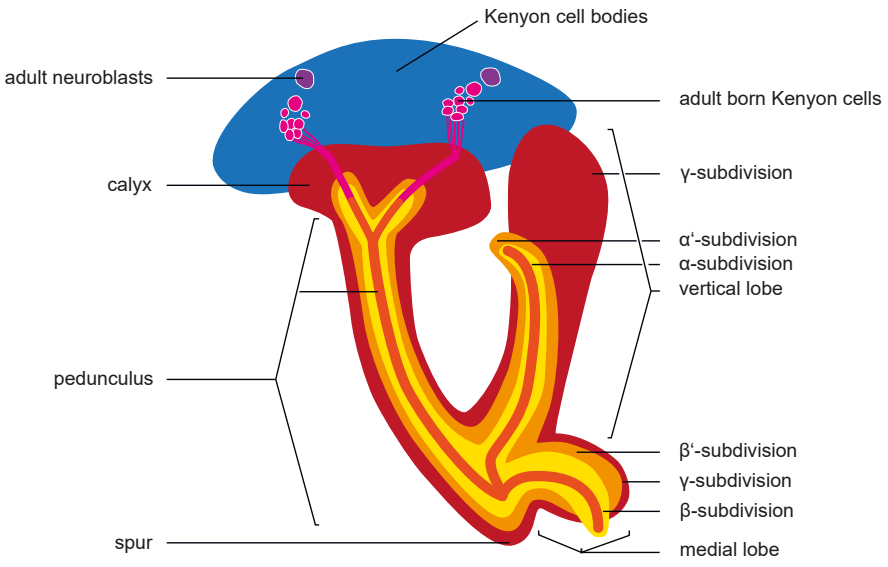

Fig. 2.1: Schematic drawing of a *T. castaneum* mushroom body (modified from [72])

The insect mushroom bodies serve as multimodal integration centers for olfactory, gustatory, visual, and mechanosensory input [73–77]. Further, they are involved in learning and memory [61, 78–80]. In the context of olfaction, they are responsible for odor discrimination [76, 81] as wells as for associative olfactory learning and memory [82, 83].

Lateral horn

Like the mushroom bodies, the lateral horn is a paired neuropil, which locates lateral within the protocerebrum. As it is not always clearly morphologically distinguishable it is often called "lateral protocerebrum". It is largely responsible for decoding the odor quality, as well as concentration, and translates the information into innate behavior by integrating the signals of the inhibitory and excitatory projection neurons of the AL [84].

2.3 Development and plasticity of the olfactory system

Metamorphic development

In holometabolous insects like beetles, the lifestyle of adult insects is often more complex compared to larvae. Consequently, the olfactory system is remodeled during metamorphosis and adopted to the new challenges. While already the larvae of holometabolous insects have olfactory appendages and processing centers, these structures are typically less complex than the adult structures.

The current picture sees the adult antennae as a separate structure that develops from imaginal discs [85–91], while the antennae of hemimetabolous insects develop gradually through molds until the adult stage [91, 92]. However, the assumption of being separate structures derives from only a few species in essentially the two orders of Diptera (mainly *Drosophila melanogaster* [87–89] and Lepidoptera (*Pieris brassicae* [85, 86], *Manduca sexta* [90, 93] and *Bombyx mori* [94]– with detailed studies of the antennal development in *Antheraea polyphemus* [95–100]. In general, the development of adult structures from imaginal discs or cells in holometabolous insects is strongly derived. In the more ancestral state, it is believed that cells of the larval appendages are used to build their adult equivalents [91].

Focusing on the development of the ALs as olfactory primary processing centers, there are fundamental differences among investigated holometabolous species. In the lepidopteran *M. sexta*, as well as in the hymenopteran *Apis mellifera*, the larval AL is not glomerular organized [101, 102], whereas the larval AL of *D. melanogaster* shows a glomerular organization [103] but with a lower number of glomeruli and a one to one wiring between receptor neurons and glomeruli. The larval ALs of the hemimetabolic insect *Periplaneta americana* display a comparable number of glomeruli as the adult AL [104].

Postmetamorphic and adult plasticity

The ground pattern of the central nervous system, and therefore also the olfactory system is genetically encoded. Following the development, when the nervous system first encounters environmental sensory input, it is crucial for the survival of an animal to adapt to the actual conditions and cues. Therefore, the genetically encoded wiring scheme of the nervous system must be altered. This plasticity typically occurs in special time windows of elevated susceptibility to sensory input (critical periods or sensitive phases) [105].

In general, the necessary plasticity can occur on the morphological level via the creation and refinement of synaptic connections [106] and proliferation or apoptosis of neurons and glial cells [107–113] but may also occur on the biochemical level with existing neurons changing their transmitter identity [114].

While research on critical periods mainly focused on vertebrates, where they were among others found during the postnatal development of the visual system [115–123] and song learning in birds [124–126], several studies also demonstrated the existence of critical periods in insects [127–131] with many focusing on the plasticity of the olfactory system in the vinegar fly *D. melanogaster* [128–134]. The results of those studies further suggest that the plasticity in the ALs is synaptic plasticity.

Considering that the mushroom bodies are linked to olfactory learning and memory [135], it is not surprising that many studies describe a high amount of plasticity within the mushroom bodies. For example, studies on several holometabolous insects, including *A. mellifera* and *D. melanogaster*, describe massive synaptic plasticity [136–144]. Further, despite being absent in *A. mellifera* and *D. melanogaster* [145, 146], neurogenesis is also part of that game.

Since first described in the hemimetabolous house cricket *Acheta domestica* [108, 147], it has also been found in holometabolous insects, such as the noctuid moth *Agrotis ipsilon* [109], as well as several beetle species [107] including the red flour beetle *T. castaneum* [148].

References

[1] Stork, N. E. "How Many Species of Insects and Other Terrestrial Arthropods Are There on Earth?" In: *Annu. Rev. Entomol.* 63.1 (2018), pp. 31–45. ISSN: 0066-4170, 1545-4487. DOI: 10.1146/annurev-ento-020117-043348.

[2] Grimaldi, D. and Engel, M. S. *Evolution of the Insects*. Reprint. New York: Cambridge University Press, 2006. 755 pp. ISBN: 978-0-521-82149-0.

[3] Shurin, J. B., Gruner, D. S., and Hillebrand, H. "All Wet or Dried up? Real Differences between Aquatic and Terrestrial Food Webs". In: *Proc. Biol. Sci.* 273.1582 (2006), pp. 1–9. ISSN: 1471-2954. DOI: 10.1098/rspb.2005.3377.

[4] Zhang, W., Ricketts, T. H., Kremen, C., Carney, K., and Swinton, S. M. "Ecosystem Services and Dis-Services to Agriculture". In: *Ecol. Econ.* 64.2 (2007), pp. 253–260. ISSN: 09218009. DOI: 10.1016/j.ecolecon.2007.02.024.

[5] Benelli, G. and Mehlhorn, H. "Declining Malaria, Rising of Dengue and Zika Virus". In: *Parasitol. Res.* 115.5 (2016), pp. 1747–1754. ISSN: 1432-1955. DOI: 10.1007/s00436-016-4971-z.

[6] Pedigo, L. P. and Rice, M. E. *Entomology and Pest Management*. Sixth edition, reissued. Long Grove, Illinois: Waveland Press, Inc, 2015. 784 pp. ISBN: 978-1-4786-2285-7 978-0-13-513295-1.

[7] Hauser, F., Cazzamali, G., Williamson, M., et al. "A Genome-Wide Inventory of Neurohormone GPCRs in the Red Flour Beetle *Tribolium Castaneum*". In: *Front. Neuroendocri.* 29.1 (2008), pp. 142–165. ISSN: 00913022. DOI: 10.1016/j.yfrne.2007.10.003.

[8] Hunt, T., Bergsten, J., Levkanicova, Z., et al. "A Comprehensive Phylogeny of Beetles Reveals the Evolutionary Origins of a Superradiation". In: *Science* 318.5858 (2007), pp. 1913–1916. ISSN: 0036-8075. DOI: 10.1126/science.1146954.

[9] Brown, S. J., Shippy, T. D., Miller, S., Bolognesi, R., Beeman, R. W., Lorenzen, M. D., Bucher, G., Wimmer, E. A., and Klingler, M. "The Red Flour Beetle, *Tribolium Castaneum* (Coleoptera)". In: *Cold Spring Harb. Protoc.* 2009.8 (2009), pdbemo126. ISSN: 1559-6095. DOI: 10.1101/pdb.emo126.

[10] Levinson, H. and Levinson, A. "Origin of Grain Storage and Insect Species Consuming Desiccated Food". In: *Anz. Schaedlingskd., Pflanzenschutz, Umweltschutz* 67.3 (1994), pp. 47–60. ISSN: 0340-7330. DOI: 10.1007/BF01906428.

[11] Arnaud, L., Brostaux, Y., Lallemand, S., and Haubruge, E. "Reproductive Strategies of *Tribolium* Flour Beetles". In: *J. Insect Sci.* 5 (2005), p. 33. ISSN: 1536-2442. DOI: 10.1093/jis/5.1.33.

[12] Buckland, P. C. "The Early Dispersal of Insect Pests of Stored Products as Indicated by Archaeological Records". In: *J. Stored Prod. Res.* 17.1 (1981), pp. 1–12. ISSN: 0022-474X. DOI: 10.1016/0022-474X(81)90025-4.

[13] Dippel, S., Kollmann, M., Oberhofer, G., et al. "Morphological and Transcriptomic Analysis of a Beetle Chemosensory System Reveals a Gnathal Olfactory Center". In: *BMC Biol.* 14.1 (2016), p. 90. ISSN: 1741-7007. DOI: 10.1186/s12915-016-0304-z.

[14] Dippel, S., Oberhofer, G., Kahnt, J., Gerischer, L., Opitz, L., Schachtner, J., Stanke, M., Schütz, S., Wimmer, E. A., and Angeli, S. "Tissue-Specific Transcriptomics, Chromosomal Localization, and Phylogeny of Chemosensory and Odorant Binding Proteins from the Red Flour Beetle *Tribolium Castaneum* Reveal Subgroup Specificities for Olfaction or More General Functions". In: *BMC Genomics* 15.1 (2014), p. 1141. ISSN: 1471-2164. DOI: 10.1186/1471-2164-15-1141.

[15] Kim, H. S., Murphy, T., Xia, J., Caragea, D., Park, Y., Beeman, R. W., Lorenzen, M. D., Butcher, S., Manak, J. R., and Brown, S. J. "BeetleBase in 2010: Revisions to Provide Comprehensive Genomic Information for *Tribolium Castaneum*". In: *Nucleic Acids Res.* 38 (Database issue 2010), pp. D437–42. ISSN: 0305-1048. DOI: 10.1093/nar/gkp807.

[16] Tribolium Genome Sequencing Consortium. "The Genome of the Model Beetle and Pest *Tribolium Castaneum*". In: *Nature* 452.7190 (2008), pp. 949–955. ISSN: 0028-0836, 1476-4687. DOI: 10.1038/nature06784.

[17] Wang, L., Wang, S., Li, Y., Paradesi, M. S. R., and Brown, S. J. "BeetleBase: The Model Organism Database for *Tribolium Castaneum*". In: *Nucleic Acids Res.* 35 (Database issue 2007), pp. D476–9. ISSN: 0305-1048. DOI: 10.1093/nar/gkl776.

[18] Gilles, A. F., Schinko, J. B., and Averof, M. "Efficient CRISPR-mediated Gene Targeting and Transgene Replacement in the Beetle *Tribolium Castaneum*". In: *Development* 142.16 (2015), pp. 2832–2839. ISSN: 1477-9129. DOI: 10.1242/dev.125054.

[19] Schinko, J. B., Weber, M., Viktorinova, I., Kiupakis, A., Averof, M., Klingler, M., Wimmer, E. A., and Bucher, G. "Functionality of the GAL4/UAS System in *Tribolium* Requires the Use of Endogenous Core Promoters". In: *BMC Dev. Biol.* 10 (2010), p. 53. ISSN: 1471-213X. DOI: 10.1186/1471-213X-10-53.

[20] Trauner, J., Schinko, J., Lorenzen, M. D., Shippy, T. D., Wimmer, E. A., Beeman, R. W., Klingler, M., Bucher, G., and Brown, S. J. "Large-Scale Insertional Mutagenesis of a Coleopteran Stored Grain Pest, the Red Flour Beetle *Tribolium Castaneum*, Identifies Embryonic Lethal Mutations and Enhancer Traps". In: *BMC Biol.* 7 (2009), p. 73. ISSN: 1741-7007. DOI: 10.1186/1741-7007-7-73.

[21] Bucher, G., Scholten, J., and Klingler, M. "Parental RNAi in *Tribolium* (Coleoptera)". In: *Curr. Biol.* 12.3 (2002), R85–R86. ISSN: 0960-9822. DOI: 10.1016/S0960-9822(02)00666-8.

[22] Tomoyasu, Y. and Denell, R. E. "Larval RNAi in *Tribolium* (Coleoptera) for Analyzing Adult Development". In: *Dev. Genes Evol.* 214.11 (2004), pp. 575–578. ISSN: 1432-041X. DOI: 10.1007/s00427-004-0434-0.

[23] Tomoyasu, Y., Miller, S. C., Tomita, S., Schoppmeier, M., Grossmann, D., and Bucher, G. "Exploring Systemic RNA Interference in Insects: A Genome-Wide Survey for RNAi Genes in *Tribolium*". In: *Genome Biol.* 9.1 (2008), R10. ISSN: 1474-760X. DOI: 10.1186/gb-2008-9-1-r10.

[24] Berghammer, A. J., Bucher, G., Maderspacher, F., and Klingler, M. "A System to Efficiently Maintain Embryonic Lethal Mutations in the Flour Beetle *Tribolium Castaneum*". In: *Dev. Genes Evol.* 209.6 (1999), pp. 382–389. ISSN: 1432-041X. DOI: 10.1007/s004270050268.

[25] Sokoloff, A. *The Biology of* Tribolium*: With Special Emphasis on Genetic Aspects. Volume 1.* Vol. 1. 3 vols. The Biology of Tribolium. Oxford: Clarendon Press, 1972. 300 pp. ISBN: 0-19-857353-1.

[26] Dicke, M. "Behavioural and Community Ecology of Plants That Cry for Help". In: *Plant Cell Environ.* 32.6 (2009), pp. 654–665. ISSN: 01407791, 13653040. DOI: 10.1111/j.1365-3040.2008.01913.x.

[27] Laska, M. "Olfactory Discrimination Ability and Odor Structure: Activity Relationships in Honeybees". In: *Chem. Senses* 24.4 (1999), pp. 429–438. ISSN: 1464-3553. DOI: 10.1093/chemse/24.4.429.

[28] Linz, J., Baschwitz, A., Strutz, A., Dweck, H. K. M., Sachse, S., Hansson, B. S., and Stensmyr, M. C. "Host Plant-Driven Sensory Specialization in *Drosophila Erecta*". In: *Proc. Biol. Sci.* 280.1760 (2013), p. 20130626. ISSN: 1471-2954. DOI: 10.1098/rspb.2013.0626.

[29] Liu, M., Yu, H., and Li, G. "Oviposition Deterrents from Eggs of the Cotton Bollworm, *Helicoverpa Armigera* (Lepidoptera: Noctuidae): Chemical Identification and Analysis by Electroantennogram". In: *J. Insect Physiol.* 54.4 (2008), pp. 656–662. ISSN: 00221910. DOI: 10.1016/j.jinsphys.2008.01.002.

[30] Paczkowski, S., Paczkowska, M., Dippel, S., Flematti, G., and Schütz, S. "Volatile Combustion Products of Wood Attract *Acanthocnemus Nigricans* (Coleoptera: Acanthocnemidae)". In: *J. Insect. Behav.* 27.2 (2014), pp. 228–238. ISSN: 0892-7553. DOI: 10.1007/s10905-013-9430-4.

[31] Stensmyr, M. C., Dweck, H. K. M., Farhan, A., et al. "A Conserved Dedicated Olfactory Circuit for Detecting Harmful Microbes in Drosophila". In: *Cell* 151.6 (2012), pp. 1345–1357. ISSN: 1097-4172. DOI: 10.1016/j.cell.2012.09.046.

[32] Sun, Y.-L., Huang, L.-Q., Pelosi, P., and Wang, C.-Z. "Expression in Antennae and Reproductive Organs Suggests a Dual Role of an Odorant-Binding Protein in Two Sibling *Helicoverpa* Species". In: *PLoS ONE* 7.1 (2012), e30040. ISSN: 1932-6203. DOI: 10.1371/journal.pone.0030040.

[33] Visser, J. H. "Host Odor Perception in Phytophagous Insects". In: *Annu. Rev. Entomol.* 31.1 (1986), pp. 121–144. ISSN: 0066-4170, 1545-4487. DOI: 10.1146/annurev.en.31.010186.001005.

[34] Weiss, L. A., Dahanukar, A., Kwon, J. Y., Banerjee, D., and Carlson, J. R. "The Molecular and Cellular Basis of Bitter Taste in Drosophila". In: *Neuron* 69.2 (2011), pp. 258–272. ISSN: 1097-4199. DOI: 10.1016/j.neuron.2011.01.001.

[35] Weissteiner, S., Huetteroth, W., Kollmann, M., Weißbecker, B., Romani, R., Schachtner, J., Schütz, S., and Marion-Poll, F. "Cockchafer Larvae Smell Host Root Scents in Soil". In: *PLoS ONE* 7.10 (2012), e45827. ISSN: 1932-6203. DOI: 10.1371/journal.pone.0045827.

[36] Whiteman, N. and Pierce, N. "Delicious Poison: Genetics of Drosophila Host Plant Preference". In: *Trends Ecol. Evol.* 23.9 (2008), pp. 473–478. ISSN: 01695347. DOI: 10.1016/j.tree.2008.05.010.

[37] Yang, C.-H., Belawat, P., Hafen, E., Jan, L. Y., and Jan, Y.-N. "Drosophila Egg-Laying Site Selection as a System to Study Simple Decision-Making Processes". In: *Science* 319.5870 (2008), pp. 1679–1683. ISSN: 0036-8075. DOI: 10.1126/science.1151842.

[38] Martin, F., Boto, T., Gomez-Diaz, C., and Alcorta, E. "Elements of Olfactory Reception in Adult Drosophila Melanogaster". In: *Anat. Rec.* 296.9 (2013), pp. 1477–1488. ISSN: 1932-8494. DOI: 10.1002/ar.22747.

[39] Shanbhag, S., Müller, B., and Steinbrecht, R. A. "Atlas of Olfactory Organs of Drosophila Melanogaster". In: *Int. J. Insect Morphol. Embryol.* 28.4 (1999), pp. 377–397. ISSN: 0020-7322. DOI: 10.1016/S0020-7322(99)00039-2.

[40] Leal, W. S. "Odorant Reception in Insects". In: *Annu. Rev. Entomol.* 58 (2013), pp. 373–391. ISSN: 1545-4487. DOI: 10.1146/annurev-ento-120811-153635.

[41] Benton, R., Vannice, K. S., Gomez-Diaz, C., and Vosshall, L. B. "Variant Ionotropic Glutamate Receptors as Chemosensory Receptors in Drosophila". In: *Cell* 136.1 (2009), pp. 149–162. ISSN: 1097-4172. DOI: 10.1016/j.cell.2008.12.001.

[42] Missbach, C., Dweck, H. K., Vogel, H., Vilcinskas, A., Stensmyr, M. C., Hansson, B. S., and Grosse-Wilde, E. "Evolution of Insect Olfactory Receptors". In: *eLife* 3 (2014), e02115. ISSN: 2050-084X. DOI: 10.7554/eLife.02115.

[43] Sato, K., Pellegrino, M., Nakagawa, T., Nakagawa, T., Vosshall, L. B., and Touhara, K. "Insect Olfactory Receptors Are Heteromeric Ligand-Gated Ion Channels". In: *Nature* 452.7190 (2008), pp. 1002–1006. ISSN: 0028-0836. DOI: 10.1038/nature06850.

[44] Wicher, D., Schäfer, R., Bauernfeind, R., Stensmyr, M. C., Heller, R., Heinemann, S. H., and Hansson, B. S. "Drosophila Odorant Receptors Are Both Ligand-Gated and Cyclic-Nucleotide-Activated Cation Channels". In: *Nature* 452.7190 (2008), pp. 1007–1011. ISSN: 0028-0836. DOI: 10.1038/nature06861.

[45] Schachtner, J., Schmidt, M., and Homberg, U. "Organization and Evolutionary Trends of Primary Olfactory Brain Centers in Tetraconata (Crustacea+Hexapoda)". In: *Arthropod. Struct. Dev.* 34.3 (2005), pp. 257–299. ISSN: 14678039. DOI: 10.1016/j.asd.2005.04.003.

[46] Anton, S. and Homberg, U. "Antennal Lobe Structure". In: *Insect Olfaction.* Ed. by Hansson, B. S. 1999, pp. 97–124.

[47] Lin, T., Li, C., Liu, J., Smith, B. H., Lei, H., and Zeng, X. "Glomerular Organization in the Antennal Lobe of the Oriental Fruit Fly Bactrocera Dorsalis". In: *Front. Neuroanat.* 12 (2018), p. 71. ISSN: 1662-5129. DOI: 10.3389/fnana.2018.00071.

[48] Riabinina, O., Task, D., Marr, E., Lin, C.-C., Alford, R., O'Brochta, D. A., and Potter, C. J. "Organization of Olfactory Centres in the Malaria Mosquito Anopheles Gambiae". In: *Nat. Commun.* 7 (2016), p. 13010. ISSN: 2041-1723. DOI: 10.1038/ncomms13010.

[49] Szyszka, P. and Galizia, C. G. "Olfaction in Insects". In: *Handbook of Olfaction and Gustation.* Ed. by Doty, R. L. 3. ed. Hoboken, NJ: Wiley, 2015, pp. 531–546. ISBN: 978-1-118-13922-6.

[50] Vosshall, L. B. "Olfaction in Drosophila". In: *Curr. Opin. Neurobiol.* 10.4 (2000), pp. 498–503. ISSN: 0959-4388. DOI: 10.1016/S0959-4388(00)00111-2.

[51] Dreyer, D., Vitt, H., Dippel, S., Goetz, B., El Jundi, B., Kollmann, M., Huetteroth, W., and Schachtner, J. "3D Standard Brain of the Red Flour Beetle *Tribolium Castaneum:* A Tool to Study Metamorphic Development and Adult Plasticity". In: *Front Syst Neurosci* 4 (2010), p. 3. ISSN: 1662-5137. DOI: 10.3389/neuro.06.003.2010.

[52] Greiner, B., Gadenne, C., and Anton, S. "Three-Dimensional Antennal Lobe Atlas of the Male Moth, Agrotis Ipsilon: A Tool to Study Structure-Function Correlation". In: *J. Comp. Neurol.* 475.2 (2004), pp. 202–210. ISSN: 0021-9967. DOI: 10.1002/cne.20173.

[53] Ignell, R., Dekker, T., Ghaninia, M., and Hansson, B. S. "Neuronal Architecture of the Mosquito Deutocerebrum". In: *J. Comp. Neurol.* 493.2 (2005), pp. 207–240. ISSN: 0021-9967. DOI: 10.1002/cne.20800.

[54] Laissue, P. P., Reiter, C., Hiesinger, P. R., Halter, S., Fischbach, K. F., and Stocker, R. F. "Three-Dimensional Reconstruction of the Antennal Lobe in Drosophila Melanogaster". In: *J. Comp. Neurol.* 405.4 (1999), pp. 543–552. ISSN: 0021-9967. DOI: 10.1002/(SICI)1096-9861(19990322)405:4<543::AID-CNE7>3.0.CO;2-A.

[55] Rospars, J. P. and Hildebrand, J. G. "Sexually Dimorphic and Isomorphic Glomeruli in the Antennal Lobes of the Sphinx Moth Manduca Sexta". In: *Chem. Senses* 25.2 (2000), pp. 119–129. ISSN: 1464-3553. DOI: 10.1093/chemse/25.2.119.

[56] Mysore, K., Subramanian, K. A., Sarasij, R. C., Suresh, A., Shyamala, B. V., VijayRaghavan, K., and Rodrigues, V. "Caste and Sex Specific Olfactory Glomerular Organization and Brain Architecture in Two Sympatric Ant Species Camponotus Sericeus and Camponotus Compressus (Fabricius, 1798)". In: *Arthropod. Struct. Dev.* 38.6 (2009), pp. 485–497. ISSN: 14678039. DOI: 10.1016/j.asd.2009.06.001.

[57] Zube, C., Kleineidam, C. J., Kirschner, S., Neef, J., and Rössler, W. "Organization of the Olfactory Pathway and Odor Processing in the Antennal Lobe of the Ant Camponotus Floridanus". In: *J. Comp. Neurol.* 506.3 (2008), pp. 425–441. ISSN: 0021-9967. DOI: 10.1002/cne.21548.

[58] Ignell, R., Anton, S., and Hansson, B. S. "The Antennal Lobe of Orthoptera - Anatomy and Evolution". In: *Brain Behav. Evol.* 57.1 (2001), pp. 1–17. ISSN: 0006-8977. DOI: 10.1159/000047222.

[59] Boeckh, J. and Tolbert, L. P. "Synaptic Organization and Development of the Antennal Lobe in Insects". In: *Microsc. Res. Tech.* 24.3 (1993), pp. 260–280. ISSN: 1059-910X. DOI: 10.1002/jemt.1070240305.

[60] Carlsson, M. A. and Hansson, B. S. "Dose-Response Characteristics of Glomerular Activity in the Moth Antennal Lobe". In: *Chem. Senses* 28.4 (2003), pp. 269–278. ISSN: 1464-3553. DOI: 10.1093/chemse/28.4.269.

[61] Galizia, C. G. and Menzel, R. "The Role of Glomeruli in the Neural Representation of Odours: Results from Optical Recording Studies". In: *J. Insect Physiol.* 47.2 (2001), pp. 115–130. ISSN: 0022-1910. DOI: 10.1016/S0022-1910(00)00106-2.

[62] Masse, N. Y., Turner, G. C., and Jefferis, G. S. X. E. "Olfactory Information Processing in *Drosophila*". In: *Curr. Biol.* 19.16 (2009), R700–13. ISSN: 0960-9822. DOI: 10.1016/j.cub.2009.06.026.

[63] Wang, J. W., Wong, A. M., Flores, J., Vosshall, L. B., and Axel, R. "Two-Photon Calcium Imaging Reveals an Odor-Evoked Map of Activity in the Fly Brain". In: *Cell* 112.2 (2003), pp. 271–282. ISSN: 0092-8674. DOI: 10.1016/S0092-8674(03)00004-7.

[64] Okada, R., Awasaki, T., and Ito, K. "Gamma-Aminobutyric Acid (GABA)-Mediated Neural Connections in the *Drosophila* Antennal Lobe". In: *J. Comp. Neurol.* 514.1 (2009), pp. 74–91. ISSN: 0021-9967. DOI: 10.1002/cne.21971.

[65] Binzer, M., Heuer, C. M., Kollmann, M., Kahnt, J., Hauser, F., Grimmelikhuijzen, C. J. P., and Schachtner, J. "Neuropeptidome of *Tribolium Castaneum* Antennal Lobes and Mushroom Bodies". In: *J. Comp. Neurol.* 522.2 (2014), pp. 337–357. ISSN: 0021-9967. DOI: 10.1002/cne.23399.

[66] Carlsson, M. A., Diesner, M., Schachtner, J., and Nässel, D. R. "Multiple Neuropeptides in the *Drosophila* Antennal Lobe Suggest Complex Modulatory Circuits". In: *J. Comp. Neurol.* 518.16 (2010), pp. 3359–3380. ISSN: 0021-9967. DOI: 10.1002/cne.22405.

[67] Siju, K. P. "Neuromodulation in the Chemosensory System of Mosquitoes". Doctoral Thesis. Alnarp: Swedish University of Agricultural Sciences, 2009.

[68] Galizia, C. G. "Olfactory Coding in the Insect Brain: Data and Conjectures". In: *Eur. J. Neurosci.* 39.11 (2014), pp. 1784–1795. ISSN: 0953-816X. DOI: 10.1111/ejn.12558.

[69] Galizia, C. G. and Rössler, W. "Parallel Olfactory Systems in Insects: Anatomy and Function". In: *Annu. Rev. Entomol.* 55 (2010), pp. 399–420. ISSN: 1545-4487. DOI: 10.1146/annurev-ento-112408-085442.

[70] Rössler, W. and Brill, M. F. "Parallel Processing in the Honeybee Olfactory Pathway: Structure, Function, and Evolution". In: *J. Comp. Physiol. A Neuroethol. Sens. Neural. Behav. Physiol.* 199.11 (2013), pp. 981–996. ISSN: 1432-1351. DOI: 10.1007/s00359-013-0821-y.

[71] Ito, K., Suzuki, K., Estes, P., Ramaswami, M., Yamamoto, D., and Strausfeld, N. J. "The Organization of Extrinsic Neurons and Their Implications in the Functional Roles of the Mushroom Bodies in *Drosophila Melanogaster* Meigen". In: *Learn. Mem.* 5.1-2 (1998), pp. 52–77. ISSN: 1549-5485.

[72] Trebels, B., Dippel, S., Schaaf, M., Balakrishnan, K., Wimmer, E. A., and Schachtner, J. "Adult Neurogenesis in the Mushroom Bodies of Red Flour Beetles (*Tribolium Castaneum*, HERBST) Is Influenced by the Olfactory Environment". In: *Sci Rep* 10.1090 (2020), pp. 1–11. ISSN: 2045-2322. DOI: 10.1038/s41598-020-57639-x.

[73] Campbell, R. A. and Turner, G. C. "The Mushroom Body". In: *Curr. Biol.* 20.1 (2010), R11–R12. ISSN: 0960-9822. DOI: 10.1016/j.cub.2009.10.031.

[74] Farris, S. M. "Evolution of Insect Mushroom Bodies". In: *Arthropod. Struct. Dev.* 34.3 (2005), pp. 211–234. ISSN: 14678039. DOI: 10.1016/j.asd.2005.01.008.

[75] Farris, S. M. "Tritocerebral Tract Input to the Insect Mushroom Bodies". In: *Arthropod. Struct. Dev.* 37.6 (2008), pp. 492–503. ISSN: 14678039. DOI: 10.1016/j.asd.2008.05.005.

[76] Heuer, C. M., Kollmann, M., Binzer, M., and Schachtner, J. "Neuropeptides in Insect Mushroom Bodies". In: *Arthropod. Struct. Dev.* 41.3 (2012), pp. 199–226. ISSN: 14678039. DOI: 10.1016/j.asd.2012.02.005.

[77] Schröter, U. and Menzel, R. "A New Ascending Sensory Tract to the Calyces of the Honeybee Mushroom Body, the Subesophageal-Calycal Tract". In: *J. Comp. Neurol.* 465.2 (2003), pp. 168–178. ISSN: 0021-9967. DOI: 10.1002/cne.10843.

[78] Heisenberg, M. "What Do the Mushroom Bodies Do for the Insect Brain? An Introduction". In: *Learn. Mem.* 5.1-2 (1998), pp. 1–10. ISSN: 1549-5485.

[79] Heisenberg, M. "Mushroom Body Memoir: From Maps to Models". In: *Nat. Rev. Neurosci.* 4.4 (2003), pp. 266–275. ISSN: 1471-0048. DOI: 10.1038/nrn1074.

[80] Strausfeld, N. J. and Hildebrand, J. G. "Olfactory Systems". In: *Curr. Opin. Neurobiol.* 9.5 (1999), pp. 634–639. ISSN: 1873-6882. DOI: 10.1016/S0959-4388(99)00019-7.

[81] Strube-Bloss, M. F. and Rössler, W. "Multimodal Integration and Stimulus Categorization in Putative Mushroom Body Output Neurons of the Honeybee". In: *R Soc Open Sci* 5.2 (2018), p. 171785. ISSN: 2054-5703. DOI: 10.1098/rsos.171785.

[82] Farris, S. M. and van Dyke, J. W. "Evolution and Function of the Insect Mushroom Bodies". In: *Curr. Opin. Insect Sci.* 12 (2015), pp. 19–25. ISSN: 22145745. DOI: 10.1016/j.cois.2015.08.006.

[83] Fiala, A. "Olfaction and Olfactory Learning in Drosophila". In: *Curr. Opin. Neurobiol.* 17.6 (2007), pp. 720–726. ISSN: 0959-4388. DOI: 10.1016/j.conb.2007.11.009.

[84] Strutz, A., Soelter, J., Baschwitz, A., Farhan, A., Grabe, V., Rybak, J., Knaden, M., Schmuker, M., Hansson, B. S., and Sachse, S. "Decoding Odor Quality and Intensity in the Drosophila Brain". In: *eLife* 3 (2014), e04147. ISSN: 2050-084X. DOI: 10.7554/elife.04147.

[85] Eassa, Y. E. E. "The Development of Imaginal Buds in the Head of *Pieris Brassicae* Linn. (Lepidoptera)". In: *Trans. R. Entomol. Soc. Lond.* 104.3 (1953), pp. 39–50. ISSN: 1365-2311. DOI: 10.1111/j.1365-2311.1953.tb01249.x.

[86] Eassa, Y. E. E. "Metamorphosis of the Cranial Capsule and Its Appendages in the Cabbage Butterfly, *Pieris Brassicae*". In: *Ann Entomol Soc Am* 56.4 (1963), pp. 510–521. ISSN: 0013-8746. DOI: 10.1093/aesa/56.4.510.

[87] Haynie, J. L. and Bryant, P. J. "Development of the Eye-Antenna Imaginal Disc and Morphogenesis of the Adult Head in *Drosophila Melanogaster*". In: *J. Exp. Zool.* 237.3 (1986), pp. 293–308. ISSN: 1097-010X. DOI: 10.1002/jez.1402370302.

[88] Lienhard, M. C. and Stocker, R. F. "The Development of the Sensory Neuron Pattern in the Antennal Disc of Wild-Type and Mutant (Lz3, Ssa) *Drosophila Melanogaster*". In: *Development* 112.4 (1991), pp. 1063–1075. ISSN: 0950-1991, 1477-9129. URL: http://dev.biologists.org/content/112/4/1063 (visited on 06/29/2018).

[89] Morata, G. and Lawrence, P. A. "Development of the Eye-Antenna Imaginal Disc of *Drosophila*". In: *Developmental Biology* 70.2 (1979), pp. 355–371. ISSN: 0012-1606. DOI: 10.1016/0012-1606(79)90033-2.

[90] Sanes, J. R. and Hildebrand, J. G. "Structure and Development of Antennae in a Moth, *Manduca Sexta*". In: *Developmental Biology* 51.2 (1976), pp. 282–299. ISSN: 0012-1606. DOI: 10.1016/0012-1606(76)90144-5.

[91] Svácha, P. "What Are and What Are Not Imaginal Discs: Reevaluation of Some Basic Concepts (Insecta, Holometabola)". In: *Developmental Biology* 154.1 (1992), pp. 101–117. ISSN: 0012-1606. DOI: 10.1016/0012-1606(92)90052-i.

[92] Schafer, R. "Postembryonic Development in the Antenna of the Cockroach, *Leucophaea Maderae*: Growth, Regeneration, and the Development of the Adult Pattern of Sense Organs". In: *J. Exp. Zool.* 183.3 (1973), pp. 353–363. ISSN: 1097-010X. DOI: 10.1002/jez.1401830309.

[93] Sanes, J. R. and Hildebrand, J. G. "Origin and Morphogenesis of Sensory Neurons in an Insect Antenna". In: *Developmental Biology* 51.2 (1976), pp. 300–319. ISSN: 0012-1606. DOI: 10.1016/0012-1606(76)90145-7.

[94] Waku, Y. "Developmental Changes of the Antenna and Its Neurons in the Silkworm, *Bombyx Mori*, with Special Regard to Larval-Pupal Transformation". In: *J. Morphol.* 207.3 (1991), pp. 253–271. ISSN: 1097-4687. DOI: 10.1002/jmor.1052070304.

[95] Keil, T. A. and Steiner, C. "Morphogenesis of the Antenna of the Male Silkmoth, *Antheraea Polyphemus*. II. Differential Mitoses of 'Dark' Precursor Cells Create the Anlagen of Sensilla". In: *Tissue and Cell* 22.5 (1990), pp. 705–720. ISSN: 0040-8166. DOI: 10.1016/0040-8166(90)90066-i.

[96] Keil, T. A. and Steiner, C. "Morphogenesis of the Antenna of the Male Silkmoth. *Antheraea Polyphemus*, III. Development of Olfactory Sensilla and the Properties of Hair-Forming Cells". In: *Tissue and Cell* 23.6 (1991), pp. 821–851. ISSN: 0040-8166. DOI: 10.1016/0040-8166(91)90034-q.

[97] Keil, T. A. and Steiner, C. "Morphogenesis of the Antenna of the Male Silkmoth, *Antheraea Polyphemus*. I. The Leaf-Shaped Antenna of the Pupa from Diapause to Apolysis". In: *Tissue and Cell* 22.3 (1990), pp. 319–336. ISSN: 0040-8166. DOI: 10.1016/0040-8166(90)90007-v.

[98] Steiner, C. and Keil, T. A. "Morphogenesis of the Antenna of the Male Silkmoth, *Antheraea Polyphemus*. IV. Segmentation and Branch Formation". In: *Tissue and Cell* 25.3 (1993), pp. 447–464. ISSN: 0040-8166. DOI: 10.1016/0040-8166(93)90085-y.

[99] Steiner, C. and Keil, T. A. "Morphogenesis of the Antenna of the Male Silkmoth, *Antheraea Polyphemus*. VI. Experimental Disturbance of Antennal Branch Formation". In: *Tissue and Cell* 27.3 (1995), pp. 289–297. ISSN: 0040-8166. DOI: 10.1016/s0040-8166(95)80049-2.

[100] Steiner, C. and Keil, T. a. "Morphogenesis of the Antenna of the Male Silkmoth, *Antheraea Polyphemus*. V. Development of the Peripheral Nervous System". In: *Tissue and Cell* 27.3 (1995), pp. 275–288. ISSN: 0040-8166. DOI: 10.1016/s0040-8166(95)80048-4.

[101] Hähnlein, I. and Bicker, G. "Glial Patterning during Postembryonic Development of Central Neuropiles in the Brain of the Honeybee". In: *Dev Gene Evol* 207.1 (1997), pp. 29–41. ISSN: 1432-041X. DOI: 10.1007/s004270050089.

[102] Hoskins, S. G., Homberg, U., Kingan, T. G., Christensen, T. A., and Hildebrand, J. G. "Immunocytochemistry of GABA in the Antennal Lobes of the Sphinx Moth *Manduca Sexta*". In: *Cell Tissue Res.* 244.2 (1986), pp. 243–252. ISSN: 1432-0878. DOI: 10.1007/bf00219199.

[103] Python, F. and Stocker, R. F. "Adult-like Complexity of the Larval Antennal Lobe of *D. Melanogaster* despite Markedly Low Numbers of Odorant Receptor Neurons". In: *J. Comp. Neurol.* 445.4 (2002), pp. 374–387. ISSN: 1096-9861. DOI: 10.1002/cne.10188.

[104] Prillinger, L. "Postembryonic Development of the Antennal Lobes in *Periplaneta Americana* L." In: *Cell Tissue Res.* 215.3 (1981), pp. 563–575. ISSN: 1432-0878. DOI: 10.1007/bf00233532.

[105] Sengpiel, F. "The Critical Period". In: *Curr. Biol.* 17.17 (2007), R742–743. ISSN: 0960-9822. DOI: 10.1016/j.cub.2007.06.017.

[106] Stevens, C. F. and Wang, Y. "Changes in Reliability of Synaptic Function as a Mechanism for Plasticity". In: *Nature* 371.6499 (1994), pp. 704–707. ISSN: 0028-0836. DOI: 10.1038/371704a0.

[107] Cayre, M., Malaterre, J., Scotto-Lomassese, S., Strambi, C., and Strambi, A. "The Common Properties of Neurogenesis in the Adult Brain: From Invertebrates to Vertebrates". In: *Comp. Biochem. Physiol. B, Biochem. Mol. Biol.* 132.1 (2002), pp. 1–15. ISSN: 1096-4959. DOI: 10.1016/S1096-4959(01)00525-5.

[108] Cayre, M., Strambi, C., and Strambi, A. "Neurogenesis in an Adult Insect Brain and Its Hormonal Control". In: *Nature* 368.6466 (1994), pp. 57–59. ISSN: 0028-0836. DOI: 10.1038/368057a0.

[109] Dufour, M.-C. and Gadenne, C. "Adult Neurogenesis in a Moth Brain". In: *J. Comp. Neurol.* 495.5 (2006), pp. 635–643. ISSN: 0021-9967. DOI: 10.1002/cne.20909.

[110] Imayoshi, I., Sakamoto, M., Ohtsuka, T., Takao, K., Miyakawa, T., Yamaguchi, M., Mori, K., Ikeda, T., Itohara, S., and Kageyama, R. "Roles of Continuous Neurogenesis in the Structural and Functional Integrity of the Adult Forebrain". In: *Nat. Neurosci.* 11.10 (2008), pp. 1153–1161. ISSN: 1546-1726. DOI: 10.1038/nn.2185.

[111] Nissant, A., Bardy, C., Katagiri, H., Murray, K., and Lledo, P.-M. "Adult Neurogenesis Promotes Synaptic Plasticity in the Olfactory Bulb". In: *Nat. Neurosci.* 12.6 (2009), pp. 728–730. ISSN: 1546-1726. DOI: 10.1038/nn.2298.

[112] Sullivan, J. M., Benton, J. L., Sandeman, D. C., and Beltz, B. S. "Adult Neurogenesis: A Common Strategy across Diverse Species". In: *J. Comp. Neurol.* 500.3 (2007), pp. 574–584. ISSN: 0021-9967. DOI: 10.1002/cne.21187.

[113] Sullivan, J. M., Sandeman, D. C., Benton, J. L., and Beltz, B. S. "Adult Neurogenesis and Cell Cycle Regulation in the Crustacean Olfactory Pathway: From Glial Precursors to Differentiated Neurons". In: *J. Mol. Histol.* 38.6 (2007), pp. 527–542. ISSN: 1567-2379. DOI: 10.1007/s10735-007-9112-7.

[114] Dulcis, D., Jamshidi, P., Leutgeb, S., and Spitzer, N. C. "Neurotransmitter Switching in the Adult Brain Regulates Behavior". In: *Science* 340.6131 (2013), pp. 449–453. ISSN: 0036-8075. DOI: 10.1126/science.1234152.

[115] Banks, M. S., Aslin, R. N., and Letson, R. D. "Sensitive Period for the Development of Human Binocular Vision". In: *Science* 190.4215 (1975), pp. 675–677. ISSN: 0036-8075, 1095-9203. DOI: 10.1126/science.1188363.

[116] Desai, N. S., Cudmore, R. H., Nelson, S. B., and Turrigiano, G. G. "Critical Periods for Experience-Dependent Synaptic Scaling in Visual Cortex". In: *Nat. Neurosci.* 5.8 (2002), pp. 783–789. ISSN: 1546-1726. DOI: 10.1038/nn878.

[117] Fagiolini, M., Pizzorusso, T., Berardi, N., Domenici, L., and Maffei, L. "Functional Postnatal Development of the Rat Primary Visual Cortex and the Role of Visual Experience: Dark Rearing and Monocular Deprivation". In: *Vision Research* 34.6 (1994), pp. 709–720. ISSN: 0042-6989. DOI: 10.1016/0042-6989(94)90210-0.

[118] Harwerth, R. S., Smith, E. L., Duncan, G. C., Crawford, M. L., and Noorden, G. von. "Multiple Sensitive Periods in the Development of the Primate Visual System". In: *Science* 232.4747 (1986), pp. 235–238. ISSN: 0036-8075, 1095-9203. DOI: 10.1126/science.3952507.

[119] Hooks, B. M. and Chen, C. "Critical Periods in the Visual System: Changing Views for a Model of Experience-Dependent Plasticity". In: *Neuron* 56.2 (2007), pp. 312–326. ISSN: 0896-6273. DOI: 10.1016/j.neuron.2007.10.003.

[120] Huang, Z. J., Kirkwood, A., Pizzorusso, T., Porciatti, V., Morales, B., Bear, M. F., Maffei, L., and Tonegawa, S. "BDNF Regulates the Maturation of Inhibition and the Critical Period of Plasticity in Mouse Visual Cortex". In: *Cell* 98.6 (1999), pp. 739–755. ISSN: 0092-8674. DOI: 10.1016/s0092-8674(00)81509-3.

[121] Hubel, D. H. and Wiesel, T. N. "The Period of Susceptibility to the Physiological Effects of Unilateral Eye Closure in Kittens". In: *J Physiol* 206.2 (1970), pp. 419–436. ISSN: 0022-3751. DOI: 10.1113/jphysiol.1970.sp009022.

[122] Issa, N. P., Trachtenberg, J. T., Chapman, B., Zahs, K. R., and Stryker, M. P. "The Critical Period for Ocular Dominance Plasticity in the Ferret's Visual Cortex". In: *J. Neurosci.* 19.16 (1999), pp. 6965–6978. ISSN: 0270-6474, 1529-2401. DOI: 10.1523/jneurosci.19-16-06965.1999.

[123] Olson, C. R. and Freeman, R. D. "Profile of the Sensitive Period for Monocular Deprivation in Kittens". In: *Exp Brain Res* 39.1 (1980), pp. 17–21. ISSN: 1432-1106. DOI: 10.1007/bf00237065.

[124] Goldman, S. A. and Nottebohm, F. "Neuronal Production, Migration, and Differentiation in a Vocal Control Nucleus of the Adult Female Canary Brain". In: *Proc. Natl. Acad. Sci. U.S.A.* 80.8 (1983), pp. 2390–2394. ISSN: 0027-8424. DOI: 10.1073/pnas.80.8.2390.

[125] Leppelsack, H.-J. "Critical Periods in Bird Song Learning". In: *Acta Otolaryngol. (Stockh.)* 101 (sup429 1986), pp. 57–60. ISSN: 0001-6489, 1651-2251. DOI: 10.3109/00016488609122731.

[126] Nottebohm, F. "The "Critical Period" for Song Learning". In: *IBIS* 111.3 (1969), pp. 386–387. ISSN: 1474-919X. DOI: 10.1111/j.1474-919x.1969.tb02551.x.

[127] Barth, M., Hirsch, H. V., Meinertzhagen, I. A., and Heisenberg, M. "Experience-Dependent Developmental Plasticity in the Optic Lobe of *Drosophila Melanogaster*". In: *J. Neurosci.* 17.4 (1997), pp. 1493–1504. ISSN: 0270-6474. DOI: 10.1523/JNEUROSCI.17-04-01493.1997.

[128] Doll, C. A. and Broadie, K. "Activity-Dependent FMRP Requirements in Development of the Neural Circuitry of Learning and Memory". In: *Development* 142.7 (2015), pp. 1346–1356. ISSN: 0950-1991, 1477-9129. DOI: 10.1242/dev.117127.

[129] Golovin, R. M., Vest, J., Vita, D. J., and Broadie, K. "Activity-Dependent Remodeling of *Drosophila* Olfactory Sensory Neuron Brain Innervation During an Early-Life Critical Period". In: *J. Neurosci.* (2019), pp. 2223–18. ISSN: 0270-6474, 1529-2401. DOI: 10.1523/jneurosci.2223-18.2019.

[130] Sachse, S., Rueckert, E., Keller, A., Okada, R., Tanaka, N. K., Ito, K., and Vosshall, L. B. "Activity-Dependent Plasticity in an Olfactory Circuit". In: *Neuron* 56.5 (2007), pp. 838–850. ISSN: 08966273. DOI: 10.1016/j.neuron.2007.10.035.

[131] Tessier, C. R. and Broadie, K. "Activity-Dependent Modulation of Neural Circuit Synaptic Connectivity". In: *Front. Mol. Neurosci.* 2 (2009), p. 8. ISSN: 1662-5099. DOI: 10.3389/neuro.02.008.2009.

[132] Devaud, J.-M., Acebes, A., Ramaswami, M., and Ferrús, A. "Structural and Functional Changes in the Olfactory Pathway of Adult *Drosophila* Take Place at a Critical Age". In: *Journal of Neurobiology* 56.1 (2003), pp. 13–23. ISSN: 0022-3034. DOI: 10.1002/neu.10215.

[133] Doll, C. A. and Broadie, K. "Neuron Class-Specific Requirements for Fragile X Mental Retardation Protein in Critical Period Development of Calcium Signaling in Learning and Memory Circuitry". In: *Neurobiology of Disease* 89 (2016), pp. 76–87. ISSN: 0969-9961. DOI: 10.1016/j.nbd.2016.02.006.

[134] Doll, C. A., Vita, D. J., and Broadie, K. "Fragile X Mental Retardation Protein Requirements in Activity-Dependent Critical Period Neural Circuit Refinement". In: *Current Biology* 27.15 (2017), 2318–2330.e3. ISSN: 0960-9822. DOI: 10.1016/j.cub.2017.06.046.

[135] Heisenberg, M., Borst, A., Wagner, S., and Byers, D. "*Drosophila* Mushroom Body Mutants Are Deficient in Olfactory Learning". In: *J. Neurogenet.* 2.1 (1985), pp. 1–30. ISSN: 0167-7063. DOI: 10.3109/01677068509100140.

[136] Cabirol, A., Cope, A. J., Barron, A. B., and Devaud, J.-M. "Relationship between Brain Plasticity, Learning and Foraging Performance in Honey Bees". In: *PLoS ONE* 13.4 (2018), e0196749. ISSN: 1932-6203. DOI: 10.1371/journal.pone.0196749.

[137] Fahrbach, S. E. and Van Nest, B. N. "Synapsin-Based Approaches to Brain Plasticity in Adult Social Insects". In: *Curr. Opin. Insect Sci.* Neuroscience * Special Section on Insect Phylogenetics 18 (2016), pp. 27–34. ISSN: 2214-5745. DOI: 10.1016/j.cois.2016.08.009.

[138] Falibene, A., Roces, F., and Rössler, W. "Long-Term Avoidance Memory Formation Is Associated with a Transient Increase in Mushroom Body Synaptic Complexes in Leaf-Cutting Ants". In: *Front. Behav. Neurosci.* 9 (2015), p. 84. ISSN: 1662-5153. DOI: 10.3389/fnbeh.2015.00084.

[139] Groh, C., Lu, Z., Meinertzhagen, I. A., and Rössler, W. "Age-Related Plasticity in the Synaptic Ultrastructure of Neurons in the Mushroom Body Calyx of the Adult Honeybee *Apis Mellifera*". In: *J. Comp. Neurol.* 520.15 (2012), pp. 3509–3527. ISSN: 1096-9861. DOI: 10.1002/cne.23102.

[140] Groh, C. and Rössler, W. "Comparison of Microglomerular Structures in the Mushroom Body Calyx of Neopteran Insects". In: *Arthropod. Struct. Dev.* 40.4 (2011), pp. 358–367. ISSN: 14678039. DOI: 10.1016/j.asd.2010.12.002.

[141] Hige, T., Aso, Y., Modi, M. N., Rubin, G. M., and Turner, G. C. "Heterosynaptic Plasticity Underlies Aversive Olfactory Learning in *Drosophila*". In: *Neuron* 88.5 (2015), pp. 985–998. ISSN: 0896-6273. DOI: 10.1016/j.neuron.2015.11.003.

[142] Hige, T., Aso, Y., Rubin, G. M., and Turner, G. C. "Plasticity-Driven Individualization of Olfactory Coding in Mushroom Body Output Neurons". In: *Nature* 526.7572 (2015), pp. 258–262. ISSN: 0028-0836. DOI: 10.1038/nature15396.

[143] Muenz, T. S., Groh, C., Maisonnasse, A., Le Conte, Y., Plettner, E., and Rossler, W. "Neuronal Plasticity in the Mushroom Body Calyx during Adult Maturation in the Honeybee and Possible Pheromonal Influences". In: *Dev. Neurobiol.* 75.12 (2015), pp. 1368–1384. ISSN: 1932-846X. DOI: 10.1002/dneu.22290.

[144] Strube-Bloss, M. F., Nawrot, M. P., and Menzel, R. "Neural Correlates of Side-Specific Odour Memory in Mushroom Body Output Neurons". In: *Proc. Biol. Sci.* 283.1844 (2016), p. 20161270. ISSN: 1471-2954. DOI: 10.1098/rspb.2016.1270.

[145] Fahrbach, S. E., Strande, J. L., and Robinson, G. E. "Neurogenesis Is Absent in the Brains of Adult Honey Bees and Does Not Explain Behavioral Neuroplasticity". In: *Neurosci. Lett.* 197.2 (1995), pp. 145–148. ISSN: 0304-3940. DOI: 10.1016/0304-3940(95)11913-H.

[146] Trotha, J. W., Egger, B., and Brand, A. H. "Cell Proliferation in the *Drosophila* Adult Brain Revealed by Clonal Analysis and Bromodeoxyuridine Labelling". In: *Neural Dev.* 4 (2009), p. 9. ISSN: 1749-8104. DOI: 10.1186/1749-8104-4-9.

[147] Cayre, M., Strambi, C., Charpin, P., Augier, R., Meyer, M. R., Edwards, J. S., and Strambi, A. "Neurogenesis in Adult Insect Mushroom Bodies". In: *J. Comp. Neurol.* 371.2 (1996), pp. 300–310. ISSN: 0021-9967. DOI: 10.1002/(SICI)1096-9861(19960722)371:2<300::AID-CNE9>3.0.CO;2-6.

[148] Zhao, C., Deng, W., and Gage, F. H. "Mechanisms and Functional Implications of Adult Neurogenesis". In: *Cell* 132.4 (2008), pp. 645–660. ISSN: 0092-8674. DOI: 10.1016/j.cell.2008.01.033.

Part II

Publications and Manuscripts

3

Adult neurogenesis in the mushroom bodies

www.nature.com/scientificreports

SCIENTIFIC REPORTS
nature research

OPEN

Adult neurogenesis in the mushroom bodies of red flour beetles (*Tribolium castaneum*, Herbst) is influenced by the olfactory environment

Björn Trebels[1], Stefan Dippel[1], Magdalina Schaaf[1], Karthi Balakrishnan[2], Ernst A. Wimmer[3] & Joachim Schachtner[1,4*]

Several studies showed adult persisting neurogenesis in insects, including the red flour beetle *Tribolium castaneum*, while it is absent in honeybees, carpenter ants, and vinegar flies. In our study, we focus on cell proliferation in the adult mushroom bodies of *T. castaneum*. We reliably labelled the progenies of the adult persisting mushroom body neuroblasts and determined the proliferation rate under several olfactory conditions within the first week after adult eclosion. We found at least two phases of Kenyon cell proliferation in the early adult beetle. Our results suggest that the generation of Kenyon cells during the first three days after adult eclosion is mainly genetically predetermined and a continuation of the developmental processes (nature), whereas from day four on proliferation seems to be mainly dependent on the odour environment (nurture). Considering that the mushroom bodies are linked to learning and memory, neurogenesis in the mushroom bodies is part of the remodelling of neuronal circuits leading to the adaption to the environment and optimization of behaviour.

The ground pattern of the central nervous system is genetically encoded. Following development, when the nervous system first encounters environmental sensory input, it is crucial for the survival of an animal to adapt to the actual conditions and cues. Therefore, the genetically encoded wiring scheme of the nervous system must be altered. This plasticity typically occurs in special time windows of elevated susceptibility to sensory input (critical periods or sensitive phases)[1].

The research on critical periods has mainly focused on vertebrates, where critical periods were among others found during the postnatal development of the visual system[2–10] and song learning in birds[11–13]. However, several studies demonstrated the existence of critical periods also in insects[14–19], with many focusing on the plasticity of the olfactory system in the vinegar fly *Drosophila melanogaster*[15,17–22].

Many insects rely on their olfactory systems to accomplish various tasks, such as the localization of food sources, mating partners, and suitable habitats. The adult olfactory system of holometabolous insects is first confronted with environmental cues upon adult eclosion. These olfactory cues are mainly detected by the olfactory sensory neurons (OSN) housed in the chemosensory sensilla of the antennae and palps[23–26]. From there the information is relayed into the primary olfactory processing centres[27–29] and further projected to the mushroom bodies (MB) and the lateral horn[26,28–30], with the former being linked to olfactory learning and memory[31–45].

Studies in adult holometabolous insects, including *Apis mellifera* and *D. melanogaster*, described synaptic plasticity, but no neurogenesis, in the mushroom bodies[36,46–55]. Since adult neurogenesis in the mushroom bodies was first described in the hemimetabolous house cricket *Acheta domestica*[56,57], it has also been found in

[1]Philipps-University Marburg, Department of Biology, Animal Physiology, Karl-von-Frisch-Str. 8, 35032, Marburg, Germany. [2]Department of Forest Zoology and Forest Conservation, Georg-August-University Göttingen, Büsgen-Institute, Büsgenweg 3, Göttingen, 37077, Germany. [3]Department of Developmental Biology, Georg-August-University Göttingen, Johann-Friedrich-Blumenbach-Institute for Zoology and Anthropology, GZMB, Ernst-Caspari-Haus, Justus-von-Liebig-Weg 11, Göttingen, 37077, Germany. [4]Clausthal University of Technology, Adolph-Roemer-Str. 2a, 38678, Clausthal-Zellerfeld, Germany. *email: joachim.schachtner@tu-clausthal.de

www.nature.com/scientificreports/

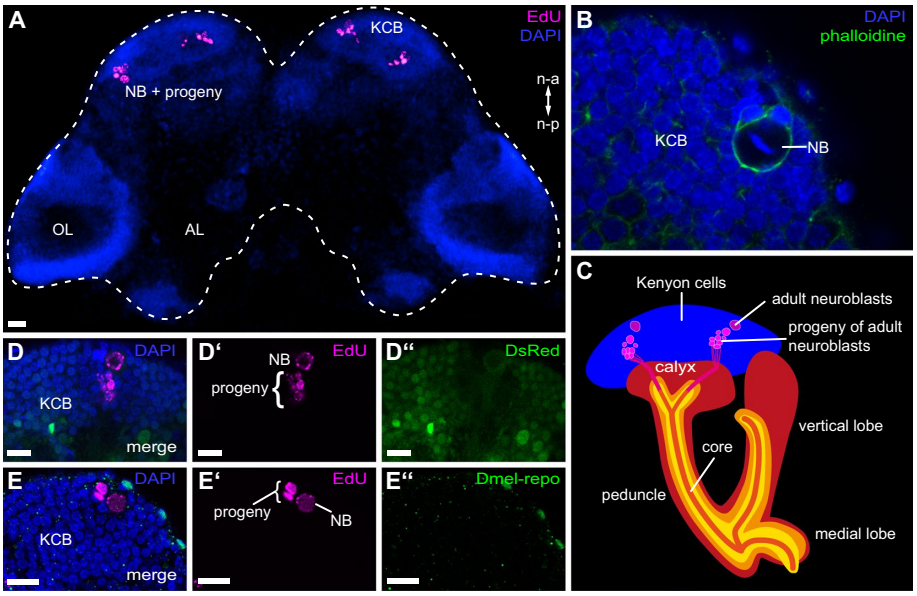

Figure 1. Localization and identification of the adult-born cells as Kenyon cells. (**A**) Volume rendering of an exemplary wholemount preparation showing the location of the adult-born neurons. Nuclei visualized with DAPI are depicted in blue, while the neuroblasts (NB) and their progeny marked by EdU are depicted in magenta. OL: optic lobes; AL: antennal lobe; KCB: cell bodies of Kenyon cells; n-a: neural axis anterior; n-p: neural axis posterior (**B**) Single confocal section showing an MB neuroblast (NB), which can be identified by its larger diameter compared to the surrounding Kenyon cells (KCB). The f-actin of the cytoskeleton is marked by phalloidin (green) and cell nuclei by DAPI (blue). (**C**) Schematic of the adult-born Kenyon cells and their integration into the mushroom bodies. They derive from usually two distinct neuroblasts per hemisphere and send their axons into the core of the mushroom body lobes as shown by Zhao and colleagues[60].(**D**-D") Single confocal slice showing colocalization between the EdU marked cells (neuroblasts [NB] and their progeny) and the DsRed reporter signal in the neuron marking transgenic EF1-B-DsRed line[77]. (**E**-E") Single confocal slice showing EdU marked cells (neuroblasts [NB] and their progeny) and immunohistochemistry against the glia cell marker reversed polarity (anti-repo)[78] in the San Bernadino wildtype strain. A colocalization cannot be identified.

holometabolous insects, such as the noctuid moth *Agrotis ipsilon*[58], as well as several beetle species[59] including the red flour beetle *Tribolium castaneum*[60].

T. castaneum is a member of the largest insect order (Coleoptera)[61,62] and a major pest of stored cereal products[61,63,64]. With its annotated genome sequence[26,65–67], an expanding genetic toolbox[68–70] including strong systemic RNA interference (RNAi)[71–73], and its relative longevity of up to two years[74], *T. castaneum* represents an eligible beetle model for studying adult plasticity.

We concentrated on olfaction which is supposed to be a main input into the mushroom bodies of *T. castaneum*[26], to answer whether the adult persisting neurogenesis is genetically predetermined and continuation of developmental processes or if it is activity-dependent.

Results

Identification of newly born cells. To label adult-born cells, we used the 5-ethynyl-2′-desoxyuridine (EdU) method[75,76]. With this method, we reliably and exclusively labelled the mushroom body neuroblasts and their progeny, while neurogenesis is not present in other areas of the cerebral ganglion of the red flour beetle (Fig. 1A). The neuroblasts were distinguished from their progeny based on their larger size (Fig. 1B).

We confirmed that in *T. castaneum*, adult-born Kenyon cells usually derive from two neuroblasts (NB) per hemisphere and send their axons into the core of the mushroom body peduncle (PED) and lobes as shown by Zhao and colleagues[60] (Fig. 1C).

The neuronal identity of the EdU labelled cells was verified by demonstrating co-localization with the reporter signal (Fig. 1D-D") in the neuron labelling EF1-B-DsRed line[77], as well as immunohistochemical staining against the glia cell marker reversed polarity[78] resulting in no co-localization (Fig. 1E-E").

Environmental conditions influence adult neurogenesis. The proliferation rates of the mushroom body neuroblasts during the first week after adult eclosion were analysed on a day-to-day basis (Fig. 2). A statistical comparison using Kruskal-Wallis test between both sexes showed no major intersexual difference in the number of newly born Kenyon cells, deriving from a single neuroblast (Supplemental Table 1). Thus, for

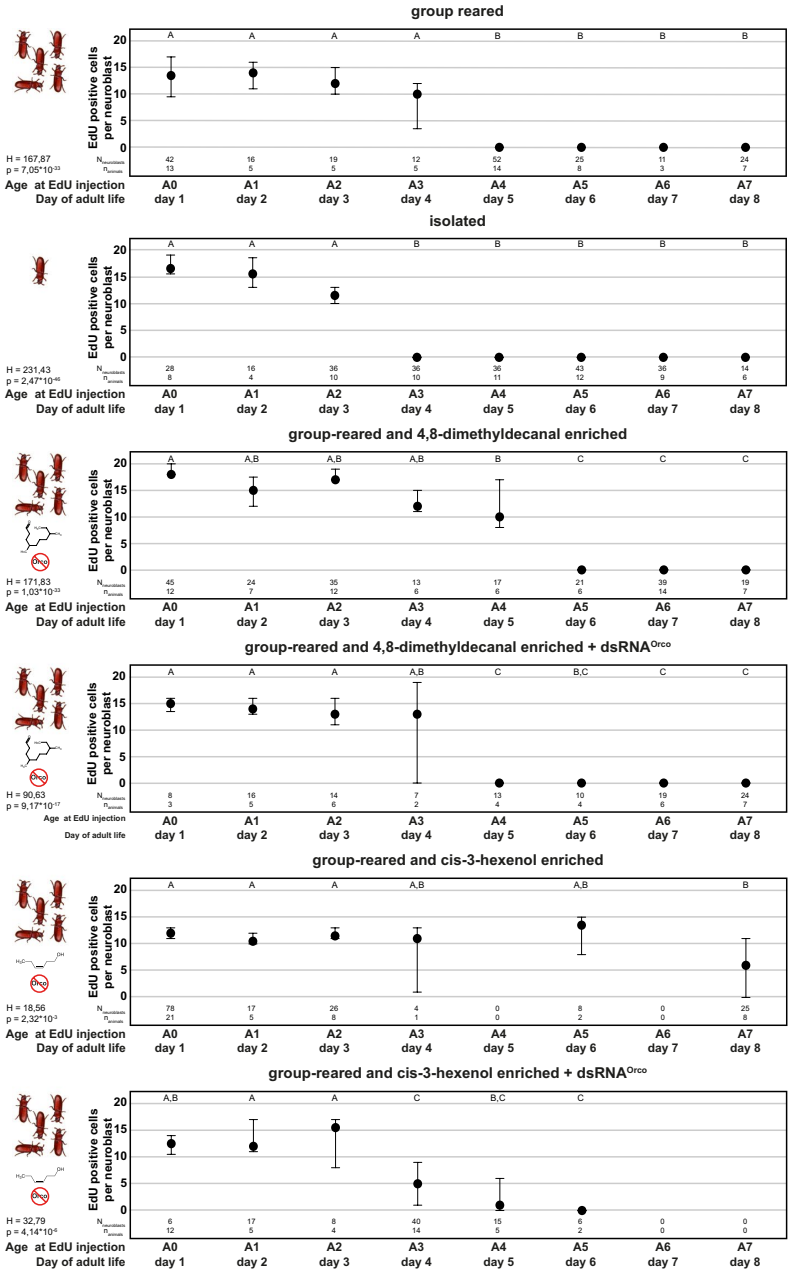

Figure 2. Kenyon cell proliferation in adult beetles under different conditions. Median numbers of EdU positive (adult-born) Kenyon cells per neuroblasts within 24 hours after EdU injection. Sample sizes for each group (analysed neuroblasts [N] and animals[n]) are given in the respective column of the plot. The circles represent the median, while the error bars represent the 95% confidence interval of the median equivalent to the standard error calculated by bootstrap analysis. Kruskal Wallis test with posthoc analysis using Dunns' multiple comparison test was used to compare the cell number over the different injection times within one experimental group. The results of the Kruskal Wallis test [test statistics corrected for ties (H), p-value (p)] for each condition is given in the figure. Same capital letters indicate groups with no significant difference to each other as obtained by Dunn's posthoc analysis ($p > 0.05$, Holm-corrected). The actual p-values of the post-hoc test are listed in Supplementary Table S2. Original photo of the beetle by Peggy Greb, USDA Agricultural Research Service (ID: D268-1).

all further analysis, both sexes were pooled. Testing for no variation between conditions and ages by means of Scheirer-Ray-Hare test resulted in rejection of the null hypothesis (olfactory conditions: $H = 114.899$, $p = 0.0$; ages; $H = 655.154$, $p = 0.0$; overall: $H = 231.580$, $p = 0.0$). Further, per condition Kruskal-Wallis analysis between ages showed significant differences between cell numbers at different days, which were further analysed by post-hoc analysis using Dunn's multiple comparison test (Fig. 2).

For enrichment of the olfactory environment we chose the beetles' aggregation pheromone 4,8-dimethyldecanal (DMD)[79] and the food-related green-leaf volatile cis-3-hexenol as both are known to elicit antennal responses in EAG recordings[80] and at least DMD causing a clear OR/Orco (TcOR1) dependent behavioural response[81].

The mushroom body neuroblasts of beetles reared in mixed-sex groups of 20 individuals generate new Kenyon cells within the first four days after adult eclosion. During the first three days of the proliferation phase, the median daily proliferation rate of each neuroblast is 10 to 15 cells, with a reduction on day four (Figs. 2, S1). At day 5 the proliferation rate drops significantly and afterwards no neurogenesis is detectable.

Isolating beetles as pupae lead to a proliferation phase lasting three days after adult eclosion. During this proliferation phase, each neuroblast gives rise to about 10 to 20 cells per day, decreasing on day three and significantly dropping at day four before from day five onwards no neurogenesis is detectable.

Enriching the environment of group-reared beetles with DMD leads to a prolonged proliferation phase of five days. During the first three days of the proliferation phase, the median daily proliferation rate of each neuroblast equals to about 15 to 20 cells, with slight decrease on days four and five. At day 6 the proliferation rate drops significantly and afterwards no neurogenesis is detectable.

Stimulating olfactory-deprived (pupal dsRNA^{orco} injection) group-reared beetles with DMD leads to a proliferation phase lasting four days after adult eclosion. During the first four days each neuroblast's median daily proliferation rate is 10 to 15 cells, with a high variation on day four (Figs. 2, S1). At day 5 the proliferation rate drops significantly and afterwards no neurogenesis is detectable.

Stimulation of group-reared beetles with cis-3-hexenol results in mushroom body neuroblasts generating new Kenyon cells during the first six days after adult eclosion with a median rate of 10 to 15 cells per day, decreasing to about 5 cells at day 8.

Stimulating olfactory-deprived (pupal dsRNA^{orco} injection) group-reared beetles with cis-3-hexenol leads to a proliferation phase lasting four days after adult eclosion. During the first three days of the proliferation phase, the daily proliferation rate per is 10 to about 15 cells, with a significant reduction on day four (Figs. 2, S1) before dropping to zero at day 6.

Antennal responses to cis-3-hexenol and 4,8-dimethyldecanal. Electroantennographical recordings (EAG) were used to demonstrate that beetles with an RNAi-mediated systemic knockdown of Orco (dsRNA^{orco}, test group) differ in their response to the tested odours, compared to beetles injected with sham (DsRed) dsRNA (dsRNA^{sham}, control group).

Stimulation with the three lowest tested concentrations ($10^{-8} - 10^{-6}$) of the beetle's aggregation pheromone DMD leads to no obvious reaction of the antennae (Fig. 3, 4,8-dimethyldecanal; Supplemental Figs. S2 and S3). Starting with a dilution of 10^{-5}, a dose-dependent reaction of the antennae is visible in dsRNA^{sham} injected beetles, but not in beetles injected with dsRNA^{orco}.

Stimulation with the five lowest tested concentrations ($10^{-8} - 10^{-4}$) of the food volatile cis-3-hexenol leads to no obvious responses. Stimulating with a dilution of 10^{-3} causes a slight response in the control group only. Whereas, at the highest tested concentration (10^{-2}) both groups respond (Fig. 3, cis-3-hexenol; Supplemental Figs. S2 and S3), but the peak response of the control group is significantly higher compared to the test group (Fig. 3, cis-3-hexenol). Furthermore, the response onset in the *orco* knock-down is delayed (Supplemental Fig. S2).

Discussion

Neurogenesis in adult brains is present to varying extents throughout invertebrates and vertebrates[57,82–89]. Several studies showed adult neurogenesis in the mushroom bodies of hemimetabolous and ametabolous insects such as crickets[56], cockroaches[90], and firebrats[91,92]. In holometabolous insects persisting adult neurogenesis in the mushroom bodies was described in the black cutworm *Agrotis ipsilon*[58] and several beetles, including the red flour beetle *T. castaneum*[59,60], while it is absent in the mushroom bodies of the honeybee *A. mellifera*[54], the carpenter ant *Camponotus floridanus*[34], and the vinegar fly *D. melanogaster*[55].

Localization of adult neurogenesis in the mushroom bodies using 5-bromo-2′-deoxyuridine (BrdU) as published for the red flour beetle by Zhao and colleagues[60] gave no reliable results in our hands and was not useful for the comparison of larger experimental groups needed for the current study. Instead, we successfully and reliably labelled mushroom body neuroblasts and their progeny using the EdU method[75,76]. Like BrdU, EdU is a thymidine analogue that is incorporated into the DNA during replication. The major advantage compared to BrdU is the labelling procedure. While BrdU is localized via immunohistochemistry and therefore requiring the DNA to be denaturized to allow binding of the antibody, EdU is labelled by selective direct chemical coupling with an azide-fluorochrome. Avoiding denaturation of the DNA with HCl provides improved overall tissue preservation. By using this reliable labelling method for newly born neurons and their neuroblasts (Fig. 1) we studied the generation of new Kenyon cells in the early adulthood of the red flour beetle *T. castaneum* under different conditions (Figs. 2, S1) to answer whether this adult neurogenesis depends on olfactory input and if there is a critical period. The activity-dependent remodelling of neuronal circuits during critical periods leads to the adaption to the environment and optimization of behaviour[93]. Previous studies in *A. mellifera* and *D. melanogaster* showed that critical periods during which the mushroom body circuitry is remodelled exist in holometabolous insects and that the underlying mechanisms are the refinement of old as well as the growth of new synapses[48–52,54], but

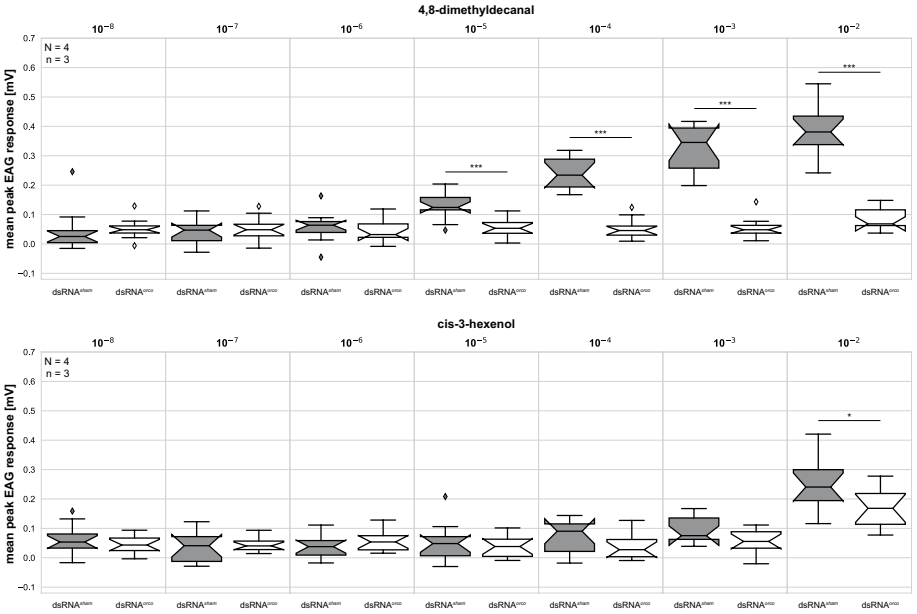

Figure 3. Peak amplitude EAG responses to 4,8-dimethyldecanal and cis-3-hexenol. Box plots with whiskers representing the 5–95% percentile of the peak amplitude EAG response after robust LOESS smoothing and normalization (subtraction of the response to silicone oil, which was used as solvent) to 4,8-dimethyldecanal (DMD) and cis-3-hexenol. Sample sizes are given in the respective subplots. [N] represents the number of animals, while [n] represents the number of replicates per animal. Notches indicate the 95% confidence interval of the median. The bar represents the 25–75 percentile, the line represents the median and the diamonds represent data points outside the 5–95% range. Statistical analysis between dsRNA^{sham} and dsRNA^{orco} was performed per odour dilution by Kruskal Wallis test. Statistical significance levels of difference in median are represented by asterisks (*$p < 0.05$, **$p < 0.01$, ***$p < 0.001$).

not neurogenesis[54,55]. The adult olfactory system of the beetle is first confronted with odour cues directly after adult eclosion.

Rearing beetles in groups of 20 animals of both sexes leads to the generation of new Kenyon cells during the first four days after adult eclosion. This phase is shortened in isolated beetles by one day and prolonged by additional olfactory stimulation. Enriching the olfactory environment of group-reared beetles with the beetles' aggregation pheromone DMD[79] prolongs the proliferation phase by one day, while stimulation with the food odour cis-3-hexenol leads to a prolongation of the proliferation phase for at least four days. This prolonging effect is mostly inhibited in beetles with a significantly reduced perception of the tested odorants (Fig. 3, dsRNA^{orco}), generated by RNAi mediated knockdown of *orco*.

A study in crickets already demonstrated that sensory deprivation by isolation results in significantly less neurogenesis among the Kenyon cells of young females, compared to group-reared females[82]. A second study based on these results asked what proportion of neurogenesis is caused by visual and olfactory stimuli[83] and demonstrated that olfactory and visual deprivation is sufficient to decrease neurogenesis in adult crickets, regardless whether reared in groups or isolation. This clearly showed a link between sensory input and adult neurogenesis.

In our study, we used a day-to-day analysis of adult neurogenesis together with the specific manipulation of the Orco dependent olfactory sensory neurons. This allowed us to temporally dissect adult neurogenesis into distinct phases and link them to olfactory activity.

Similarly to the results from crickets[82], our data suggest that isolation reduces adult neurogenesis. We were able to demonstrate that this reduction is based on a shortened proliferation phase rather than an altered proliferation rate.

It seems that the generation of Kenyon cells during the first three days after adult eclosion is mainly genetically predetermined and a continuation of developmental processes rather than depending on sensory activity.

The shorter proliferation phase in isolated beetles compared to group-reared beetles suggest an influence of social interactions. This is supported by the fact that the proliferation phase after *orco* knock-down in odour stimulated beetles is still longer than in isolated beetles. Since the beetles were kept under constant darkness, visual stimulation can be excluded, making tactile and gustatory cues the most likely triggers. This is partially in accordance with findings in crickets, were unilateral removal of the antennae, causing the loss of chemosensory as well as mechanosensory antennal input in the ipsilateral hemisphere, lead to less adult neurogenesis in the ipsilateral hemisphere[83].

The significant differences in the proliferation rate within the first three days might indicate an influence of odour stimulation. However, as the results for DMD and cis-3-hexenol are contradicting, we conclude that these differences are very likely artificial.

However, the main and most striking effect of DMD stimulation is the prolongation of the proliferation phase compared to group-reared beetles, which is not present in dsRNA^{orco} injected beetles. Since after a RNAi mediated knockdown of *orco* the EAG response towards DMD is significantly reduced (Fig. 3) and no longer measurable (Supplemental Fig. S2) and the behavioural response towards DMD is abolished[81], the prolongation is olfactory induced and driven via activity of the OR/Orco complex.

Interestingly, the potential for a longer capacity of the MB system to produce new Kenyon cells seems to depend on the odour, as the stimulation with the food-related odour cis-3-hexenol leads to a longer proliferation phase when compared to DMD stimulation, with cis-3-hexenol causing an increased proliferation rate even at day eight. This seems to contradict the EAG data that suggest a higher sensitivity towards DMD. However, the lack of responses to cis-3-hexenol at lower concentrations does not necessarily mean that it is not perceived, as the recorded response likely depends on the localisation of the OSNs relative to the recording electrode[94].

This longer proliferation phase is massively shortened in dsRNA^{orco} injected beetles, clearly demonstrating that this effect is most likely olfactory but not solely driven via the activity of the OR/Orco complex. While after knockdown of *orco*, the EAG responses to DMD are fully abolished, the EAG responses to cis-3-hexenol show a significantly lower, but still exiting reaction (Fig. 3) with a delayed response onset (Supplemental Fig. S2), which suggests the involvement of another receptor type. As Getahun and colleagues[95] already described in *D. melanogaster* the best candidates with slower responses are the ionotropic glutamate-like receptors (IR)[26].

The different effects of DMD and cis-3-hexenol on the duration of the proliferation phase (five vs. eight days) might be explained already on the receptor level, as IRs, unlike ORs, do not exhibit adaptation to longer stimulations[95]. This could mean that continued exposure to high DMD concentration leads to a desensitisation of the OR/Orco complex, causing the shorter proliferation phase. Whereas, the response to cis-3-hexenol seemingly also perceived by IRs persists longer. Furthermore, there is the possibility of different pheromone vs. normal odour processing networks in the antennal lobes that provide the input to the MB as shown among others in *Manduca sexta*[96], *D. melanogaster*[97], and *A. mellifera*[98]. However, so far, such separate olfactory processing networks were not described in the red flour beetle and it remains unclear whether they exist.

The EAG responses showed that the reaction of both odorants is significantly reduced in adult female beetles seven days after dsRNA^{orco} injection, corresponding roughly to A4. Besides, we performed immunohistochemical staining against Orco in freshly eclosed (A0) and seven days old beetles (A7) using the cross-reactive Moth-R2 antiserum[26]. This resulted in no immunoreactivity after pupal injection of dsRNA^{orco} (Supplemental Fig. S4) demonstrating the effectivity of the RNAi within the studied ages. Furthermore, the RNAi effect in *T. castaneum* has already been published to last from weeks to months[99].

T. castaneum has a life span of up to two years[74] and studies on the origin of the beetle[63] together with a large variety of odorant receptors[26,81] suggest a broad spectrum of potential food sources, which may change over time. Adapting the MB neuronal network via newly born cells could be part of the strategy to cope with ongoing environmental changes. The process might be triggered by changes in the OR repertoire in response to the environmental changes, as speculated by Dippel and colleagues[26]. This could explain why Zhao *et al.*[60]. occasionally found neurogenesis in 88 days old beetles without stimulation. The involvement of adult proliferation in behavioural adaption to the changing odorant environment has already been suggested in crickets[82,83]. In analogy, a study on the mouse hippocampus demonstrated that adult neurogenesis is not triggered by continued long-term exposure to enriched environments, but by novel complex stimuli[100].

Considering that the mushroom bodies are linked to learning and memory[39], adult neurogenesis might contribute to the formation of new odorant memories. As Zhao and colleagues demonstrated, the adult-born Keyon cells send their axons into the core of the mushroom bodies[60], which were shown to be involved in differential olfactory learning in *D. melanogaster*[101,102]. Suppression of adult neurogenesis in crickets leads to a significant impairment in olfactory learning and memory[44], undermining the role of adult-born neurons in learning and memory. Furthermore, studies in vertebrates show that olfactory enrichment leads to increased neurogenesis in the hippocampus and plays a role in olfactory learning[103–106].

Methods

Animals. Red flour beetles (*Tribolium castaneum*, Herbst 1797; Insecta, Coleoptera) of the wild-type strains "San Bernadino"[107] and *"black"*[108], as well as the neuron labelling[26,77] transgenic line EF1-B-DsRed (elongation factor1-alpha regulatory region-DsRedExpress; kindly provided by Michalis Averof, Institut de Génomique Fonctionnelle de Lyon, France) were used. The beetles were bred under constant darkness at about 28 °C and 40–50% relative humidity on organic whole grain wheat flour supplemented with 5% dried yeast powder and 0.05% Fumagilin-B (Medivet Pharmaceuticals Ltd., High River, Alberta, Canada) to prevent sporozoan infections[109]. For age determination, freshly eclosed beetles (A0) were collected and kept in mixed-sex groups of 20 in 68 ml *Drosophila* vials on about 20 g substrate.

For isolation experiments, individuals were separated as pupae into 5 ml glass vials on about 2 g substrate.

EdU injections. Cold anaesthetized beetles were mounted ventral-up on microscope slides using double-faced adhesive tape and were subsequently injected with about 1 µl 5-ethynyl-2′-desoxyuridine (EdU) solution (100 µM EdU in injection buffer: 1.4 mM NaCl, 0.07 mM Na_2HPO_4, 0.03 mM KH_2PO_4, 4 mM KCL, and 5% phenol red). Injection was performed with glass micropipettes made from thin-walled glass capillaries (TW150-4, World Precision Instruments, Sarasota, FL, USA; micropipette puller: Sutter Model P-30, Sutter Instrument, Novato, CA, USA) attached to a pressure ejection system (PDES-02T; npi electronics, Tamm,

Name	Abbreviation	Host species	Dilution	Used to label	Vendor/Donor (catalogue #, batch #, RRID/CAS #)	References/ Specificity
4′,6-diamidin-2-phenylindol	DAPI		1:20,000	Cell nuclei (DNA)	Sigma Aldrich, Steinheim, Germany (D9542, n/a, 28718-90-3)	120
5-ethynyl-2′-desoxyuridine	EdU		100 µM	newly born cells (newly synthesized DNA)	Thermo Fischer Scientific, Rockford, IL, USA (A10044; 1259424; 61135-33-9)	75,76
Alexa Flour 488 coupled phalloidine	Phalloidin		1:200	Ubiquitous neuroanatomy (F-Actin)	Thermo Fischer Scientific, Rockford, IL, USA (A12379; n/a; n/a)	121
Alexa Flour 488 Azide	488-azide		1 µM	5-ethynyl-2′-desoxuridine	Thermo Fischer Scientific, Rockford, IL, USA (A10260; 1320994; n/a)	
Anti-*Drosophila melanogaster* reversed polarity (4α3)	anti-repo	Rabbit	1:5,000	Glia cells	B. Altenhain, University of Mainz, Germany (n/a; n/a; n/a)	78,122
Anti-Red fluorescent protein	RFP	Chicken	1:3,000	DsRed	Rockland Immunochemicals INC, Limerick, PA, USA (600-901-379, 26274, AB_10704808)	
Cy3 coupled goat anti-chicken	GACh-Cy3	Goat	1:300	Primary antibodies raised in chicken	Jackson ImmunoResearch; Westgrove, PA, USA (103-165-155, 93117, AB_2337386)	
Cy3 coupled goat anti-rabbit	GAR-Cy3	Goat	1:300	Primary antibodies raised in rabbit	Jackson ImmunoResearch; Westgrove, PA, USA (111-165-144, n/a, AB_2338006)	
Cy5 Azide	Cy5-azide		1 µM	5-ethynyl-2′-desoxuridine	Jena Bioscience, Jena, Germany (CLK-CCA-9295-1; Kli008-078; n/a)	
Cy5-Sulfo Azide			1 µM	5-ethynyl-2′-desoxuridine	Jena Bioscience, Jena, Germany (CLK-AZ118-1; Kli009-030; n/a)	
Moth-R2, Orco antiserum	Moth-R2	Rabbit	1:5,000	Olfactory sensory neurons	J. Krieger, University Halle-Wittenberg, Germany (n/a; n/a; n/a)	26

Table 1. Overview of used antibodies and markers.

Germany). After injection, the beetles were transferred into a para-film sealed petri dish and incubated at 28 °C for 24 hours.

Immunohistochemistry and EdU detection. The brains of cold anaesthetized beetles were dissected in PBS (phosphate-buffered saline, 0.01 M, pH 7.4) and fixed in 0.01 M PBS containing 4% paraformaldehyde for 1–2 hours at room temperature or at 4 °C overnight. Fixation was stopped by rinsing 4 × 10 min in PBS supplemented with 0.3% Triton X-100 (PBS-TrX). Afterwards, the brains were transferred into a blocking solution (5% normal goat serum (NGS, Dianova, Hamburg, Germany) in PBS-TrX) and incubated for 3–4 hours at room temperature or overnight at 4 °C. The brains were then incubated with primary antibody solution (PBS-TrX, 2% NGS, concentrations and details see Table 1). After 2–3 days at 4 °C, the antibodies were removed by rinsing 5 × 10 minutes in PBS-TrX. Subsequently, the brains were incubated for 2–3 days at 4 °C in constant darkness with secondary antisera and fluorescent markers (for details see Table 1). Afterwards, the brains were rinsed 5 times in PBS-TrX for 10 min and 2 times in 0,1 M TRIS buffer (pH 8,5; Tris-Base, HCL) and the incorporated EdU was detected using copper-catalysed click-chemistry[76]. Therefore, the brains were incubated for 1 to 2 hours at room temperature in constant darkness in freshly prepared reaction solution (4 mM $CuSO^4$, 10 µM azide-fluorochrome (see Table 1), and 500 mM ascorbic acid in 0.1 M TRIS buffer pH 8.5). Afterwards, the brains were embedded in a mixture of glycerol and PBS (80% glycerol, 20% PBS) or Mowiol[110] between two coverslips using a layer of two reinforcing rings as spacers.

Olfactory stimulation. For enhanced olfactory stimulation we reared 20 freshly eclosed adults in mixed-sex groups in para-film sealed 68 ml *Drosophila* vials on about 20 g substrate, supplemented with 1 µl pure green-leaf alcohol (cis-3-hexen-1-ol; Sigma-Aldrich) or 1 µl of the beetles aggregation pheromone 4,8-dimethyldecanal[79] in a dilution of 1:1000 in silicone oil (4,8-dimethyldecanal; Trécé Inc., Adair, OK, USA; Silicone oil M 10, Carl Roth, Karlsruhe, Germany), on filter paper (1 cm^2).

Orco-knockdown. *Orco* dsRNA (dsRNA^{orco}) and *DsRed* dsRNA (dsRNA^{sham}) used as a control were synthesized as previously published[26]. Both dsRNAs were injected into pupae at about 30%–40% of total metamorphosis. The Orco knockdown was verified by immunohistochemistry against Orco (Moth-R2, kindly provided by J. Krieger, University of Hohenheim, Germany) on cryo-sections of antennae as previously published[26] (Supplemental Fig. S4).

Image acquisition and processing. Fluorescent preparations were imaged using a widefield microscope setup (Axio Observer Z1; Carl Zeiss Microscopy, Jena, Germany) and a confocal laser scanning microscope (TCS SP5, Leica Microsystems, Wetzlar, Germany). Confocal image stacks were analysed with Amira 6 graphics software (FEI Visualization Sciences Group, Mérignac Cedex, France).

For further processing, snapshots of single sections and projections generated in Amira were processed (global level adjustments, contrast and brightness optimization) in Adobe Photoshop CC (Adobe Systems, San Jose, CA, USA). Final figure arrangements were performed in Adobe Illustrator CC.

EAG recordings. For electronantennographical recordings, we followed a previously published protocol[80]. The tests were performed using five female beetles aged seven days after dsRNA injection, corresponding to about A4, with three repeated measurements per animal. The antennal response was recorded at 25 Hz via a custom-build amplifier attached to a data acquisition controller (IDAC-4 A/D converter, Syntech, Hilversum, The Netherlands) using EAG 2000 software (Syntech). During the EAG recordings, the antennae were exposed to a constant flow (~3 l/min) of filtered and humidified air. The green leaf volatile cis-3-hexenol and the beetle's aggregation pheromone DMD[111] were used as test odours. They were presented as 1 s pulse via a stimulus controller (CS-02, Syntech) that looped in the odour diluted in silicone oil from a filter paper impregnated with 20 µl odour sample. Measurements were performed in minute-long intervals with increasing concentrations (10^{-8}–10^{-2}). Each repeat was preceded by the measurement of the reaction to DMD (positive control) and silicone oil, which was used as solvent)

Data analysis and plotting. Analysis of cell numbers and EAG responses including statistical comparison and plotting was performed using Python (version 3.7.3, Python Software Foundation, www.python.org) based custom scripts. Those scripts utilize the SciPy ecosystems (www.scipy.org) modules SciPy (version 1.2.1)[112], Numpy (version 1.16.2)[113], Matplotlib (version 3.0.3)[114], and Pandas (version 0.24.2)[115], as well as the additional modules scikit-posthocs (version 0.5.1, https://github.com/maximtrp/scikit-posthocs)[116], Seaborn (version 0.9.0)[117], and localreg (version 0.2.1, https://github.com/sigvaldm/localreg).

To test for significant differences between experimental groups, Scheirer-Ray-Hare[118] test (https://github.com/jpinzonc/Scheirer-Ray-Hare-Test), Kruskal-Wallis test from SciPy and posthoc analysis by Dunn's multiple comparison from scikit-posthocs with p-value correction using the Holm method[119] were used.

Raw EAG voltage trains exported from EAG 2000 were initially smoothed using robust LOESS (local regression) method from localreg to account for local spikes and subsequently normalized by subtracting the corresponding responses to silicone oil which was used as the solvent to dilute the test odours.

Figures were plotted as vector graphics and final figure arrangements were performed in Adobe Illustrator CC.

Ethics approval and consent to participate. All experiments involving animals were performed in compliance with the guidelines of the European Union (Directive 2010/63/EU). As all experiments were on insects an approval of the study by an ethics committee was unnecessary.

Data availability

Except for the original microscope images/stacks, all data generated or analysed during this study and all analysis scripts are included in this published article [and its Supplemental Information]. The confocal image stacks are available from the corresponding author upon request.

Received: 4 October 2019; Accepted: 2 January 2020;
Published online: 23 January 2020

References

1. Sengpiel, F. The critical period. *Curr. Biol. CB* **17**, R742–743 (2007).
2. Banks, M. S., Aslin, R. N. & Letson, R. D. Sensitive period for the development of human binocular vision. *Science* **190**, 675–677 (1975).
3. Desai, N. S., Cudmore, R. H., Nelson, S. B. & Turrigiano, G. G. Critical periods for experience-dependent synaptic scaling in visual cortex. *Nat. Neurosci.* **5**, 783–789 (2002).
4. Fagiolini, M., Pizzorusso, T., Berardi, N., Domenici, L. & Maffei, L. Functional postnatal development of the rat primary visual cortex and the role of visual experience: Dark rearing and monocular deprivation. *Vision Res.* **34**, 709–720 (1994).
5. Harwerth, R. S., Smith, E. L., Duncan, G. C., Crawford, M. L. & Noorden, Gvon Multiple sensitive periods in the development of the primate visual system. *Science* **232**, 235–238 (1986).
6. Hooks, B. M. & Chen, C. Critical Periods in the Visual System: Changing Views for a Model of Experience-Dependent Plasticity. *Neuron* **56**, 312–326 (2007).
7. Huang, Z. J. *et al.* BDNF Regulates the Maturation of Inhibition and the Critical Period of Plasticity in Mouse Visual Cortex. *Cell* **98**, 739–755 (1999).

8. Issa, N. P., Trachtenberg, J. T., Chapman, B., Zahs, K. R. & Stryker, M. P. The Critical Period for Ocular Dominance Plasticity in the Ferret's Visual Cortex. *J. Neurosci.* **19**, 6965–6978 (1999).
9. Olson, C. R. & Freeman, R. D. Profile of the sensitive period for monocular deprivation in kittens. *Exp. Brain Res.* **39**, 17–21 (1980).
10. Hubel, D. H. & Wiesel, T. N. The period of susceptibility to the physiological effects of unilateral eye closure in kittens. *J. Physiol.* **206**, 419–436 (1970).
11. Goldman, S. A. & Nottebohm, F. Neuronal production, migration, and differentiation in a vocal control nucleus of the adult female canary brain. *Proc. Natl. Acad. Sci. USA* **80**, 2390–2394 (1983).
12. Leppelsack, H.-J. Critical Periods in Bird Song Learning. *Acta Otolaryngol. (Stockh.)* **101**, 57–60 (1986).
13. Nottebohm, F. The "Critical Period" for Song Learning. *Ibis* **111**, 386–387 (1969).
14. Barth, M., Hirsch, H. V., Meinertzhagen, I. A. & Heisenberg, M. Experience-dependent developmental plasticity in the optic lobe of Drosophila melanogaster. *J. Neurosci.* **17**, 1493–1504 (1997).
15. Doll, C. A. & Broadie, K. Activity-dependent FMRP requirements in development of the neural circuitry of learning and memory. *Development* **142**, 1346–1356 (2015).
16. Fielde, A. M. Power of recognition among ants. *Biol. Bull.* **7**, 227–250 (1904).
17. Golovin, R. M., Vest, J., Vita, D. J. & Broadie, K. Activity-Dependent Remodeling of Drosophila Olfactory Sensory Neuron Brain Innervation During an Early-Life Critical Period. *J. Neurosci.* 2223–18, https://doi.org/10.1523/jneurosci.2223-18.2019 (2019).
18. Sachse, S. *et al.* Activity-Dependent Plasticity in an Olfactory Circuit. *Neuron* **56**, 838–850 (2007).
19. Tessier, C. R. & Broadie, K. Activity-dependent modulation of neural circuit synaptic connectivity. *Front. Mol. Neurosci.* **2** (2009).
20. Devaud, J.-M., Acebes, A., Ramaswami, M. & Ferrús, A. Structural and functional changes in the olfactory pathway of adult Drosophila take place at a critical age. *J. Neurobiol.* **56**, 13–23 (2003).
21. Doll, C. A. & Broadie, K. Neuron class-specific requirements for Fragile X Mental Retardation Protein in critical period development of calcium signaling in learning and memory circuitry. *Neurobiol. Dis.* **89**, 76–87 (2016).
22. Doll, C. A., Vita, D. J. & Broadie, K. Fragile X Mental Retardation Protein Requirements in Activity-Dependent Critical Period Neural Circuit Refinement. *Curr. Biol.* **27**, 2318–2330.e3 (2017).
23. Steinbrecht, R. A. Structure and function of insect olfactory sensilla. in Olfaction in mosquito-host interactions (eds. Bock, G. & Cardew, G.) 158–74; discussion 174-7 (John Wiley, 1996).
24. Bruyne, M. & Warr, C. G. Molecular and cellular organization of insect chemosensory neurons. *BioEssays* **28**, 23–34 (2006).
25. Hansson, B. S. & Stensmyr, M. C. Evolution of insect olfaction. *Neuron* **72**, 698–711 (2011).
26. Dippel, S. *et al.* Morphological and Transcriptomic Analysis of a Beetle Chemosensory System Reveals a Gnathal Olfactory Center. *BMC Biol.* **14**, 90 (2016).
27. Schachtner, J., Schmidt, M. & Homberg, U. Organization and evolutionary trends of primary olfactory brain centers in Tetraconata (Crustacea+Hexapoda). *Arthropod Struct. Dev.* **34**, 257–299 (2005).
28. Masse, N. Y., Turner, G. C. & Jefferis, G. S. X. E. Olfactory information processing in Drosophila. *Curr. Biol.* **19**, R700–13 (2009).
29. Galizia, C. G. & Rössler, W. Parallel olfactory systems in insects: anatomy and function. *Annu. Rev. Entomol.* **55**, 399–420 (2010).
30. Farris, S. M. Tritocerebral tract input to the insect mushroom bodies. *Arthropod Struct. Dev.* **37**, 492–503 (2008).
31. Awata, H. *et al.* Knockout crickets for the study of learning and memory. *Sci. Rep.* **5**, 15885 (2015).
32. Erber, J., Masuhr, T. & Menzel, R. Localization of short-term memory in the brain of the bee, Apis mellifera. *Physiol. Entomol.* **5**, 343–358 (1980).
33. Falibene, A., Roces, F. & Rössler, W. Long-term avoidance memory formation is associated with a transient increase in mushroom body synaptic complexes in leaf-cutting ants. *Front. Behav. Neurosci.* **9** (2015).
34. Gronenberg, W., Heeren, S. & Hölldobler, B. Age-dependent and task-related morphological changes in the brain and the mushroom bodies of the ant Camponotus floridanus. *J. Exp. Biol.* **199**, 2011–2019 (1996).
35. Grünewald, B. Physiological properties and response modulations of mushroom body feedback neurons during olfactory learning in the honeybee, Apis mellifera. *J. Comp. Physiol. A* **185**, 565–576 (1999).
36. Haenicke, J., Yamagata, N., Zwaka, H., Nawrot, M. & Menzel, R. Neural Correlates of Odor Learning in the Presynaptic Microglomerular Circuitry in the Honeybee Mushroom Body Calyx. *eNeuro* **5** (2018).
37. Heisenberg, M. Mushroom body memoir: from maps to models. *Nat. Rev. Neurosci.* **4**, 266–275 (2003).
38. Heisenberg, M. What do the mushroom bodies do for the insect brain? an introduction. *Learn. Mem.* **5**, 1–10 (1998).
39. Heisenberg, M., Borst, A., Wagner, S. & Byers, D. Drosophila mushroom body mutants are deficient in olfactory learning. *J. Neurogenet.* **2**, 1–30 (1985).
40. Keene, A. C. & Waddell, S. Drosophila olfactory memory: single genes to complex neural circuits. *Nat. Rev. Neurosci.* **8**, 341–354 (2007).
41. Menzel, R. Searching for the memory trace in a mini-brain, the honeybee. *Learn. Mem.* **8**, 53–62 (2001).
42. Mizunami, M., Weibrecht, J. M. & Strausfeld, N. J. Mushroom bodies of the cockroach: Their participation in place memory. *J. Comp. Neurol.* **402**, 520–537 (1998).
43. Scheiner, R., Weiß, A., Malun, D. & Erber, J. Learning in honey bees with brain lesions: how partial mushroom-body ablations affect sucrose responsiveness and tactile antennal learning. *Anim. Cogn.* **3**, 227–235 (2001).
44. Scotto-Lomassese, S. *et al.* Suppression of adult neurogenesis impairs olfactory learning and memory in an adult insect. *J. Neurosci.* **23**, 9289–9296 (2003).
45. Seid, M. A., Goode, K., Li, C. & Traniello, J. F. A. Age- and subcaste-related patterns of serotonergic immunoreactivity in the optic lobes of the ant Pheidole dentata. *Dev. Neurobiol.* **68**, 1325–1333 (2008).
46. Cabirol, A., Cope, A. J., Barron, A. B. & Devaud, J.-M. Relationship between brain plasticity, learning and foraging performance in honey bees. *PLOS ONE* **13**, e0196749 (2018).
47. Fahrbach, S. E. & Van Nest, B. N. Synapsin-based approaches to brain plasticity in adult social insects. *Curr. Opin. Insect Sci.* **18**, 27–34 (2016).
48. Groh, C. & Rössler, W. Comparison of microglomerular structures in the mushroom body calyx of neopteran insects. *Arthropod Struct. Dev.* **40**, 358–367 (2011).
49. Groh, C., Lu, Z., Meinertzhagen, I. A. & Rössler, W. Age-related plasticity in the synaptic ultrastructure of neurons in the mushroom body calyx of the adult honeybee Apis mellifera. *J. Comp. Neurol.* **520**, 3509–3527 (2012).
50. Hige, T., Aso, Y., Rubin, G. M. & Turner, G. C. Plasticity-driven individualization of olfactory coding in mushroom body output neurons. *Nature* **526**, 258–262 (2015).
51. Hige, T., Aso, Y., Modi, M. N., Rubin, G. M. & Turner, G. C. Heterosynaptic Plasticity Underlies Aversive Olfactory Learning in Drosophila. *Neuron* **88**, 985–998 (2015).
52. Muenz, T. S. *et al.* Neuronal plasticity in the mushroom body calyx during adult maturation in the honeybee and possible pheromonal influences. *Dev. Neurobiol.* **75**, 1368–1384 (2015).
53. Strube-Bloss, M. F., Nawrot, M. P. & Menzel, R. Neural correlates of side-specific odour memory in mushroom body output neurons. *Proc. Biol. Sci.* **283** (2016).
54. Fahrbach, S. E., Strande, J. L. & Robinson, G. E. Neurogenesis is absent in the brains of adult honey bees and does not explain behavioral neuroplasticity. *Neurosci. Lett.* **197**, 145–148 (1995).
55. Trotha, J. W., Egger, B. & Brand, A. H. Cell proliferation in the Drosophila adult brain revealed by clonal analysis and bromodeoxyuridine labelling. *Neural Develop.* **4**, 9 (2009).

56. Cayre, M., Strambi, C. & Strambi, A. Neurogenesis in an adult insect brain and its hormonal control. *Nature* **368**, 57–59 (1994).
57. Cayre, M. *et al*. Neurogenesis in adult insect mushroom bodies. *J. Comp. Neurol.* **371**, 300–310 (1996).
58. Dufour, M.-C. & Gadenne, C. Adult neurogenesis in a moth brain. *J. Comp. Neurol.* **495**, 635–643 (2006).
59. Cayre, M., Malaterre, J., Scotto-Lomassese, S., Strambi, C. & Strambi, A. The common properties of neurogenesis in the adult brain: from invertebrates to vertebrates. *Comp. Biochem. Physiol. B Biochem. Mol. Biol.* **132**, 1–15 (2002).
60. Zhao, X., Coptis, V. & Farris, S. M. Metamorphosis and adult development of the mushroom bodies of the red flour beetle, Tribolium castaneum. *Dev. Neurobiol.* **68**, 1487–1502 (2008).
61. Meusemann, K. *et al*. A phylogenomic approach to resolve the arthropod tree of life. *Mol. Biol. Evol.* **27**, 2451–2464 (2010).
62. Wiegmann, B. M. *et al*. Episodic radiations in the fly tree of life. *Proc. Natl. Acad. Sci. USA* **108**, 5690–5695 (2011).
63. Levinson, H. & Levinson, A. Origin of grain storage and insect species consuming desiccated food. *Anz. Fuer Schaedlingskunde Pflanzenschutz Umweltschutz* **67**, 47–60 (1994).
64. Misof, B. *et al*. Phylogenomics resolves the timing and pattern of insect evolution. *Science* **346**, 763–767 (2014).
65. Dippel, S. *et al*. Tissue-specific transcriptomics, chromosomal localization, and phylogeny of chemosensory and odorant binding proteins from the red flour beetle Tribolium castaneum reveal subgroup specificities for olfaction or more general functions. *BMC Genomics* **15**, 1141 (2014).
66. Kim, H. S. *et al*. BeetleBase in 2010: revisions to provide comprehensive genomic information for Tribolium castaneum. *Nucleic Acids Res.* **38**, D437–42 (2010).
67. Tribolium Genome Sequencing Consortium. The genome of the model beetle and pest Tribolium castaneum. *Nature* **452**, 949–955 (2008).
68. Gilles, A. F., Schinko, J. B. & Averof, M. Efficient CRISPR-mediated gene targeting and transgene replacement in the beetle Tribolium castaneum. *Development* **142**, 2832–2839 (2015).
69. Schinko, J. B. *et al*. Functionality of the GAL4/UAS system in Tribolium requires the use of endogenous core promoters. *BMC Dev. Biol.* **10**, 53 (2010).
70. Trauner, J. *et al*. Large-scale insertional mutagenesis of a coleopteran stored grain pest, the red flour beetle Tribolium castaneum, identifies embryonic lethal mutations and enhancer traps. *BMC Biol.* **7**, 73 (2009).
71. Bucher, G., Scholten, J. & Klingler, M. Parental RNAi in Tribolium (Coleoptera). *Curr. Biol.* **12**, R85–R86 (2002).
72. Tomoyasu, Y. & Denell, R. E. Larval RNAi in Tribolium (Coleoptera) for analyzing adult development. *Dev. Genes Evol.* **214**, 575–578 (2004).
73. Tomoyasu, Y. *et al*. Exploring systemic RNA interference in insects: a genome-wide survey for RNAi genes in Tribolium. *Genome Biol.* **9**, R10 (2008).
74. Sokoloff, A. The biology of Tribolium: with special emphasis on genetic aspects. Volume 1. vol. 1 (Clarendon Press, 1972).
75. Chehrehasa, F., Meedeniya, A. C. B., Dwyer, P., Abrahamsen, G. & Mackay-Sim, A. EdU, a new thymidine analogue for labelling proliferating cells in the nervous system. *J. Neurosci. Methods* **177**, 122–130 (2009).
76. Salic, A. & Mitchison, T. J. A chemical method for fast and sensitive detection of DNA synthesis *in vivo*. *Proc. Natl. Acad. Sci. USA* **105**, 2415–2420 (2008).
77. Posnien, N., Koniszewski, N. D. B., Hein, H. J. & Bucher, G. Candidate gene screen in the red flour beetle Tribolium reveals six3 as ancient regulator of anterior median head and central complex development. *PLoS Genet.* **7**, e1002416 (2011).
78. Halter, D. A. *et al*. The homeobox gene repo is required for the differentiation and maintenance of glia function in the embryonic nervous system of Drosophila melanogaster. *Development* **121**, 317–332 (1995).
79. Arnaud, L. *et al*. Is dimethyldecanal a common aggregation pheromone of Tribolium flour beetles? *J. Chem. Ecol.* **28**, 523–532 (2002).
80. Balakrishnan, K., Holighaus, G., Weißbecker, B. & Schütz, S. Electroantennographic responses of red flour beetle Tribolium castaneum Herbst (Coleoptera: Tenebrionidae) to volatile organic compounds. *J. Appl. Entomol.* **141**, 477–486 (2017).
81. Engsontia, P. *et al*. The red flour beetle's large nose: an expanded odorant receptor gene family in Tribolium castaneum. *Insect Biochem. Mol. Biol.* **38**, 387–397 (2008).
82. Scotto Lomassese, S. *et al*. Influence of environmental stimulation on neurogenesis in the adult insect brain. *J. Neurobiol.* **45**, 162–171 (2000).
83. Scotto-Lomassese, S., Strambi, C., Aouane, A., Strambi, A. & Cayre, M. Sensory inputs stimulate progenitor cell proliferation in an adult insect brain. *Curr. Biol.* **12**, 1001–1005 (2002).
84. van Praag, H. *et al*. Functional neurogenesis in the adult hippocampus. *Nature* **415**, 1030–1034 (2002).
85. van Praag, H., Shubert, T., Zhao, C. & Gage, F. H. Exercise Enhances Learning and Hippocampal Neurogenesis in Aged Mice. *J. Neurosci.* **25**, 8680–8685 (2005).
86. Aimone, J. B., Wiles, J. & Gage, F. H. Potential role for adult neurogenesis in the encoding of time in new memories. *Nat. Neurosci.* **9**, 723–727 (2006).
87. Deng, W., Aimone, J. B. & Gage, F. H. New neurons and new memories. *Nat. Rev. Neurosci.* **11**, 339 (2010).
88. Bruel-Jungerman, E., Davis, S., Rampon, C. & Laroche, S. Long-Term Potentiation Enhances Neurogenesis in the Adult Dentate Gyrus. *J. Neurosci.* **26**, 5888–5893 (2006).
89. Cayre, M., Scotto-Lomassese, S., Malaterre, J., Strambi, C. & Strambi, A. Understanding the regulation and function of adult neurogenesis: contribution from an insect model, the house cricket. *Chem. Senses* **32**, 385–395 (2007).
90. Gu, S.-H., Tsia, W.-H., Chiang, A.-S. & Chow, Y.-S. Mitogenic effects of 20-hydroxyecdysone on neurogenesis in adult mushroom bodies of the cockroach, Diploptera punctata. *J. Neurobiol.* **39**, 264–274 (1999).
91. Farris, S. M. Evolution of insect mushroom bodies. *Arthropod Struct. Dev.* **34**, 211–234 (2005).
92. Farris, S. M. & Roberts, N. S. Coevolution of generalist feeding ecologies and gyrencephalic mushroom bodies in insects. *Proc. Natl. Acad. Sci. USA* **102**, 17394–17399 (2005).
93. Hensch, T. K. Critical period regulation. *Annu. Rev. Neurosci.* **27**, 549–579 (2004).
94. Jacob, V. E. J. M. Current Source Density Analysis of Electroantennogram Recordings: A Tool for Mapping the Olfactory Response in an Insect Antenna. *Front. Cell. Neurosci.* **12** (2018).
95. Getahun, M. N., Wicher, D., Hansson, B. S. & Olsson, S. B. Temporal response dynamics of Drosophila olfactory sensory neurons depends on receptor type and response polarity. *Front. Cell. Neurosci.* **6** (2012).
96. Christensen, T. A. & Hildebrand, J. G. Pheromonal and host-odor processing in the insect antennal lobe: how different? *Curr. Opin. Neurobiol.* **12**, 393–399 (2002).
97. Jefferis, G. S. X. E. *et al*. Comprehensive maps of Drosophila higher olfactory centers: spatially segregated fruit and pheromone representation. *Cell* **128**, 1187–1203 (2007).
98. Kropf, J., Kelber, C., Bieringer, K. & Rössler, W. Olfactory subsystems in the honeybee: sensory supply and sex specificity. *Cell Tissue Res.* **357**, 583–595 (2014).
99. Brown, S. J. *et al*. The red flour beetle, Tribolium castaneum (Coleoptera). *Cold Spring Harb. Protoc.* **2009**, pdb.emo126 (2009).
100. Kempermann, G. & Gage, F. H. Experience-dependent regulation of adult hippocampal neurogenesis: Effects of long-term stimulation and stimulus withdrawal. *Hippocampus* **9**, 321–332 (1999).
101. McGuire, S. E., Le, P. T. & Davis, R. L. The Role of Drosophila Mushroom Body Signaling in Olfactory Memory. *Science* **293**, 1330–1333 (2001).

102. Akalal, D.-B. G. *et al.* Roles for Drosophila mushroom body neurons in olfactory learning and memory. *Learn. Mem.* **13**, 659–668 (2006).
103. Leuner, B., Gould, E. & Shors, T. J. Is there a link between adult neurogenesis and learning? *Hippocampus* **16**, 216–224 (2006).
104. Ma, D. K., Kim, W. R., Ming, G. & Song, H. Activity-dependent extrinsic regulation of adult olfactory bulb and hippocampal neurogenesis. *Ann. N. Y. Acad. Sci.* **1170**, 664–673 (2009).
105. Snyder, J. S., Hong, N. S., McDonald, R. J. & Wojtowicz, J. M. A role for adult neurogenesis in spatial long-term memory. *Neuroscience* **130**, 843–852 (2005).
106. Yau, S., Li, A. & So, K.-F. Involvement of Adult Hippocampal Neurogenesis in Learning and Forgetting. *Neural Plast.* **2015** (2015).
107. Sokoloff, A. The Genetics of Tribolium and Related Species. vol. Supplement 1 (Academic Press, 1966).
108. Sokoloff, A., Slatis, H. M. & Stanley, J. The black mutation of Tribolium castaneum. *J. Hered.* **51**, 131–135 (1960).
109. Berghammer, A. J., Bucher, G., Maderspacher, F. & Klingler, M. A system to efficiently maintain embryonic lethal mutations in the flour beetle Tribolium castaneum. *Dev. Genes Evol.* **209**, 382–389 (1999).
110. Mowiol embedding medium. Cold Spring Harb. *Protoc.* **2010**, pdb.rec12110–pdb.rec12110 (2010).
111. Kim, J., Matsuyama, S. & Suzuki, T. 4,8-Dimethyldecanal, the aggregation pheromone of Tribolium castaneum, is biosynthesized through the fatty acid pathway. *J. Chem. Ecol.* **31**, 1381–1400 (2005).
112. Virtanen, P. *et al.* SciPy 1.0–Fundamental Algorithms for Scientific Computing in Python. *ArXiv190710121 Phys.* (2019).
113. van der Walt, S., Colbert, S. C. & Varoquaux, G. The NumPy Array: A Structure for Efficient Numerical Computation. *Comput. Sci. Eng.* **13**, 22–30 (2011).
114. Hunter, J. D. Matplotlib: A 2D Graphics Environment. *Comput. Sci. Eng.* **9**, 90–95 (2007).
115. McKinney, W. Data Structures for Statistical Computing in Python. in Proceedings of the 9th Python in Science Conference (eds. Walt, S. van der & Millman, J.) 51–56 (2010).
116. Terpilowski, M. scikit-posthocs: Pairwise multiple comparison tests in Python. *J. Open Source Softw.* **4**, 1169 (2019).
117. Waskom, M. *et al.* mwaskom/seaborn: v0.9.0 (July 2018), https://doi.org/10.5281/zenodo.1313201 (Zenodo, 2018).
118. Scheirer, C. J., Ray, W. S. & Hare, N. The Analysis of Ranked Data Derived from Completely Randomized Factorial Designs. *Biometrics* **32**, 429 (1976).
119. Holm, S. A Simple Sequentially Rejective Multiple Test Procedure. *Scand. J. Stat.* **6**, 65–70 (1979).
120. Tanious, F. A., Veal, J. M., Buczak, H., Ratmeyer, L. S. & Wilson, W. D. DAPI (4′,6-diamidino-2-phenylindole) binds differently to DNA and RNA: minor-groove binding at AT sites and intercalation at AU sites. *Biochemistry* **31**, 3103–3112 (1992).
121. Vandekerckhove, J., Deboben, A., Nassal, M. & Wieland, T. The phalloidin binding site of F-actin. *EMBO J.* **4**, 2815–2818 (1985).
122. Koniszewski, N. D. B. *et al.* The insect central complex as model for heterochronic brain development-background, concepts, and tools. *Dev. Genes Evol.* **226**, 209–219 (2016).

Acknowledgements
We thank Jürgen Krieger for providing the cross-reactive Orco antiserum, Benjamin Altenhain for providing the cross-reactive reversed-polarity antiserum, Gregor Bucher and Michaelis Averof for sharing transgenic beetle lines, and Martina Kern for technical assistance. Parts of this study were funded within the Deutsche Forschungsgemeinschaft SPP 1392: SCHA 678/13-1 (J.S.) and WI 1797/4-1 (E.A.W.). The funders had no role in the study design, data collection, interpretation, or the decision to submit the work for publication.

Author contributions
B.T. conceived and designed the study, acquired, analysed, and interpreted the data; and drafted and revised the article; M.S., K.B. acquired and analysed the data; S.D., J.S., and E.A.W. conceived and designed the study; analysed and interpreted the data; and drafted and revised the article. All authors read and approved the final manuscript.

Competing interests
The authors declare no competing interests.

Additional information
Supplementary information is available for this paper at https://doi.org/10.1038/s41598-020-57639-x.

Correspondence and requests for materials should be addressed to J.S.

Reprints and permissions information is available at www.nature.com/reprints.

Publisher's note Springer Nature remains neutral with regard to jurisdictional claims in published maps and institutional affiliations.

4

Metamorphic development of the olfactory system

Trebels et al. BMC Biology (2021) 19:155
https://doi.org/10.1186/s12915-021-01055-8

BMC Biology

RESEARCH ARTICLE Open Access

Metamorphic development of the olfactory system in the red flour beetle (*Tribolium castaneum*, HERBST)

Björn Trebels[1*†], Stefan Dippel[1†], Brigitte Goetz[1], Maria Graebner[1], Carolin Hofmann[1], Florian Hofmann[1], Freya-Rebecca Schmid[1], Mara Uhl[1], Minh-Phung Vuong[1], Vanessa Weber[1] and Joachim Schachtner[1,2*]

Abstract

Background: Insects depend on their olfactory sense as a vital system. Olfactory cues are processed by a rather complex system and translated into various types of behavior. In holometabolous insects like the red flour beetle *Tribolium castaneum*, the nervous system typically undergoes considerable remodeling during metamorphosis. This process includes the integration of new neurons, as well as remodeling and elimination of larval neurons.

Results: We find that the sensory neurons of the larval antennae are reused in the adult antennae. Further, the larval antennal lobe gets transformed into its adult version. The beetle's larval antennal lobe is already glomerularly structured, but its glomeruli dissolve in the last larval stage. However, the axons of the olfactory sensory neurons remain within the antennal lobe volume. The glomeruli of the adult antennal lobe then form from mid-metamorphosis independently of the presence of a functional OR/Orco complex but mature dependent on the latter during a postmetamorphic phase.

Conclusions: We provide insights into the metamorphic development of the red flour beetle's olfactory system and compared it to data on *Drosophila melanogaster*, *Manduca sexta*, *and Apis mellifera*. The comparison revealed that some aspects, such as the formation of the antennal lobe's adult glomeruli at mid-metamorphosis, are common, while others like the development of sensory appendages or the role of Orco seemingly differ.

Keywords: *Tribolium castaneum*, Olfaction, Insect, Metamorphic development, Antennae, Antennal lobe, Gnathal olfactory center, Neuroanatomy

Background

In insects, olfactory perception usually starts at the chemosensory sensilla of the antennae and palps. The sensilla house the chemosensory neurons (CSNs). CSNs divide into olfactory sensory neurons (OSNs) and gustatory sensory neurons (GSNs). The OSNs present the olfactory receptors, either odorant receptors (ORs) or ionotropic glutamate-like receptors (IRs), in their membranes [1–5]. Notably, most sensory information received by the OSNs of insects stems from a functional heteromer of specific odorant receptors (ORs) and the odorant receptor co-receptor (Orco) [6]. Thus, elimination of Orco typically leads to a loss of most olfactory transduction [7–12].

The OSNs then relay the olfactory information via their axons to the respective primary processing centers. For the antennal OSNs, these centers are the antennal lobes, while those of the palpal OSNs differ among species. In hemimetabolous insects, the signal from palpal OSNs gets processed in the glomerular lobes (LGs) [13].

* Correspondence: bjoern@famtrebels.de; joachim.schachtner@tu-clausthal.de
†Björn Trebels and Stefan Dippel contributed equally to this work.
[1]Department of Biology, Animal Physiology, Philipps-University Marburg, Karl-von-Frisch-Str. 8, 35032 Marburg, Germany
Full list of author information is available at the end of the article

The current picture of olfaction in holometabolous insects states that the palpal signals are also processed in the ALs [14–18]. However, at least in the red flour beetle, the palpal OSNs do not project into the ALs but into the paired LGs and the unpaired gnathal olfactory center (GOC), which is a glomerularly organized neuropil within the gnathal ganglion [5].

In holometabolous insects, the lifestyle of imagines and larvae typically differs. Consequently, during metamorphosis, the olfactory system's morphology is remodeled to reflect the new challenges. Already the larvae of holometabolous insects possess olfactory appendages, while the complexity of the primary processing centers differs among species. The larvae of *Tribolium castaneum* possess elaborate antennae with three distinguishable segments (scape, pedicel, flagellum) [19, 20], which is also described for the red flour beetle's close relative *Tenebrio molitor* [21] and some other beetles [22–24]. The larval antennae of the hawkmoth *Manduca sexta* are similar in structure [25, 26], whereas the larvae of flies only possess functional equivalent dorsal organs [27, 28].

The adult antennae of the vinegar fly *Drosophila melanogaster* [29, 30] and the hawkmoth *Manduca sexta* [31] are built from imaginal disks during the pupal stage, whereas the antennae of the hemimetabolous American cockroach *Periplaneta americana* grow gradually with every molt [32, 33]. Previous studies on appendage development in holometabolous insects focused on species with imaginal discs or cells. However, it is discussed that reusing larval appendages to build their adult equivalents is the more ancestral state [34]. This mechanism is found during the development of the adult legs of the red flour beetle [35], of which the antennae are serial homologs [36]. We used transgenic lines labeling CSNs and OSNs, in combination with cell birth detection, to visualize and follow the sensory neurons of the antennae throughout pupal formation and metamorphosis to investigate the origin of the beetle's adult antennae.

Previous studies showed that the organization of the larval antennal lobes (ALs) differs between holometabolous insect species. In the lepidopteran *M. sexta* and the hymenopteran *Apis mellifera,* the larval ALs are not glomerularly organized [37, 38], whereas the larval ALs of *the mealworm beetle Tenebrio molitor* are glomerularly organized [39]. Further, the larval ALs of *D. melanogaster* possess glomeruli but with a lower count and one-to-one wiring between receptor neurons and glomeruli [40]. Besides, in the hemimetabolous American cockroach *Periplaneta americana,* the ALs show similar numbers of glomeruli in nymphs (larvae) and adults [41].

So far, studies indicate that OSNs are required for the proper formation of the adult AL glomeruli. In *M. sexta,* de-antennation leads to non-glomerular ALs [42]. Further, in the clonal raider ant *Ooceraea biroi,* de-antennation leads to a heavily reduced glomeruli number [43]. In the ant, the same result was achieved in Orco knock-out experiments [44, 45]. The authors suggest that the effect is more likely due to the loss of the majority of OSNs caused by the knock-out. Knock-out studies on the metamorphic development of the ALs of *D. melanogaster* indicate that activity of the OR/Orco complex is not necessary for the formation of AL glomeruli [7, 46, 47], which is also reported for the malaria mosquito *Anopheles gambiae* [48].

In our study, we used (immuno)-histochemistry to visualize the formation of the adult glomeruli of the ALs and the GOC of the red flour beetle. We took advantage of the strong dsRNA injection-induced systemic RNA interference [49–51] to effectively knockdown Orco just before the pupal formation to study the role of Orco on the formation of the AL glomeruli in *T. castaneum*.

Within the ALs, the olfactory information perceived by the OSNs is processed by a network of glomeruli connecting local interneurons (LNs). Olfactory representations, shaped by the LNs, are mainly due to the inhibitory transmitter gamma amino-butyric acid (GABA), the excitatory transmitter acetylcholine [52–65], and numerous neuropeptides [13, 66–68]. As evident from *D. melanogaster* [60] and many other insects [13, 69], the vast majority of LNs use the inhibitory transmitter GABA, therefore providing a good estimate for LN numbers.

Insight into the LN development in beetles is provided for *T. molitor*, a close relative of *T. castaneum*. In *T. molitor,* GABA expressing LNs (somata in the cluster "CL7") are present in larvae, remain present with similar numbers with the onset of metamorphosis, and eventually rise in numbers throughout metamorphosis [39]. To study the development of the AL LNs in the red flour beetle, we labeled GABAergic neurons by immunohistochemistry against glutamic acid decarboxylase (GAD), which catalyzes the decarboxylation of glutamate to GABA. We determined the number of GAD immunoreactive cells in a lateral cluster comparable to the cluster "CL7" in *T. molitor* and used reliable neurogenesis detection with EdU [10] to determine their origins.

Results

Antennae, sensory neurons, and antennal lobe glomeruli

The *T. castaneum* larvae possess a pair of three-parted antennae, each consisting of scape, pedicel, and a reduced flagellum (Fig. 1) [19, 20]. The distal trichoid sensillum (sTri) and the placoid sensillum or plate organ (sPla) of the larval antenna are both labeled in the CSN-labeling EF-1-B-DsRed line (Fig. 2), as well as in the OSN-labeling partial Orco-Gal4xUAS-DsRed line (Fig. 3A).

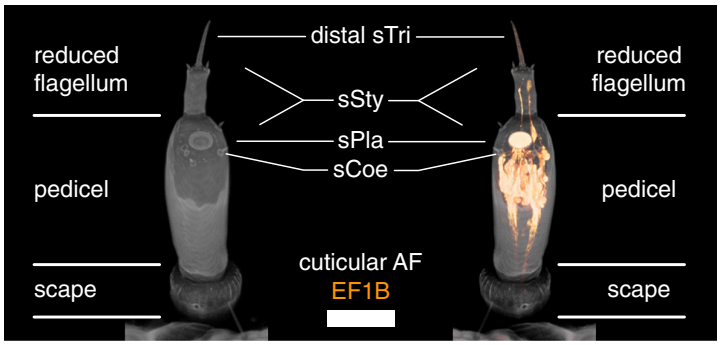

Fig. 1 Structure of the larval antenna. Volume rendering of a confocal image stack. Depicted in gray the cuticular autofluorescence and orange the reporter signal in the EF-1-B-DsRed line representing CSNs. sTri – trichoid sensilla, sSty – styloconic sensilla, sPla – placoid sensilla, sCoe – coeloconic sensilla. Scale bar 50 μm

Late during the last larval instar and within the first few hours of the prepupal stage, the CSNs retract their dendrites. Further, their somata relocate into the head capsule, where they are detectable in later prepupal stages (Figs. 2B, C; 3B; 4). At this time, the gross morphology of the adult antenna is already found beneath the larval cuticle (Fig. 4; Additional file 1: Figure S1 A, B)—with the labeled CSNs (Additional file 1: Figure S1 A', C) and OSNs (Additional file 1: Figure S1 D) located in its tip (Fig. 4, Additional file 1: Figure S1 A'). As the partial Orco-Gal4xUAS-DsRed line labels fewer neurons, which results in a much weaker signal, and as imaging requires scanning through two cuticles (larval and pupal), we were not able to acquire confocal stacks of the OSNs in prepupae suitable for volume rendering as provided for the CSNs.

Simultaneously, OSN axons are found within the antennal lobe (Fig. 4; Additional file 2: Figure S2). During the last hours of pupal stage P0%, the gross distribution of OSNs in the last three segments of the flagellum becomes readily visible (Figs. 2d and 3D, Additional file 3: Video S1 and Additional file 4: Video S2). During the following stages, the OSN number rises (Figs. 2E, F and 3E, F; Additional file 3: Video S1 and Additional file 4: Video S2) and mostly resembles the adult distribution (Figs. 2G and 3G) at about P50% (Fig. 2F). EdU injections into the prepupa with subsequent dissection at P0% revealed that the CSNs found in the antennae of

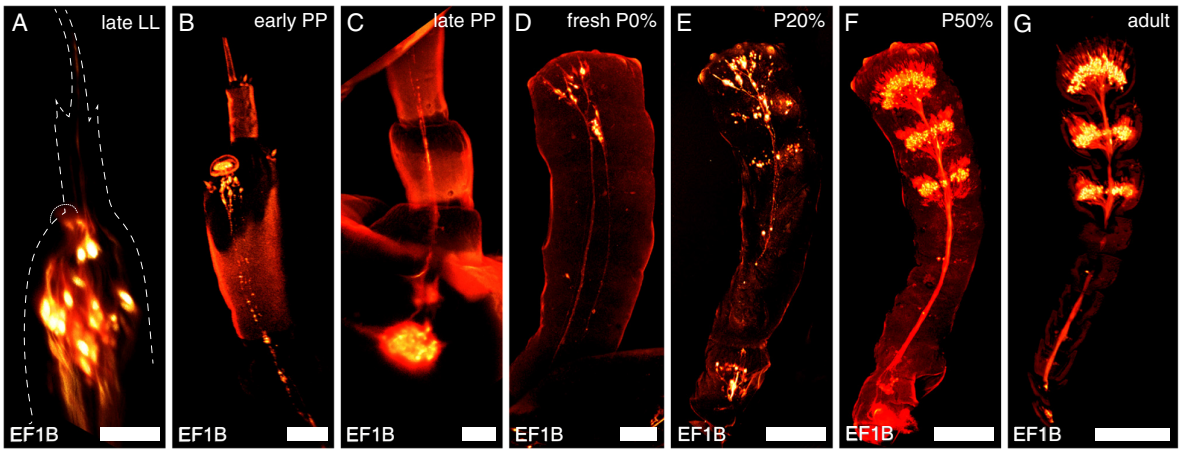

Fig. 2 Development of the antennal chemosensory neurons (CSNs). Volume rendering of the reporter signal in the antenna at different developmental stages in the EF-1-B-DsRed line. **A** The dashed line depicts the outline of the antenna based on the autofluorescence of the cuticula. In the last larval instar (LL), CSNs innervate the placoid and the distal trichoid sensillum. **B**, **C** The neurons retract from the larval antenna during the prepupa (PP), and the somas relocate into the head capsule. **D** With the onset of metamorphosis, CSNs are found at the distal end of the adult antennae. **E**–**G** Their number rises until stage P50% when their gross distribution already resembles that of the adult antenna. Scale bars **A**–**C** 25 μm; **D**–**G** 100 μm

Trebels *et al. BMC Biology* (2021) 19:155

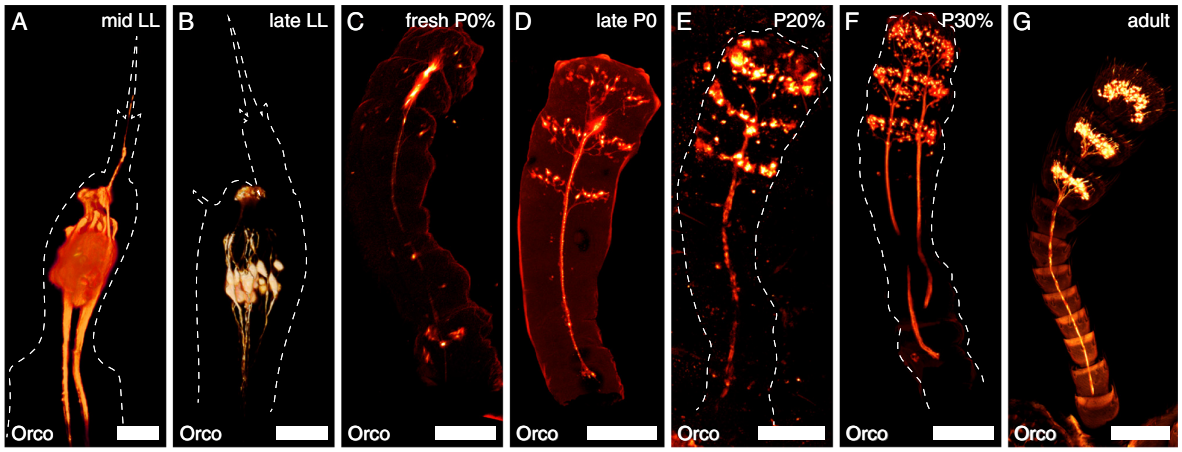

Fig. 3 Development of the antennal olfactory sensory neurons (OSNs). Volume renderings from confocal image stacks of the reporter signal in the antenna at different developmental stages within the Orco-GAL4xUAS-DsRed line. The dashed lines depict the outline of the antenna based on the autofluorescence of the cuticula. **A**, **B** In the last larval instar (LL), OSNs innervate the placoid and the distal trichoid sensillum. **C** The OSNs retract from the larval antenna during the prepupa (PP) and are with the onset of metamorphosis found at the distal end of the adult antenna. **E**–**G** Their number rises until P50% when their distribution already resembles the adult antenna. Scale bars **A**, **B** 25 μm; **C**–**G** 100 μm. Two time-lapse videos of approx. the first 30 h of OSN-development are available as Additional file 3: Video S1 and Additional file 4: Video S2

fresh pupae are born before pupation (Fig. 5A, B), while EdU injections at P0% and detection at A0 revealed that the majority of adult CSNs are born during metamorphosis (Fig. 5C).

In the early phase of the last instar larvae, the about 45 AL glomeruli (mean = 44.75, SD = 3.42; N_{ALs} = 12) are defined in the f-actin and synapsin labeling (Fig. 6A-A"). The glomerular organization vanishes during the late phase of last instar larvae in the f-actin and synapsin labeling (Fig. 6B-B"). In the prepupa up to pupal stage P30%, a glomerular organization within the antennal lobe is absent (Fig. 6C-C", D-D"). At pupal stage P40% (Fig. 6E-E"), glomerulization becomes visible in the f-actin staining, with incipient glomerulization visible in the synapsin staining. At mid-metamorphosis (P50%; Fig. 6F-F"), glomerulization is obvious in the f-actin

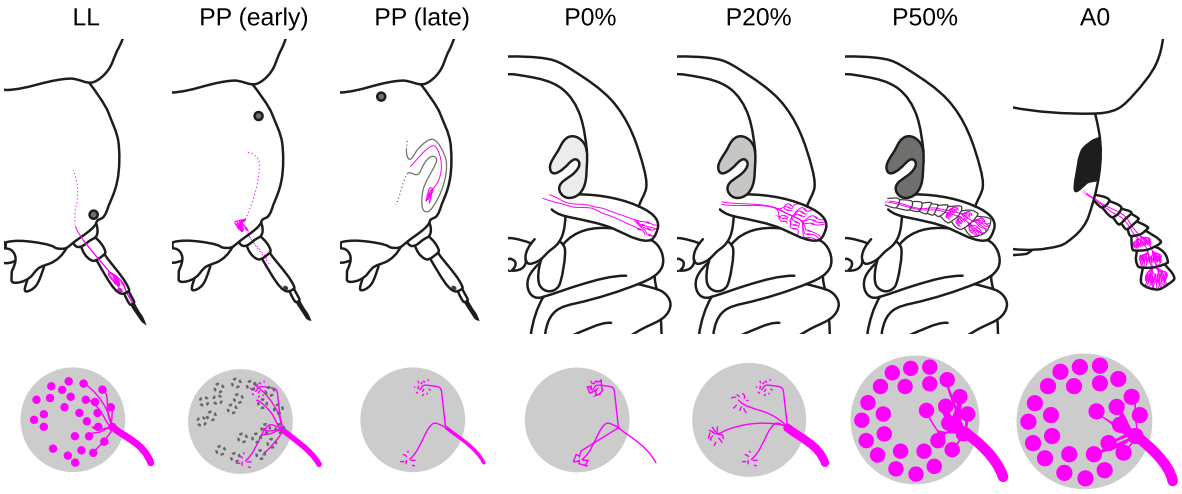

Fig. 4 Metamorphic development of the *T. castaneum* antennae and antennal lobes. The upper row visualizes the location of the OSNs (magenta) within the antennae and head capsule, while the lower row displays the OSN axons and their arborizations within the ALs, as well as the state of AL glomerulization. LL - last larval instar, PP - prepupa

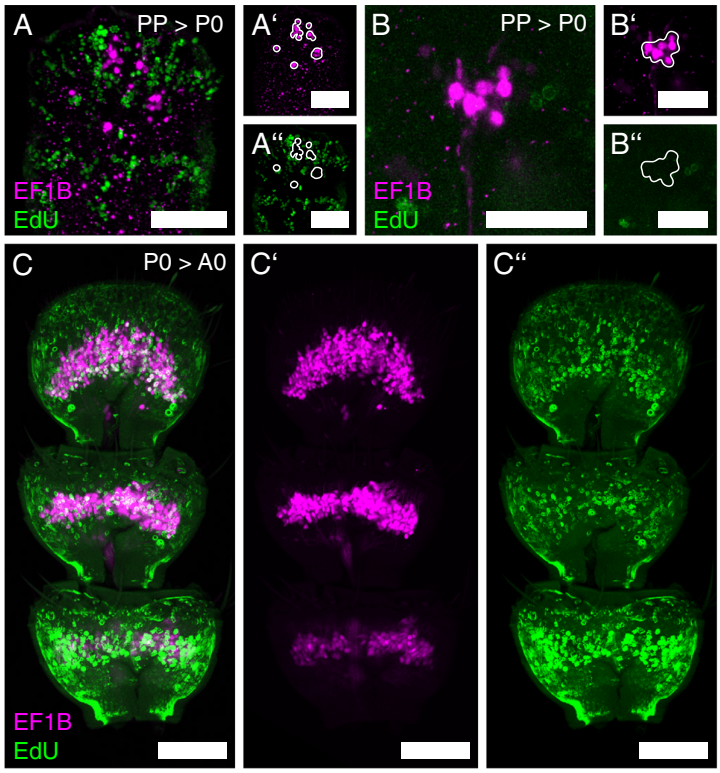

Fig. 5 Genesis of the antennal CSNs. Antennal maximum projections of the reporter signal in the EF-1-B-DsRed line (magenta), as well as EdU-labeled cells (green). **A**-**A″**, **B**-**B″** After EdU injection in the prepupa (PP), none of the CSNs in the antenna at P0% is labeled with EdU. **C**-**C″** After EdU injection at P0%, a large amount of CSNs in the adult antenna at A0 is labeled. Scale bars **A**-**A″**, **C**-**C″** 50 μm, **B**-**B″** 25 μm

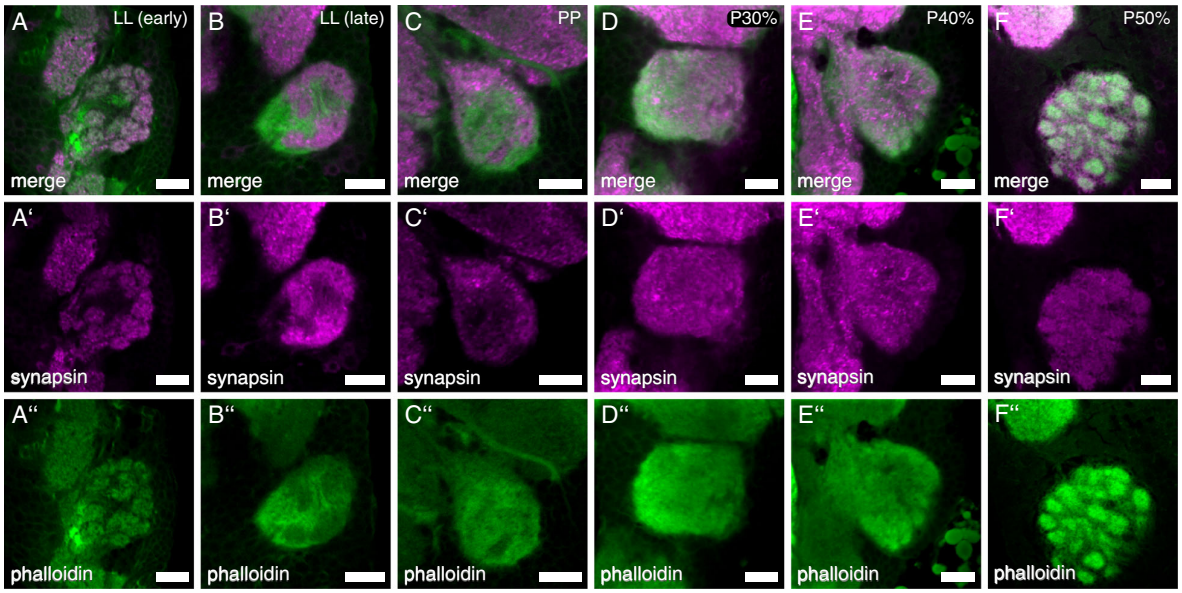

Fig. 6 Development of the adult antennal lobe glomeruli. Representative optical slices of the antennal lobes of the red flour beetle *T. castaneum* at different developmental stages (LL - last larval instar, PP - prepupa, P - pupal stages), visualized by synapsin (magenta) and phalloidin (green) staining. Scale bars 10 μm

staining. In the synapsin staining, weak yet distinct glomerulization is visible. At this stage, the antennal lobes consist of about 70 (mean = 68.44, SD = 1.89; N_{ALs} = 9) glomeruli, which is also the number found in freshly eclosed (A0) beetles [70].

Role of Orco during the formation of the antennal lobe glomerular map

We find Orco-expression in pupae already before glomerulization of the adult ALs starts (Fig. 3, Additional file 5: Figure S3). In experiments using dsRNA-injection-induced systemic RNA interference (RNAi) against Orco and thereby effectively blocking OR/Orco driven olfactory transduction [10], we find that a knockdown of Orco induced in late larvae seemingly does not block the formation of the olfactory glomeruli. The AL glomeruli are still easily distinguishable in freshly eclosed (A0) knockdown beetles (n = 8; Fig. 7A) as they are in wildtype beetles (n = 7; Fig. 7B; compare also [70]). Further, the same experiments showed that in 7-day-old (A7) beetles, glomerulization is heavily reduced in knockdown beetles (n = 7; Fig. 7C), while they are clearly visible in the wildtype (n = 7; Fig. 7D; compare also [5, 67]). However, even in 7-day-old knockdown beetles, the OSNs still locate in the antennae, with their dendrites within the olfactory sensilla (Fig. 8B).

Local neurons of the antennal lobe (AL)

In *D. melanogaster* [60] and many other insects [13, 69], the vast majority of the AL LNs use the inhibitory transmitter GABA, which is synthesized by GAD. We used immunohistochemistry against GAD (pupae: GADr; adults: GADs) to follow the development of the AL LNs. From at least P30%, the antennal lobes are innervated by GAD immunoreactive fibers, while a distinct glomerular pattern in the GAD immunostaining is first visible in adult stage A7 (Fig. 9). The number of GAD immunoreactive somata rises during metamorphosis. At pupal stages P30% and P40%, about 65 (P30%: mean = 64.00, SD = 5.72; N_{ALs} = 7; P40%: mean = 65.75, SD = 1.71, N_{ALs} = 4) immunoreactive cells locate in the lateral cluster of each antennal lobe. At pupal stage P50%, the clusters consist of about 70 cells each but display a high variation (mean = 70.40, SD = 49.30, N_{ALs} = 5). At P70% about 130 cells (mean = 130.83, SD = 4.96, N_{ALs} = 6) and at P90% about 155 cells (mean = 154.5, SD = 11.79, N_{ALs} = 4) are found in each lateral cluster. The number then rises to about 165 cells in 7-day-old adult beetles (A7; mean = 164.3, SD = 23.46, N_{ALs} = 10).

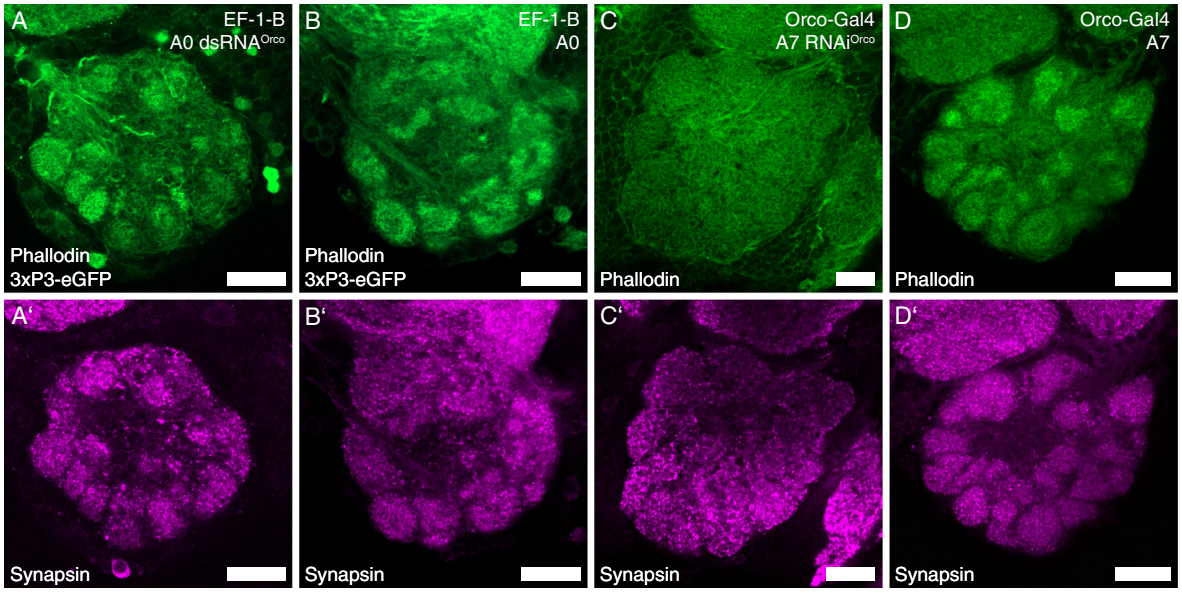

Fig. 7 Antennal lobe (AL) glomeruli after larval *RNAi*^{Orco}. *R*epresentative single optical slices of the AL of freshly eclosed (A0) beetles of the EF-1-B line (**A**, **A'**, **B**, **B'**) and 7-day-old beetles (A7) of the Orco-GAL4 line (**C**, **C'**, **D**, **D'**) after *dsRNA*^{Orco} injection in late larvae with comparison to wildtype beetles visualized by phalloidin (**A**–**D**; green) and synapsin (**A'**–**D'**; magenta). **A**, **B** In freshly eclosed beetles, the AL glomeruli are clearly visible in the phalloidin and synapsin staining under both conditions. **c**, **d** At A7 glomeruli are clearly visible in both stainings in untreated beetles, while glomeruli in knockdown beetles are hardly visible in the phalloidin staining, and only vague glomeruli are visible in the synapsin staining. Scale bars 20 μm

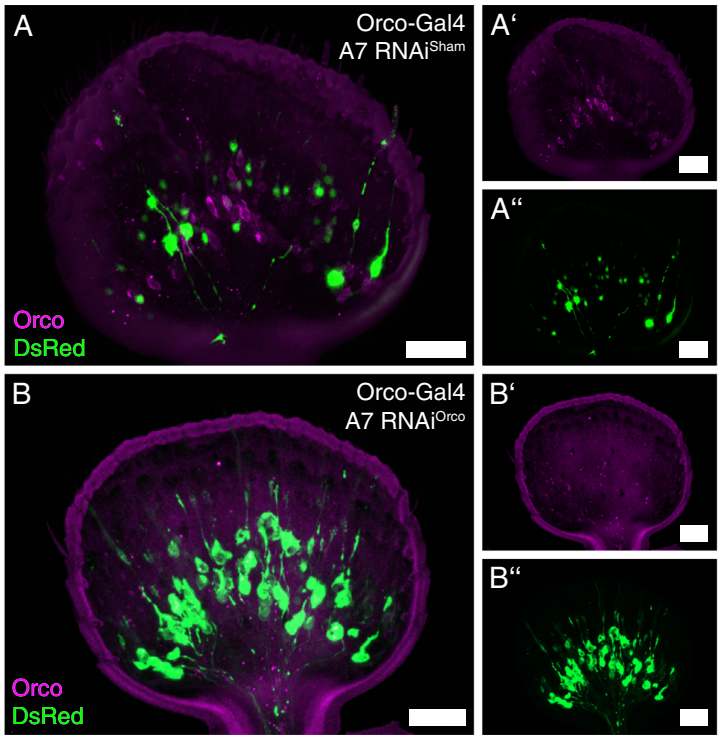

Fig. 8 Olfactory sensory neurons and Orco immunoreactivity in the antennae after larval *RNAi* induction. Representative maximum projections of 50 µm cryo-section of antennae of seven days old beetles (A7) in the Orco-GAL4 line after $dsRNA^{Sham}$ (**A**-**A''**) and $dsRNA^{Orco}$ (**B**-**B''**) injection in late larvae. The reporter signal of the transgenic line is depicted in green, while the Orco immunostaining is depicted in magenta. Scale bars 20 µm

Injection of EdU at P0% with dissection at A0 and EdU injection at different metamorphic stages (P20%, P50%, P70%, P80%) with subsequent dissection after 24 h did not result in labeled neurons within the AL, while in the same specimen labeled cells and thus presumably newborn neurons are found in the mushroom bodies and optic lobes (data not shown).

Glomeruli of the gnathal olfactory center (GOC)

In the red flour beetle, palpal olfactory input is not processed within the AL as in *D. melanogaster* but in the LGs and the GOC [5]. The GOC is already present as glomerularly organized neuropil in the first larval stage (L1) (Fig. 10A). The glomeruli vanish during the last larval stage (Fig. 10B) and are no longer distinguishable in the early pupae (P10%; Fig. 10C). At pupal stage P30%, a non-glomerular GOC is clearly distinguishable in the phalloidin staining (Fig. 10D). At about mid-metamorphosis (P50%), incipient glomerulization becomes visible in the phalloidin staining (Fig. 10E). About 30 h later, at stage P70% (Fig. 10F), the glomerulization becomes more clearly visible in the f-actin staining (Fig. 10F). Glomerulization is clearly visible another 35 h later at P95% (Fig. 10G).

Apis mellifera AL LNs

In adult honeybees, all AST-A immunoreactive neurons are co-labeled with an anti-GABA antiserum. They are a subpopulation of the inhibitory GABA local neuron network in the ALs [71]. We used immunohistochemical labeling of AST-A expressing neurons to follow the development of the AL LN subpopulation.

In pupal stage P1 (P10%), first, stained fibers are visible in the AL (Additional file 7: Figure S5 A). First somata become visible at stage P2 (P20%; Additional file 7: Figure S5 B, C), and their number rises after glomeruli formation. Incipient glomeruli formation becomes first visible in the AST-A staining at P4 (P40%; Additional file 7: Figure S5 D). At P50%, glomerulization is obvious (Additional file 7: Figure S5 E). Innervation of the olfactory glomeruli then increases throughout metamorphosis (Additional file 7: Figure S5 F, G) and eventually reaches the adult pattern (Additional file 7: Figure S5 H).

Trebels *et al. BMC Biology* (2021) 19:155

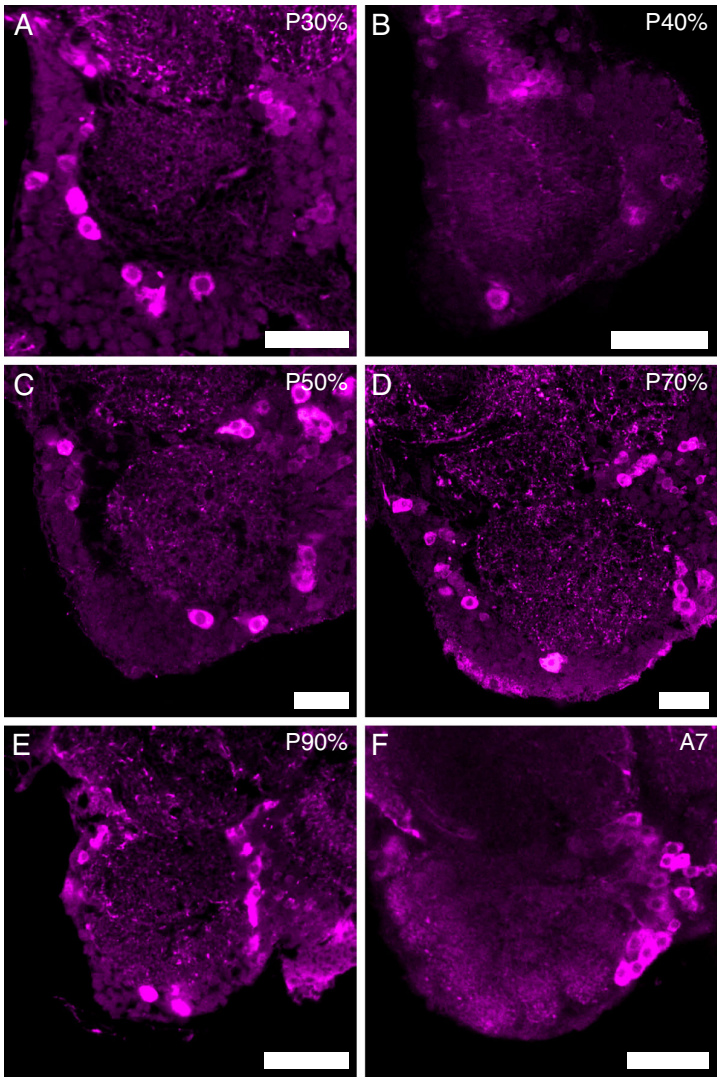

Fig. 9 GAD immunostaining in the developing AL. Representative single optical slices of the antennal lobes stained against GAD (pupae: GADr; adults: GADs) at different time points during metamorphosis (P30%, P50%, P70%, P90%) and adult stage A7. Scale bars 20 μm

Discussion

The anatomy of the adult olfactory system of the red flour beetle *T. castaneum* is well described [5]. To date, information about the metamorphic development and the origin of the structures of the olfactory system in *T. castaneum* is not and in beetles generally rarely available [39, 72]. In the current developmental study, we asked at which stage of metamorphosis the structures of the olfactory system form and aimed to reveal the origins of OSNs and LNs. To accomplish this, we used a combination of immunohistochemical staining, reporter expression in the CSN-labeling EF-1-B-DsRed [73], and the OSN-labeling partial Orco-GAL4xUAS-DsRed [5] line, as well as neurogenesis detection with EdU [10] and systemic RNAi against *Orco*. An overview of the developmental events including an interspecies comparison is given in Fig. 11.

Development of the antennae and their sensory neurons

Starting at the periphery, we find a segmented larval antenna consisting of scape, pedicel, and a reduced flagellum (Fig. 1), as already described earlier [19, 20]. Analysis of the reporter signal in the transgenic lines showed that the distal large trichoid sensillum functions in chemosensation. This result fits previous studies that supposed a function in contact chemoreception [19].

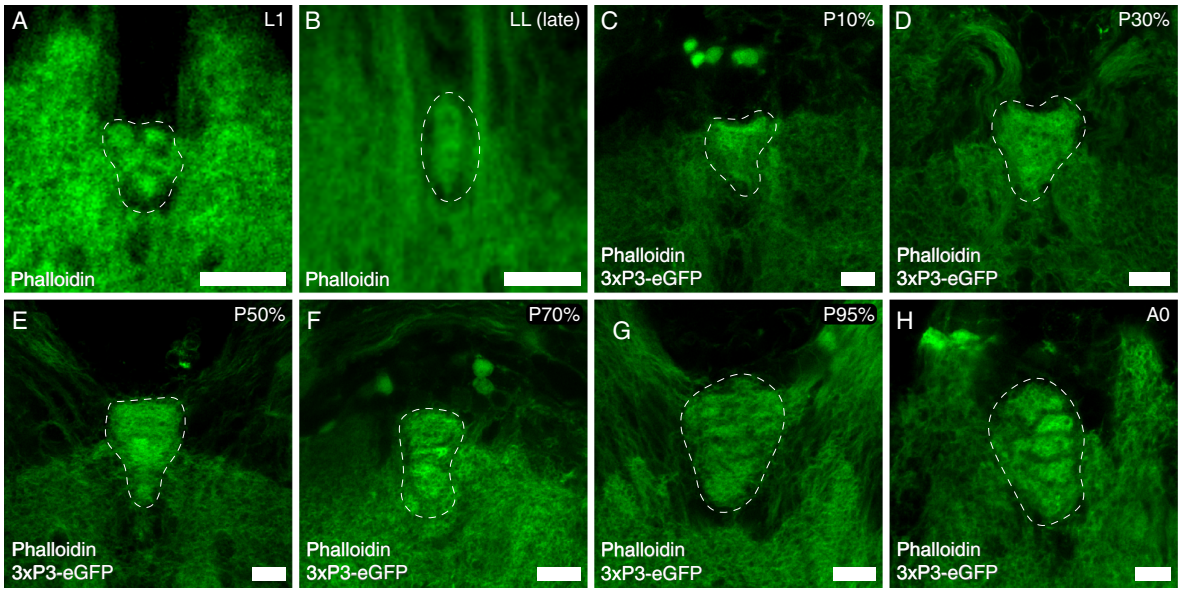

Fig. 10 Glomeruli formation within the gnathal olfactory center. Representative optical slices of the GOC at different developmental stages (L1 - first larval instar, LL - last larval instar, P - pupal stages, A0 - freshly eclosed), visualized by **A**, **B** phalloidin in the SB line and **C**–**H** phalloidin plus 3xP3-eGFP in the EF-1-B-DsRed line. Scale bars 10 μm

Trichoid sensilla, in general, might also act in mechanoreception and/or airborne chemoreception [74, 75]. As the distal large trichoid sensillum was not only labeled in the CSN-labeling EF-1-B DsRed line but also the OSN-labeling Orco-Gal4xUAS-DsRed line, we further suggest an olfactory function (Fig. 3A). This corresponds to the fact that also the adult antennae possess olfactory trichoid sensilla [5]. However, the main olfactory function of the larval antennae is provided via the placoid sensillum (Fig. 3A). It is considered a fusion of several basiconic sensilla [20], which again corresponds with the olfactory function of the basiconic sensilla on the beetle's adult antenna [5].

The gross structure of the larval antennae, with three distinguishable segments, is also described in the red flour beetle's close relative *T. molitor* [21] and other beetles [22–24]. It is similar to the structure of the larval antennae of *M. sexta* [25, 26], whereas flies possess functionally but not serially homolog appendages (dorsal organs) [27, 28]. Interestingly, lepidopterans and dipterans are phylogenetic sister groups [76]. Therefore, the presence of an elaborate larval antenna seems to be the more ancestral form. The current scientific picture sees the adult antennae of holometabolous insects as separate structures that develop from imaginal discs [29–31, 77–80], while the antennae of hemimetabolous insects develop gradually through larval molts until the adult stage [80, 81]. However, this derives from only a few species in essentially two orders: Diptera [29, 30, 79] and Lepidoptera [31, 77, 78, 82–89]. Both belong to the same phylogenetic branch, which is the sister branch to that including the Coleoptera [76].

In general, the development of adult structures from imaginal discs or cells in holometabolous insects is highly derived. In the more ancestral state, it is discussed that cells of the larval appendages are used to build their adult equivalents [34]. In the red flour beetle, this ancestral state is found during the development of the adult legs, which are built from reused polymorphic larval cells, while the legs of *D. melanogaster* are built from imaginal discs and those of *M. sexta* employing a mixture of reused larval cells and imaginal cells [35]. Consequently, it is concluded that the red flour beetle also lacks antennal imaginal discs from which the antenna may arise [36]. Our results indeed support the conclusion that the adult antennae of *T. castaneum* are not formed de novo from imaginal cells/discs but by reuse of polymorphic larval cells. We observed that during the last larval instar, the CSNs retract from the larval antennae and relocate into the head capsule, rather than dissolve as described in *D. melanogaster* [90, 91]. In the prepupal stage, they are then found in the tip of the freshly formed adult antennae (Fig. 4)—by this point still within the larval head cuticle (Additional file 1: Figure S1).

At pupal stage P0%, CSNs (Fig. 2) including OSNs (Fig. 3) are already located in the three distal segments of the flagellum, as they are in the adult beetle [5]. This finding is a major difference to results in *D. melanogaster*, where OSNs are not found in the antennae of fresh pupae but first at about 15% of metamorphosis [90]. The

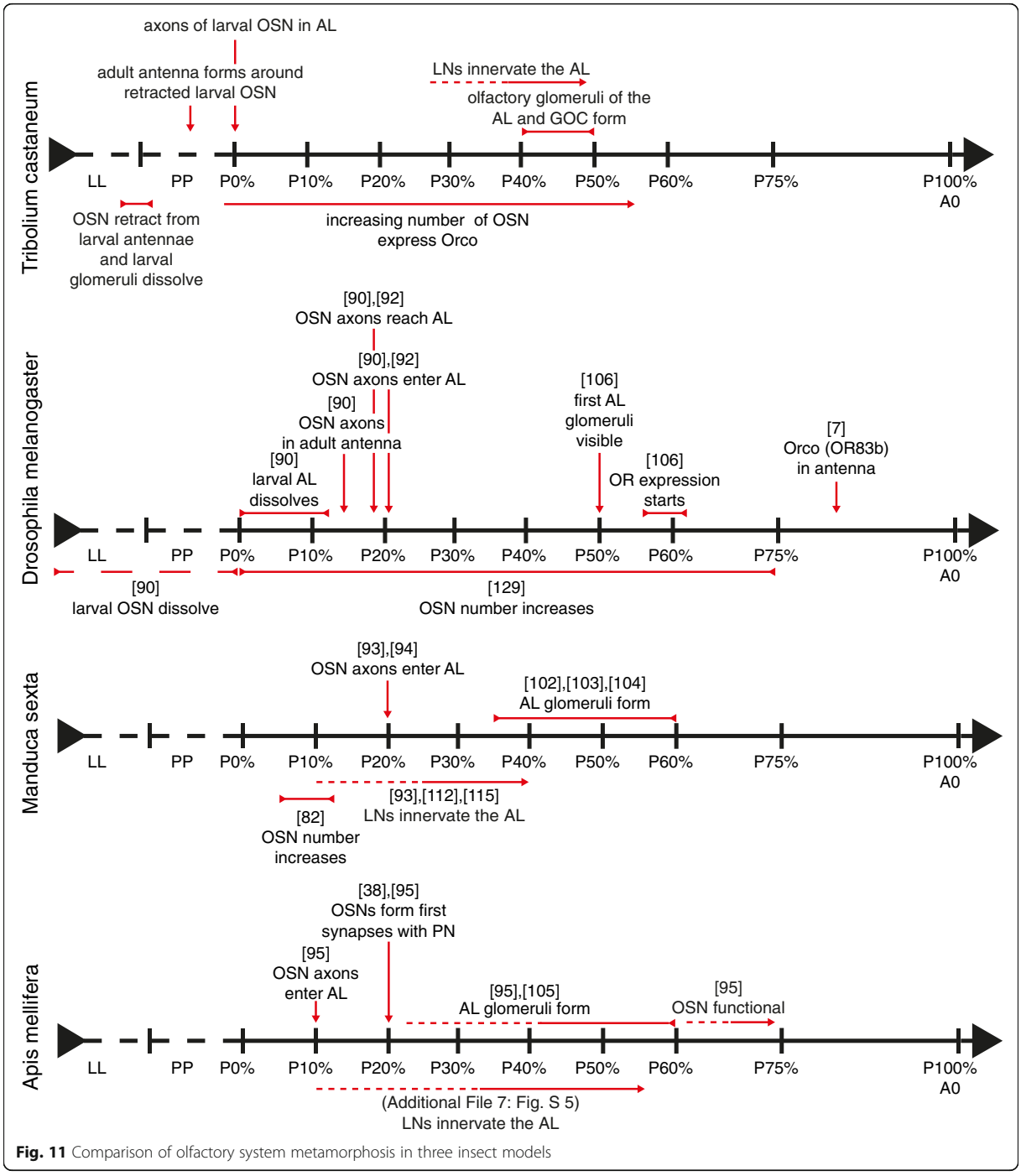

Fig. 11 Comparison of olfactory system metamorphosis in three insect models

OSN number then obviously rises until pupal stage P50%, when the gross distribution is akin to the adult one. We found that, in all pupal stages, the antennal nerves are present and already or still at P0% axonal terminals of the OSNs are found in the AL and remain detectable in all further pupal stages. This again contrasts results in *D. melanogaster*, where OSNs first reach and enter the AL at about P20% [90, 92], which is also found in *M. sexta* [93, 94], while they reach the AL at about P10% in *A. mellifera* [95].

This persistence of the OSN axons in the ALs, as well as in the GOC and LGs (Additional file 2: Figure S2)

leads us to the assumption that those neurons might serve as guidance for the newly born sensory neurons.

Formation of the olfactory glomeruli

Direct comparison of the f-actin staining via phalloidin and the immunostaining against synapsin showed that during most metamorphic stages, the AL glomeruli were more readily visible in the f-actin staining. For the analysis of the GOCs development, we therefore only used phalloidin staining of f-actin.

In general, f-actin seems to be heavily aggregated in olfactory glomeruli [96]. The same study showed that while f-actin in vertebrates is mostly located on the postsynaptic site, this is not true for insects. Examples from *M. sexta* and *A. mellifera* clearly show that the OSNs are labeled by phalloidin. They further showed that projection neurons do not contribute to the phalloidin staining within the glomeruli. Besides, f-actin serves a key role in neuronal growth and regulation of synaptic vesicle dynamics [97, 98]. Transferring these findings to the beetle, we conclude that the OSNs are in the first place responsible for the formation of glomeruli. This conclusion is supported by results from *M. sexta*, where de-antennation, and therefore lack of OSNs, prevents the formation of the olfactory glomeruli [42]. Further, results from ants clearly show that, without OSNs, the ALs are heavily reduced [43–45].

Unlike *M. sexta* [99] and *A. mellifera* [38], but similar to *D. melanogaster* [100], the larvae of *T. castaneum* possess glomerular organized ALs (Fig. 6A). Like the ALs, also the GOC in larvae is glomerularly organized (Fig. 10A). The larval ALs glomeruli dissolve before pupation, and as in other insects, e.g., *M. sexta* [101–104], *A. mellifera* [95, 105], or *D. melanogaster* [106, 107], the adult AL glomeruli form in the middle of metamorphosis (Fig. 11). Similarly, the adult glomeruli in the GOC form during metamorphosis (Fig. 10).

The glomeruli of the ALs and GOC become first visible in the f-actin staining at 40% of metamorphosis. Considering the functions of f-actin in neuronal growth and regulating synaptic vesicle dynamics [97, 98], at this time, the cytoskeleton of the synaptic structures within the ALs is likely formed. Since the AL glomeruli are first visible in the synapsin staining at P50%, it seems convincing, that only then, synaptic vesicles are recruited, and the first functional synapses are formed.

In *M. sexta,* the process of glomeruli formation was shown to be triggered by a rising 20E titer in the hemolymph [108]. This rise is also present in pupae of *T. castaneum*. In the beetle, a sharp titer increase occurs between P40% and P50% [109]. With roughly 70, the number of glomeruli found at P50% resembles the number found in freshly eclosed beetles [70], increasing to about 90 glomeruli in 7-day-old beetles [5]. Therefore, a basic set of AL glomeruli seems to be genetically encoded and built during metamorphosis. However, after adult eclosion, modifications seemingly occur.

We find Orco expression in the OSNs during all metamorphic stages, which is similar to results in the lepidopteran *Spodoptera litura* (cotton leafworm) [110] and the hymenopteran *Ooceraea biroi* (clonal raider ant) [43]. In contrast, in the dipteran *D. melanogaster,* Orco vanishes before pupation and becomes first detectable again after the formation of the AL glomeruli at about P80% [7] (Fig. 11). This led to the conclusion that Orco, and therefore functional olfactory receptors, are not necessary for the formation of AL glomeruli [7, 46, 47]. In ants, the lack of Orco leads to heavily reduced glomeruli numbers in the AL and total numbers of OSNs [44, 45]. Therefore, the authors conclude that the reduced ALs are an effect of the missing OSNs rather than a direct effect of Orco lacking, which is also supported by a more recent study [43].

To learn about the role of Orco during the metamorphic development in the red flour beetle, we used RNAi interference (RNAi). This results in a nearly complete knockdown of Orco, which results in a massive reduction of Orco-dependent odor responses [10]. Contrasting a knock-out, which is generally present from embryogenesis onwards, the RNAi-mediated knockdown, induced by dsRNA injection [5, 10, 111], has the advantage to be induced at any time. For example, as we did, just before pupation in late larvae. We find that at A0, glomerulization is still clearly visible in knockdown beetles (Fig. 7A), while a heavily reduced glomerulization could be observed at A7 (Fig. 7C). Notably, at both ages, the OSNs still locate normally in the antennae (Fig. 8A; Additional file 6: Figure S4 A). Therefore, we suggest that Orco is not necessary for the initial formation of olfactory glomeruli and their maturation during metamorphosis. However, OR/Orco driven olfactory activity seems to be necessary during the differentiation and adaption of the olfactory system after adult eclosion.

Origin and metamorphosis of the AL local neurons (LNs)

The vast majority of the AL LNs are GABAergic [13, 37, 60, 69] but also express various neuropeptides, which may also provide an estimate for LN numbers [13, 66, 67, 71, 112, 113].

In the red flour beetle, we identified GABAergic neurons by immunohistochemical staining of GAD. Labeled LNs locate in a cluster lateral to the AL, which is comparable to the "antero-dorsal DC cluster" (CL7) described in *Tenebrio molitor* [39]. In the first half of metamorphosis, the number of labeled neurons is relatively stable. It is first, after glomeruli formation, at

mid-metamorphosis, that their number rises. We used neurogenesis detection via the EdU technique [10] to reveal the origin of the rising LN numbers and did not find evidence for newly born neurons. Thus, we conclude that all AL LNs in the red flour beetle are of larval or embryonic origin and gain transmitter identity during metamorphosis. Further, the majority of LNs being recruited coinciding with glomeruli formation might be a common feature, as also most LNs of *M. sexta* ALs seem to be recruited just after the onset of glomeruli formation [112–114].

Similar to GABA immunostaining in *T. molitor* [39], we could first observe a glomerular pattern in the GAD staining in adult *T. castaneum*. Nevertheless, immunoreactive fibers were already visible within the AL volume at stage P30% (Fig. 9A), which corresponds to results from *M. sexta*, where GABAergic fibers are present in the AL at P20% [115]. In *M. sexta*, AST-A immunoreactive fibers occur at stage P10% [112]—just when the LNs start innervating the AL [93]. Similarly, in the honeybee's ALs, AST-A immunoreactive fibers are found at stage P10% (Additional file 7: Figure S5 A). In *M. sexta* both, GABA and AST-A fibers enter the forming glomeruli at P35% [112, 115]. The same is true for AST-A immunoreactive fibers in the honey bee, which enter the forming glomeruli around P40% (Additional file 7: Figure S5 D). Thus, the LN fibers entering the ALs before glomeruli formation seem to be a common feature.

Conclusions

In our study, we provide evidence that the adult antennae of the red flour beetle are built from reused polymorphic larval cells, that the CSNs of the beetle's larval antennae are reused in the adult antennae, and that the larval antennal lobe gets transformed into its adult version. OSN axons are present in the ALs during the whole process. Further, we find that Orco is seemingly not necessary during the initial formation of the AL glomeruli, while the activity of Orco expressing OSNs seems to be required during differentiation after adult eclosion. Comparing our results from the beetle to other model insects, it seems that some features, such as the timepoint of adult glomeruli formation or ingrowth of the AL LNs, are common among insects, while others, e.g., development of sensory appendages or the role of Orco seem to differ. These differences among species should be a reminder to be careful on using generalizations derived from results in a specific insect.

Methods

Animals

Experiments were performed using red flour beetles (*Tribolium castaneum*, Herbst 1797; Insecta, Coleoptera) of the wild-type strain "San Bernadino" [116], the transgenic EF1-B-DsRed line (elongation factor1-alpha regulatory region-DsRedExpress; kindly provided by Michalis Averof, Institut de Génomique Fonctionnelle de Lyon, France) [5, 73], or the partial Orco-Gal4 line [5].

The beetles were bred under constant darkness at about 30°C (wildtype) or 28°C (transgenes) and 40–50% relative humidity on organic whole grain wheat flour supplemented with 5% dried yeast powder and 0.05% Fumagilin-B (Medivet Pharmaceuticals Ltd., High River, Alberta, Canada) to prevent sporozoan infections [117].

Pupae of the San Bernadino wildtype were staged using external markers, like eye development and sclerotization of elytra and appendages using a refined version (Additional file 8: Figure S6) of a previously published staging scheme [118, 119]. Due to missing eye color, transgenic beetles were collected at P0% and reared to the desired ages according to a conversion table based upon data collected by time-lapse recordings of total metamorphosis at 28°C.

For the Orco-knockdown experiments, injected individuals were separated as pupae into 5-ml glass vials containing about a 2-g substrate and reared to the desired age.

For the bee experiments, we used the western honeybees (*Apis mellifera*). Honeybee breeding combs (kindly provided by Stefan Berg and Ralph Buechler, Bieneninstitut Kirchhain, Landesbetrieb Landwirtschaft Hessen, Kirchhain, Germany; and Wolfgang Roessler; University of Wuerzburg, Wuerzburg, Germany) were kept under constant darkness at about 34°C, and individual pupae were removed from their comb and staged against a previously published scheme [105].

EdU injections

5-Ethynyl-2′-desoxuridine (EdU) injections followed a previously published protocol [10]. Cold anesthetized larvae and pupae of different ages were placed in a chilled metal block. Injection of a 100-μM EdU-solution was performed using glass micropipettes made from thin-walled glass capillaries (TW150-4, World Precision Instruments, Sarasota, FL, USA; micropipette puller: Sutter Model P-30, Sutter Instrument, Novato, CA, USA) attached to a pressure ejection system (PDES-02T; npi electronics, Tamm, Germany) until individuals were slightly inflated. After injection, the beetles were transferred into a para-film sealed Petri dish and incubated at 28°C.

Immunohistochemistry and EdU detection

EdU detections, as well as immunohistochemistry, followed previously published protocols (*T. castaneum* [10, 70]; *A. mellifera* [120]).

For histochemical analysis, dissected ganglia were fixed in either 4% paraformaldehyde or 4% formaldehyde. Due

to their larger size, after fixation, honeybee brains were embedded into a gelatin/albumin medium which was hardened overnight in 4 or 8% formaldehyde in PBS at 4°C. Afterward, blocks were cut into 40-μm sections using a vibratome (VT1000S, Leica Biosystems, Nussloch, Germany).

Blocking was performed either in 5% normal goat serum (NGS; Jackson ImmunoResearch, Westgrove, PA, USA) or normal donkey serum (NDS; Jackson ImmunoResearch) based on the primary antisera (for concentrations and details see Table 1).

Wholemounts of ganglia were mounted either aqueous in the Mowiol [121] or after dehydration in an ascending ethanol series and clearing with methyl salicylate (Merck KGaA, Darmstadt, Germany) in Permount mounting medium (Fisher Scientific, Pittsburgh, PA) between two coverslips using reinforcing rings as spacers to prevent squeezing. Vibratome sections were dehydrated in an ascending ethanol series and cleared in xylol, before being mounted in Entellan (Merck) between a microscope slide and a coverslip.

Western blotting

To demonstrate the specificity of the used anti-GAD antibodies in *T. castaneum*, western blot analysis was performed as previously described [113]. Twenty brains were dissected and homogenized in 20 μl reducing sample buffer and boiled for 5 min. A 10 μl of the sample was loaded and run on a discontinuous 10% SDS polyacrylamide gel and blotted onto Optitran BA-S 83 nitrocellulose membranes (Carl Roth GmbH & Co. KG, Karlsruhe, Germany). After blocking, the membrane was incubated with the GAD antisera (1:10,000) overnight at 4°C, washed, and incubated with HRP conjugated anti-sheep/rabbit secondary antibody (1:1,000; see Table 1) for 2 h at room temperature. Finally, the blot was incubated with chemiluminescent substrate (SuperSignal™ West Pico, Thermo Fischer Scientific, Rockford, IL,

Table 1 Overview of used antibodies and markers

Name	Abbreviation	Host species	Dilution	Vendor/donor (catalogue #, batch #, RRID/CAS #)	References	Specificity
5-Ethynyl-2′-desoxuridine	EdU		100 μM	Thermo Fischer Scientific, Rockford, IL, USA (A10044; 1259424; 61135-33-9)	[122, 123]	
Alexa Fluor 488-coupled phalloidin	Phalloidin		1:200	Thermo Fischer Scientific, Rockford, IL, USA (A12379; n/a; n/a)	[124]	
Alexa Fluor 488 Azide	488-azide		1 μM	Thermo Fischer Scientific, Rockford, IL, USA (A10260; 1320994; n/a)		
Cy2-coupled donkey anti-sheep	DAS-Cy2	Donkey	1:300	Jackson ImmunoResearch; Westgrove, PA, USA (713-225-147, n/a, AB_2340735)		
Cy3-coupled goat anti-chicken	GACh-Cy3	Goat	1:300	Jackson ImmunoResearch; Westgrove, PA, USA (103-165-155, 93117 / 139580, AB_2337386)		
Cy3-coupled goat anti-rabbit	GAR-Cy3	Goat	1:300	Jackson ImmunoResearch; Westgrove, PA, USA (111-165-144, n/a, AB_2338006)		
Cy5-coupled donkey anti-mouse	DAS-Cy5	Donkey	1:300	Jackson ImmunoResearch; Westgrove, PA, USA (715-005-150,132236, RB_2340758)		
Cy5-coupled goat anti-mouse	GAM-Cy5	Goat	1:300	Jackson ImmunoResearch; Westgrove, PA, USA (115-175-146, n/a, AB_2338713)		
Cy5-Sulfo Azide	Cy5-azide		1 μM	Jena Bioscience, Jena, Germany (CLK-AZ118-1; Kli009-030; n/a)		
Diploptera punctata Allatostatin I	Dip-AST	Rabbit	1:20,000	H.J. Agricola (Friedrich Schiller University, Jena, Germany) (n/a, n/a, AB_2314318)	[125]	Ame: [71]
Drosophila melanogaster Synapsin I (SYNORF1)	Synapsin	Mouse	1:50	E. Bucher, University of Würzburg, Germany (n/a, n/a, AB_2313617)	[126]	Ame: [127] Tcas: [113]
HRP-coupled donkey anti-sheep	DAS-HRP	Donkey	1:1,000	Jackson ImmunoResearch; Westgrove, PA, USA (713-035-147, 69205, AB_2340710)		
HRP-coupled goat anti-rabbit	GAR-HRP	Goat	1:1,000	Jackson ImmunoResearch; Westgrove, PA, USA (111-035-003, 130223, AB_2313567)		
Moth-R2, Orco antiserum	Moth-R2	Rabbit	1:5,000	J. Krieger, University Halle-Wittenberg, Germany (n/a; n/a; n/a)	[5]	Tcas: [5]
Rattus norvegicus glutamate decarboxylase (rabbit)	GADr	Rabbit	1:1,000	Sigma-Aldrich; now Merck KGaA, Darmstadt, Germany (G5163; 113M4772; AB_477019)		Tcas: This study by Western blot
Rattus norvegicus glutamate decarboxylase (sheep)	GADs	Sheep	1:5,000	W. Oertel, Laboratory of Clinical Science, Mansfield, MA, USA (n/a; n/a; AB_2314497)	[128]	Tcas: This study by Western blot
Red fluorescent protein	RFP	Chicken	1:3,000	Rockland Immunochemicals INC, Limerick, PA, USA (600-901-379, 26274, AB_10704808)		

USA) and either exposed to Amersham Hyperfilm ECL (GE Healthcare Europe GmbH, Freiburg, Germany) and digitized with a flatbed scanner (9900F Mark II, Canon Inc, Tokyo, Japan) or imaged using a CCD image system (Image Station 440CF, Kodak Digital Science, Rochester, NY, USA). A single band at about 55 kDa was recognized for the sheep antibody, as well as for the rabbit antibody matching to the predicted size of Tcas-GAD (UniProt ID: D6WRJ1) of about 58 kDa (Additional file 9: Figure S7).

Orco-knockdown

Tcas-orco-5´ (1067 bp) dsRNA (*RNAi*^{Orco}) and *Cmor-MIP2* dsRNA (*RNAi*^{Sham}) were synthesized from PCR templates following a previously published protocol [5], using the HiScribe T7 High Yield RNA Synthesis Kit (New England Biolabs, Ipswich, MA, ISA). Both dsRNAs (about 0.3 to 0.5 μg/μl in injection buffer) were injected with the same setup as used for EdU injection into last-stage larvae (LL) until individuals were slightly stretched. The Orco knockdown was verified by immunohistochemistry against Orco (Moth-R2, kindly provided by J. Krieger, University of Hohenheim, Germany) on cryosections of antennae (Additional file 6: Figure S4) as previously published [5, 10].

Image acquisition and analysis

Fluorescent preparations were imaged using a confocal laser scanning microscope (TCS SP2 or TCS SP5, Leica Microsystems, Wetzlar, Germany) and analyzed with Amira 6.5 graphics software (FEI SAS a part of Thermo Fisher Scientific, Mérignac Cedex, France). In Amira, AL glomeruli numbers were acquired through manual 3D reconstruction and LN cell bodies were manually counted using the "landmark" tool.

Images of larvae and pupae were acquired in Progress Capture Pro 2.10 (Jenoptik, Jena, Germany) using a CCD camera (Progress C4 or C12plus, Jenoptik) attached to a (fluorescence) stereomicroscope (Stereo Lumar.V12, Carl Zeiss Microscopy, Jena Germany; Wild M3, Herbrugg, CH).

Further image processing (global level adjustments, contrast, and brightness optimization) was performed in Photoshop CC (Adobe Systems, San Jose, CA, USA), while final figure arrangements were made in Illustrator CC (Adobe Systems).

For basic statistics (arithmetic mean and standard deviation) on the number of immunoreactive local neurons, we used Excel 2019 (Microsoft Corporation, Redmond, WA, USA).

Time-lapse series

Time-lapse series images were acquired as stated above for larvae and pupae, but in a temperature-controlled environment at about 30°C. Afterward, images were further processed (cropping, global level adjustments; contrast, and brightness optimization) in Photoshop CC. Graphical annotations were prepared in Illustrator CC and final video assembly, and annotations were performed using Premiere CC (Adobe Systems).

Supplementary Information

The online version contains supplementary material available at https://doi.org/10.1186/s12915-021-01055-8.

Additional file 1: Figure S1. Localization of the adult appendages and sensory neurons in the head capsule of the prepupa. (A-A') Stereo microscopic image in ventral view of a prepupa with the opened larval head capsule, showing the location of the adult appendages within the prepupal head capsule, as well as the location of the CSNs in the adult antennae. (B) Schematic drawing of the location of the adult head within the prepupal head capsule in dorsal view. (C, D) Confocal image of the DsRed reporter signal (magenta) of the EF-1-B-line (C) and Orco-Gal4xUAS-DsRed-line (D), showing the position of the CSNs / OSNs cell cluster in the intact head capsule of prepupae. Scale bars 50 μm.

Additional file 2: Figure S2. OSNs in primary processing centers at P0%. Representative optical slices showing the DsRed reporter signal (magenta) of the Orco-GAL4 line, indicating OSNs, counterstained with phalloidin (green) to visualize the general neuroarchitecture. Scale bars 10 μm.

Additional file 3: Video S1. Timelapse of OSN development (whole head capsule). Visualized by the fluorescent reporter in the Orco-Gal4 x UAS-DsRed line covering approximately the first 30 hours of metamorphosis.

Additional file 4: Video S2. Timelapse of antennal OSN development (single antenna). Visualized by the fluorescent reporter in the Orco-Gal4 x UAS-DsRed line covering approximately the first 30 hours of metamorphosis.

Additional file 5: Figure S3. Orco in the antennae before glomeruli formation. Confocal maximum projection of 50μm slice a P10% antenna showing OSNs labeled by immunohistochemistry using the crossreactive Moth-R2 antiserum. Scale bars 50μm.

Additional file 6: Figure S4. Immunohistochemical Orco knock-down verification. Representative maximum projections of 50 μm cry-sections of the antennae of freshly eclosed (A0) beetles of the CSN-labeling EF-1-B-DsRed line after (A) *RNAi*^{Orco} and (B) *RNAi*^{Sham} injection. (A – A", B – B") The DsRed reporter signal is depicted in green, while Orco immunostaining is depicted in magenta. This channel also includes the autofluorescence of the antennal cuticle. In both treatment groups, the gross CSN distribution is very similar, while Orco cannot be detected in the *RNAi*^{Orco} group (A). Scale bars 20 μm.

Additional file 7: Figure S5. Development of AST-A immunoreactivity in the AL of *Apis mellifera*. Representative optical slices of AST-A immunoreactivity in the AL of A. mellifera workers at different developmental stages. (A) In the AL of P10% pupae, AST-A fibers are restricted to the lateral portion of the AL. (B, C) At P20% AST-A fibers penetrate the AL. (D) At P40% immunoreactive fibers locate in most of the forming glomeruli. (E-H) From P50% AST-A immunoreactivity shows clearly distinguishable glomeruli, which grow until adult eclosion. Scale bars 40μm.

Additional file 8: Figure S6. Staging of wild-type beetles during metamorphosis. The comparison of time-lapse recordings of nine pupae led to an averaged time for the metamorphosis of 126 h (5,25 d) at 30°C with a deviation of 5,3 h. The development of the eyes [118, 119], as well as the sclerotization of mandibles, elytra, and legs, served as external markers, in a time-dependent context. The fresh eclosed pupae are brighter and glossy with a maximum of three rows of ommatidia. After about 20% (25 h after pupa formation (APF)), about six rows of ommatidia are visible and form a kidney-shaped eye. At 30% (40 h APF) the

formation of the seventh row is in progress and the distance between the ommatidia shrinks. At about 50% all ommatidia are visible and outgrowth to the sides of the antennal pocket, thus the eyes look horseshoe-shaped. After 68% (86 h APF; SD 2,6 h) the outlines of ommatidia are resolved and the eye appears homogeneous. Besides the eye, at 76% (96 h APF, SD 3,6 h) the majority of mandibles are amber followed by the coloration of the elytra at 85% (106 h APF, SD 2,9 h) and sclerotization of the legs and antennae at 91% (114 h APF, SD 3.3). Finally, the imago eclosed after 126 h (SD 5.3 h).

Additional file 9: Figure S7. Specificity of the used antisera against GAD. Western blot analysis on *Tribolium castaneum* brain tissue shows a single band of about 55 kDa for both antibodies which corresponds to the predicted size of Tcas-GAD (UniProt ID: D6WRJ1) of about 58 kDa.

Acknowledgements
We thank Jürgen Krieger for providing the cross-reactive Orco antiserum; Hans-Jürgen Agricola for providing the cross-reactive Dip-AST antiserum; Gregor Bucher and Michaelis Averof for sharing transgenic beetle lines; Stefan Berg, Ralph Buechler, and Wolfgang Roessler and his lab for their generous support with honey bee combs and handling; and Martina Kern and Dr. Thorsten Stehlik for technical assistance and expertise.

Authors' contributions
B.T. and S.D. conceived and designed the study; acquired, analyzed, and interpreted the data; and drafted and revised the article; B.G., M.G., C.H., F.H., F.S., M.U., M-P.V., and V.W. acquired and analyzed the data; J.S. conceived and designed the study, analyzed and interpreted the data, and drafted and revised the article. The authors read and approved the final manuscript.

Funding
Parts of this study were funded within the Deutsche Forschungsgemeinschaft SPP 1392: SCHA 678/13-1 (J.S.). The funders had no role in the study design, data collection, interpretation, or the decision to submit the work for publication. Open Access funding enabled and organized by Projekt DEAL.

Availability of data and materials
The datasets generated and/or analyzed during the current study are either included in this published article and its additional files and/or available in the University of Marburg's institutional data (data_UMR) repository at https://data.uni-marburg.de/handle/dataumr/73 [129–137].

Declarations

Ethics approval and consent to participate
All experiments involving animals were performed in compliance with the guidelines of the European Union (Directive 2010/63/EU). As all experiments were on insects, approval of the study by an ethics committee was unnecessary.

Consent for publication
Not applicable.

Competing interests
The authors declare that they have no competing interests.

Author details
[1]Department of Biology, Animal Physiology, Philipps-University Marburg, Karl-von-Frisch-Str. 8, 35032 Marburg, Germany. [2]Clausthal University of Technology, Adolph-Roemer-Str. 2a, 38678 Clausthal-Zellerfeld, Germany.

Received: 28 December 2020 Accepted: 25 May 2021
Published online: 30 July 2021

References
1. Sato K, Pellegrino M, Nakagawa T, Nakagawa T, Vosshall LB, Touhara K. Insect olfactory receptors are heteromeric ligand-gated ion channels. Nature. 2008;452(7190):1002–6. https://doi.org/10.1038/nature06850.
2. Wicher D, Schäfer R, Bauernfeind R, Stensmyr MC, Heller R, Heinemann SH, et al. Drosophila odorant receptors are both ligand-gated and cyclic-nucleotide-activated cation channels. Nature. 2008;452(7190):1007–11. https://doi.org/10.1038/nature06861.
3. Benton R, Vannice KS, Gomez-Diaz C, Vosshall LB. Variant ionotropic glutamate receptors as chemosensory receptors in Drosophila. Cell. 2009; 136(1):149–62. https://doi.org/10.1016/j.cell.2008.12.001.
4. Missbach C, Dweck HK, Vogel H, Vilcinskas A, Stensmyr MC, Hansson BS, et al. Evolution of insect olfactory receptors. eLife. 2014;3:e02115. https://doi.org/10.7554/eLife.02115.
5. Dippel S, Kollmann M, Oberhofer G, Montino A, Knoll C, Krala M, et al. Morphological and transcriptomic analysis of a beetle chemosensory system reveals a gnathal olfactory center. BMC Biol. 2016;14(1):90. https://doi.org/10.1186/s12915-016-0304-z.
6. Butterwick JA, del Mármol J, Kim KH, Kahlson MA, Rogow JA, Walz T, Ruta, V. Cryo-EM structure of the insect olfactory receptor Orco. Nature. 2018;560: 447–52. https://doi.org/10.1038/s41586-018-0420-8.
7. Larsson MC, Domingos AI, Jones WD, Chiappe ME, Amrein H, Vosshall LB. Or83b encodes a broadly expressed odorant receptor essential for *Drosophila* olfaction. Neuron. 2004;43(5):703–14. https://doi.org/10.1016/j.neuron.2004.08.019.
8. DeGennaro M, McBride CS, Seeholzer L, Nakagawa T, Dennis EJ, Goldman C, et al. orco mutant mosquitoes lose strong preference for humans and are not repelled by volatile DEET. Nature. 2013;498:487–91.
9. Li Y, Zhang J, Chen D, Yang P, Jiang F, Wang X, et al. CRISPR/Cas9 in locusts: successful establishment of an olfactory deficiency line by targeting the mutagenesis of an odorant receptor co-receptor (Orco). Insect Biochem Mol Biol. 2016;79:27–35. https://doi.org/10.1016/j.ibmb.2016.10.003.
10. Trebels B, Dippel S, Schaaf M, Balakrishnan K, Wimmer EA, Schachtner J. Adult neurogenesis in the mushroom bodies of red flour beetles (*Tribolium castaneum*, Herbst) is influenced by the olfactory environment. Sci Rep. 2020;10:1–11.
11. Fandino RA, Haverkamp A, Bisch-Knaden S, Zhang J, Bucks S, Nguyen TAT, et al. Mutagenesis of odorant coreceptor Orco fully disrupts foraging but not oviposition behaviors in the hawkmoth Manduca sexta. Proc Natl Acad Sci USA. 2019;116:15677–85. https://doi.org/10.1073/pnas.1902089116.
12. Lin W, Yu Y, Zhou P, Zhang J, Dou L, Hao Q, et al. Identification and knockdown of the olfactory receptor (OrCo) in gypsy moth. Lymantria dispar. Int J Biol Sci. 2015;11(7):772–80. https://doi.org/10.7150/ijbs.11898.
13. Schachtner J, Schmidt M, Homberg U. Organization and evolutionary trends of primary olfactory brain centers in Tetraconata (Crustacea+ Hexapoda). Arthropod Struct Dev. 2005;34(3):257–99. https://doi.org/10.1016/j.asd.2005.04.003.
14. Anton S, Homberg U. Antennal Lobe Structure. In: Hansson BS, editor. Insect olfaction. Berlin, Heidelberg: Springer Berlin Heidelberg; 1999. p. 97–124.
15. Vosshall LB. Olfaction in Drosophila. Curr Opin Neurobiol. 2000;10(4):498–503. https://doi.org/10.1016/S0959-4388(00)00111-2.
16. Szyszka P, Galizia CG. Olfaction in Insects. In: Doty RL, editor. Handbook of olfaction and gustation. 3rd ed. Hoboken: Wiley; 2015. p. 531–46. https://doi.org/10.1002/9781118971758.ch22.
17. Riabinina O, Task D, Marr E, Lin C-C, Alford R, O'Brochta DA, et al. Organization of olfactory centres in the malaria mosquito Anopheles gambiae. Nat Commun. 2016;7(1):13010. https://doi.org/10.1038/ncomms13010.
18. Lin T, Li C, Liu J, Smith BH, Lei H, Zeng X. Glomerular organization in the antennal lobe of the oriental fruit fly Bactrocera dorsalis. Front Neuroanat. 2018;12:71. https://doi.org/10.3389/fnana.2018.00071.
19. Ryan MF, Behan M. The sensory receptors of *Tribolium* larvae. Physiol Zool. 1973;46(3):238–44. https://doi.org/10.1086/physzool.46.3.30155605.
20. Behan M, Ryan MF. Ultrastructure of antennal sensory receptors of *Tribolium* larvae (Coleoptera: Tenebrionidae). Int J Insect Morphol Embryol. 1978;7(3): 221–36. https://doi.org/10.1016/0020-7322(78)90005-3.
21. Bloom JW, Zacharuk RY, Holodniuk AE. Ultrastructure of the larval antenna of *Tenebrio molitor* L. (Coleoptera: Tenebrionidae): structure of the trichoid and uniporous peg sensilla. Can J Zool. 1982;60(7):1528–44. https://doi.org/10.1139/z82-202.
22. Corbière G. Anatomie sensorielle des appendices céphaliques de la larve du *Speophyes lucidulus* (Delar.)(Colèopteré cavernicole de la sous-famille des Bathysciinae). In: Annales de Spéléologie; 1967. p. 417–31.
23. Roppel RM, Arbogast RT, Zeigler JA. Antennal sensilla of the larval sawtoothed grain beetle, *Oryzaephilus surinamensis* (Coleoptera, Cucujidae). Rev Can Biol. 1972;31(1):9–20.
24. Zacharuk RY. Sense organs of the head of larvae of some Elateridae (Coleoptera): their distribution, structure and innervation. J Morphol. 1962; 111(1):1–33. https://doi.org/10.1002/jmor.1051110102.

25. Dethier VG. The function of the antennal receptors in lepidopterous larvae. Biol Bull. 1941;80(3):403–14. https://doi.org/10.2307/1537725.
26. Dethier VG, Schoonhoven LM. Olfactory coding by lepidopterous larvae. Entomol Exp Appl. 1969;12(5):535–43. https://doi.org/10.1111/j.1570-7458.1969.tb02551.x.
27. Chu I-W, Axtell RC. Fine structure of the dorsal organ of the house fly larva, *Musca domestica* L. Z Für Zellforsch Mikrosk Anat. 1971;117(1):17–34. https://doi.org/10.1007/BF00331098.
28. Singh RN, Singh K. Fine structure of the sensory organs of *Drosophila melanogaster* Meigen larva (Diptera : Drosophilidae). Int J Insect Morphol Embryol. 1984;13(4):255–73. https://doi.org/10.1016/0020-7322(84)90001-1.
29. Morata G, Lawrence PA. Development of the eye-antenna imaginal disc of *Drosophila*. Dev Biol. 1979;70(2):355–71. https://doi.org/10.1016/0012-1606(79)90033-2.
30. Haynie JL, Bryant PJ. Development of the eye-antenna imaginal disc and morphogenesis of the adult head in *Drosophila melanogaster*. J Exp Zool. 1986;237(3):293–308. https://doi.org/10.1002/jez.1402370302.
31. Sanes JR, Hildebrand JG. Structure and development of antennae in a moth, *Manduca sexta*. Dev Biol. 1976;51(2):282–99. https://doi.org/10.1016/0012-1606(76)90144-5.
32. Imms AD. Memoirs: on growth processes in the antennae of insects. J Cell Sci. 1940;s2-81:585–93.
33. Haas H. Untersuchungen zur Segmentbildung an der Antenne von *Periplaneta americana*, L. Wilhelm Roux Arch Für Entwicklungsmechanik Org. 1955;147(4-5):434–73. https://doi.org/10.1007/BF00575998.
34. Truman JW, Riddiford LM. Endocrine insights into the evolution of metamorphosis in insects. Annu Rev Entomol. 2002;47(1):467–500. https://doi.org/10.1146/annurev.ento.47.091201.145230.
35. Villarreal CM, Darakananda K, Wang VR, Jayaprakash PM, Suzuki Y. Hedgehog signaling regulates imaginal cell differentiation in a basally branching holometabolous insect. Dev Biol. 2015;404(2):125–35. https://doi.org/10.1016/j.ydbio.2015.05.020.
36. Smith FW, Angelini DR, Jockusch EL. A functional genetic analysis in flour beetles (Tenebrionidae) reveals an antennal identity specification mechanism active during metamorphosis in Holometabola. Mech Dev. 2014;132:13–27. https://doi.org/10.1016/j.mod.2014.02.002.
37. Hoskins SG, Homberg U, Kingan TG, Christensen TA, Hildebrand JG. Immunocytochemistry of GABA in the antennal lobes of the sphinx moth *Manduca sexta*. Cell Tissue Res. 1986;244(2):243–52. https://doi.org/10.1007/BF00219199.
38. Hähnlein I, Bicker G. Glial patterning during postembryonic development of central neuropiles in the brain of the honeybee. Dev Genes Evol. 1997;207(1):29–41. https://doi.org/10.1007/s004270050089.
39. Wegerhoff R. GABA and serotonin immunoreactivity during postembryonic brain development in the beetle *Tenebrio molitor*. Microsc Res Tech. 1999;45(3):154–64. https://doi.org/10.1002/(SICI)1097-0029(19990501)45:3<154::AID-JEMT3>3.0.CO;2-5.
40. Python F, Stocker RF. Adult-like complexity of the larval antennal lobe of *D. melanogaster* despite markedly low numbers of odorant receptor neurons. J Comp Neurol. 2002;445(4):374–87. https://doi.org/10.1002/cne.10188.
41. Prillinger L. Postembryonic development of the antennal lobes in *Periplaneta americana* L. Cell Tissue Res. 1981;215(3):563–75. https://doi.org/10.1007/BF00233532.
42. Boeckh J, Tolbert LP. Synaptic organization and development of the antennal lobe in insects. Microsc Res Tech. 1993;24(3):260–80. https://doi.org/10.1002/jemt.1070240305.
43. Ryba AR, McKenzie SK, Olivos-Cisneros L, Clowney EJ, Pires PM, Kronauer DJC. Comparative development of the ant chemosensory system. Curr Biol. 2020;30:3223–3230.e4.
44. Trible W, Olivos-Cisneros L, McKenzie SK, Saragosti J, Chang N-C, Matthews BJ, et al. orco Mutagenesis causes loss of antennal lobe glomeruli and impaired social behavior in ants. Cell. 2017;170:727–735.e10.
45. Yan H, Opachaloemphan C, Mancini G, Yang H, Gallitto M, Mlejnek J, et al. An engineered orco mutation produces aberrant social behavior and defective neural development in ants. Cell. 2017;170:736–747.e9.
46. Berdnik D, Chihara T, Couto A, Luo L. Wiring stability of the adult *Drosophila* olfactory circuit after lesion. J Neurosci. 2006;26(13):3367–76. https://doi.org/10.1523/JNEUROSCI.4941-05.2006.
47. Chiang A, Priya R, Ramaswami M, VijayRaghavan K, Rodrigues V. Neuronal activity and Wnt signaling act through Gsk3-β to regulate axonal integrity in mature *Drosophila* olfactory sensory neurons. Development. 2009;136(8):1273–82. https://doi.org/10.1242/dev.031377.
48. Maguire SE, Afify A, Goff LA, Potter CJ. A Feedback Mechanism Regulates *Odorant Receptor* Expression in the Malaria Mosquito, *Anopheles gambiae*. bioRxiv. 2020. https://doi.org/10.1101/2020.07.23.218586.
49. Bucher G, Scholten J, Klingler M. Parental RNAi in *Tribolium* (Coleoptera). Curr Biol. 2002;12(3):R85–6. https://doi.org/10.1016/S0960-9822(02)00666-8.
50. Tomoyasu Y, Denell RE. Larval RNAi in *Tribolium* (Coleoptera) for analyzing adult development. Dev Genes Evol. 2004;214(11):575–8. https://doi.org/10.1007/s00427-004-0434-0.
51. Tomoyasu Y, Miller SC, Tomita S, Schoppmeier M, Grossmann D, Bucher G. Exploring systemic RNA interference in insects: a genome-wide survey for RNAi genes in *Tribolium*. Genome Biol. 2008;9(1):R10. https://doi.org/10.1186/gb-2008-9-1-r10.
52. Stopfer M, Bhagavan S, Smith BH, Laurent G. Impaired odour discrimination on desynchronization of odour-encoding neural assemblies. Nature. 1997;390(6655):70–4. https://doi.org/10.1038/36335.
53. Sachse S, Galizia CG. Role of inhibition for temporal and spatial odor representation in olfactory output neurons: a calcium imaging study. J Neurophysiol. 2002;87(2):1106–17. https://doi.org/10.1152/jn.00325.2001.
54. Wilson RI, Laurent G. Role of GABAergic inhibition in shaping odor-evoked spatiotemporal patterns in the *Drosophila* antennal lobe. J Neurosci Off J Soc Neurosci. 2005;25(40):9069–79. https://doi.org/10.1523/JNEUROSCI.2070-05.2005.
55. Olsen SR, Bhandawat V, Wilson RI. Excitatory interactions between olfactory processing channels in the *Drosophila* antennal lobe. Neuron. 2007;54(1):89–103. https://doi.org/10.1016/j.neuron.2007.03.010.
56. Olsen SR, Bhandawat V, Wilson RI. Divisive normalization in olfactory population codes. Neuron. 2010;66(2):287–99. https://doi.org/10.1016/j.neuron.2010.04.009.
57. Shang Y, Claridge-Chang A, Sjulson L, Pypaert M, Miesenböck G. Excitatory local circuits and their implications for olfactory processing in the fly antennal lobe. Cell. 2007;128(3):601–12. https://doi.org/10.1016/j.cell.2006.12.034.
58. Silbering AF, Galizia CG. Processing of odor mixtures in the *Drosophila* antennal lobe reveals both global inhibition and glomerulus-specific interactions. J Neurosci. 2007;27(44):11966–77. https://doi.org/10.1523/JNEUROSCI.3099-07.2007.
59. Olsen SR, Wilson RI. Lateral presynaptic inhibition mediates gain control in an olfactory circuit. Nature. 2008;452(7190):956–60. https://doi.org/10.1038/nature06864.
60. Okada R, Awasaki T, Ito K. Gamma-aminobutyric acid (GABA)-mediated neural connections in the *Drosophila* antennal lobe. J Comp Neurol. 2009;514(1):74–91. https://doi.org/10.1002/cne.21971.
61. Tanaka NK, Ito K, Stopfer M. Odor-evoked neural oscillations in *Drosophila* are mediated by widely branching interneurons. J Neurosci. 2009;29(26):8595–603. https://doi.org/10.1523/JNEUROSCI.1455-09.2009.
62. Chou Y-H, Spletter ML, Yaksi E, Leong JCS, Wilson RI, Luo L. Diversity and wiring variability of olfactory local interneurons in the *Drosophila* antennal lobe. Nat Neurosci. 2010;13(4):439–49. https://doi.org/10.1038/nn.2489.
63. Root CM. Propagation and modulation of activity in early olfactory processing and its relevance to odor-driven behavior: Dissertation. San Diego: University of California; 2010. https://escholarship.org/uc/item/20q9w0st
64. Wilson RI. Early olfactory processing in *Drosophila* : mechanisms and principles. Annu Rev Neurosci. 2013;36(1):217–41. https://doi.org/10.1146/annurev-neuro-062111-150533.
65. Nagel KI, Hong EJ, Wilson RI. Synaptic and circuit mechanisms promoting broadband transmission of olfactory stimulus dynamics. Nat Neurosci. 2015;18(1):56–65. https://doi.org/10.1038/nn.3895.
66. Carlsson MA, Diesner M, Schachtner J, Nässel DR. Multiple neuropeptides in the *Drosophila* antennal lobe suggest complex modulatory circuits. J Comp Neurol. 2010;518(16):3359–80. https://doi.org/10.1002/cne.22405.
67. Binzer M, Heuer CM, Kollmann M, Kahnt J, Hauser F, Grimmelikhuijzen CJP, et al. Neuropeptidome of *Tribolium castaneum* antennal lobes and mushroom bodies. J Comp Neurol. 2014;522(2):337–57. https://doi.org/10.1002/cne.23399.
68. Siju KP, Reifenrath A, Scheiblich H, Neupert S, Predel R, Hansson BS, et al. Neuropeptides in the antennal lobe of the yellow fever mosquito, *Aedes aegypti*. J Comp Neurol. 2014;522(3):592–608. https://doi.org/10.1002/cne.23434.
69. Kay LM, Stopfer M. Information processing in the olfactory systems of insects and vertebrates. Semin Cell Dev Biol. 2006;17(4):433–42. https://doi.org/10.1016/j.semcdb.2006.04.012.

70. Dreyer D, Vitt H, Dippel S, Goetz B, El Jundi B, Kollmann M, et al. 3D standard brain of the red flour beetle *Tribolium castaneum:* a tool to study metamorphic development and adult plasticity. Front Syst Neurosci. 2010;4:3.
71. Kreissl S, Strasser C, Galizia CG. Allatostatin immunoreactivity in the honeybee brain. J Comp Neurol. 2010;518(9):1391–417. https://doi.org/10.1002/cne.22343.
72. Wegerhoff R. Metamorphic development of locusta-tachykinin immunoreactive neurons of the antennal lobes of the beetle Tenebrio molitor and the effect of fenvalerate application. Exp Biol Online. 1997;2(14):1–13. https://doi.org/10.1007/s00898-997-0014-7.
73. Posnien N, Koniszewski NDB, Bucher G. Insect Tc-six4 marks a unit with similarity to vertebrate placodes. Dev Biol. 2011;350(1):208–16. https://doi.org/10.1016/j.ydbio.2010.10.024.
74. Lewis CT. Structure and function in some external receptors. In: Roy Entomol Soc London Symp; 1970.
75. Schneider D, Steinbrecht RA. Checklist of insect olfactory sensilla. In: Symposia of the Zoological Society London; 1968. p. 279–97. http://hdl.handle.net/11858/00-001M-0000-002B-19CA-E.
76. Misof B, Liu S, Meusemann K, Peters RS, Donath A, Mayer C, et al. Phylogenomics resolves the timing and pattern of insect evolution. Science. 2014;346(6210):763–7. https://doi.org/10.1126/science.1257570.
77. Eassa YEE. Metamorphosis of the cranial capsule and its appendages in the cabbage butterfly, *Pieris brassicae*. Ann Entomol Soc Am. 1963;56(4):510–21. https://doi.org/10.1093/aesa/56.4.510.
78. Eassa YEE. The development of imaginal buds in the head of *Pieris Brassicae* Linn. (lepidoptera). Trans R Entomol Soc Lond. 1953;104:39–50.
79. Lienhard MC, Stocker RF. The development of the sensory neuron pattern in the antennal disc of wild-type and mutant (lz3, ssa) *Drosophila melanogaster*. Development. 1991;112(4):1063–75. https://doi.org/10.1242/dev.112.4.1063.
80. Svácha P. What are and what are not imaginal discs: reevaluation of some basic concepts (insecta, holometabola). Dev Biol. 1992;154(1):101–17. https://doi.org/10.1016/0012-1606(92)90052-I.
81. Schafer R. Postembryonic development in the antenna of the cockroach, *Leucophaea maderae*: growth, regeneration, and the development of the adult pattern of sense organs. J Exp Zool. 1973;183(3):353–63. https://doi.org/10.1002/jez.1401830309.
82. Sanes JR, Hildebrand JG. Origin and morphogenesis of sensory neurons in an insect antenna. Dev Biol. 1976;51(2):300–19. https://doi.org/10.1016/0012-1606(76)90145-7.
83. Waku Y. Developmental changes of the antenna and its neurons in the silkworm, *Bombyx mori*, with special regard to larval-pupal transformation. J Morphol. 1991;207(3):253–71. https://doi.org/10.1002/jmor.1052070304.
84. Steiner C, Keil TA. Morphogenesis of the antenna of the male silkmoth, *Antheraea polyphemus*. VI. Experimental disturbance of antennal branch formation. Tissue Cell. 1995;27(3):289–97. https://doi.org/10.1016/S0040-8166(95)80049-2.
85. Steiner C. Keil T a. Morphogenesis of the antenna of the male silkmoth, *Antheraea polyphemus*. V. Development of the peripheral nervous system. Tissue Cell. 1995;27(3):275–88. https://doi.org/10.1016/S0040-8166(95)80048-4.
86. Steiner C, Keil TA. Morphogenesis of the antenna of the male silkmoth, *Antheraea polyphemus*. IV. Segmentation and branch formation. Tissue Cell. 1993;25(3):447–64. https://doi.org/10.1016/0040-8166(93)90085-Y.
87. Keil TA, Steiner C. Morphogenesis of the antenna of the male silkmoth, *Antheraea polyphemus*. I. The leaf-shaped antenna of the pupa from diapause to apolysis. Tissue Cell. 1990;22(3):319–36. https://doi.org/10.1016/0040-8166(90)90007-V.
88. Keil TA, Steiner C. Morphogenesis of the antenna of the male silkmoth, *Antheraea polyphemus*. II. Differential mitoses of 'dark' precursor cells create the Anlagen of sensilla. Tissue Cell. 1990;22(5):705–20. https://doi.org/10.1016/0040-8166(90)90066-I.
89. Keil TA, Steiner C. Morphogenesis of the antenna of the male silkmoth. *Antheraea polyphemus*, III. Development of olfactory sensilla and the properties of hair-forming cells. Tissue Cell. 1991;23(6):821–51. https://doi.org/10.1016/0040-8166(91)90034-Q.
90. Jefferis GSXE. Developmental origin of wiring specificity in the olfactory system of *Drosophila*. Development. 2004;131(1):117–30. https://doi.org/10.1242/dev.00896.
91. Stocker RF. The organization of the chemosensory system in *Drosophila melanogaster*: a rewiew. Cell Tissue Res. 1994;275(1):3–26. https://doi.org/10.1007/BF00305372.
92. Jhaveri D, Sen A, Rodrigues V. Mechanisms underlying olfactory neuronal connectivity in *Drosophila* - the atonal lineage organizes the periphery while sensory neurons and glia pattern the olfactory lobe. Dev Biol. 2000;226(1):73–87. https://doi.org/10.1006/dbio.2000.9855.
93. Oland LA, Orr G, Tolbert LP. Construction of a protoglomerular template by olfactory axons initiates the formation of olfactory glomeruli in the insect brain. J Neurosci. 1990;10(7):2096–112. https://doi.org/10.1523/JNEUROSCI.10-07-02096.1990.
94. Oland LA, Tolbert LP. Glial patterns during early development of antennal lobes of *Manduca sexta*: a comparison between normal lobes and lobes deprived of antennal axons. J Comp Neurol. 1987;255(2):196–207. https://doi.org/10.1002/cne.902550204.
95. Schröter U, Malun D. Formation of antennal lobe and mushroom body neuropils during metamorphosis in the honeybee, *Apis mellifera*. J Comp Neurol. 2000;422(2):229–45. https://doi.org/10.1002/(SICI)1096-9861(20000626)422:2<229::AID-CNE6>3.0.CO;2-N.
96. Rössler W, Kuduz J, Schürmann FW, Schild D. Aggregation of f-actin in olfactory glomeruli: a common feature of glomeruli across phyla. Chem Senses. 2002;27(9):803–10. https://doi.org/10.1093/chemse/27.9.803.
97. De Camili P, Haucke V, Takei K, Mignani E. The structure of synapses. In: Cowan MW, Südhof TL, Stevens CF, editors. Synapses. Baltimore: Johns Hopkins University Press; 2001. p. 89–133.
98. Morales M, Colicos MA, Goda Y. Actin-dependent regulation of neurotransmitter release at central synapses. Neuron. 2000;27(3):539–50. https://doi.org/10.1016/S0896-6273(00)00064-7.
99. Tolbert LP, Oland LA, Tucker ES, Gibson NJ, Higgins MR, Lipscomb BW. Bidirectional influences between neurons and glial cells in the developing olfactory system. Prog Neurobiol. 2004;73(2):73–105. https://doi.org/10.1016/j.pneurobio.2004.04.004.
100. Ramaekers A, Magnenat E, Marin EC, Gendre N, Jefferis GSXE, Luo L, et al. Glomerular maps without cellular redundancy at successive levels of the *Drosophila* larval olfactory circuit. Curr Biol. 2005;15(11):982–92. https://doi.org/10.1016/j.cub.2005.04.032.
101. Dubuque SH, Schachtner J, Nighorn AJ, Menon KP, Zinn K, Tolbert LP. Immunolocalization of synaptotagmin for the study of synapses in the developing antennal lobe of *Manduca sexta*. J Comp Neurol. 2001;441(4):277–87. https://doi.org/10.1002/cne.1412.
102. Hildebrand JG, Rössler W, Tolbert LP. Postembryonic development of the olfactory system in the moth *Manduca sexta*: primary-afferent control of glomerular development. Semin Cell Dev Biol. 1997;8(2):163–70. https://doi.org/10.1006/scdb.1996.0139.
103. Huetteroth W, El Jundi B, El Jundi S, Schachtner J. 3D-Reconstructions and virtual 4D-visualization to study metamorphic brain development in the sphinx moth *Manduca sexta*. Front Syst Neurosci. 2010;4:7.
104. Tolbert LP, Matsumoto SG, Hildebrand JG. Development of synapses in the antennal lobes of the moth *Manduca sexta* during metamorphosis. J Neurosci. 1983;3(6):1158–75. https://doi.org/10.1523/JNEUROSCI.03-06-01158.1983.
105. Groh C, Rössler W. Caste-specific postembryonic development of primary and secondary olfactory centers in the female honeybee brain. Arthropod Struct Dev. 2008;37(6):459–68. https://doi.org/10.1016/j.asd.2008.04.001.
106. Clyne PJ, Warr CG, Freeman MR, Lessing D, Kim J, Carlson JR. A novel family of divergent seven-transmembrane proteins. Neuron. 1999;22(2):327–38. https://doi.org/10.1016/S0896-6273(00)81093-4.
107. Jefferis GSXE, Hummel T. Wiring specificity in the olfactory system. Semin Cell Dev Biol. 2006;17(1):50–65. https://doi.org/10.1016/j.semcdb.2005.12.002.
108. Schachtner J, Trosowski B, D'Hanis W, Stubner S, Homberg U. Development and steroid regulation of RFamide immunoreactivity in antennal-lobe neurons of the sphinx moth *Manduca sexta*. J Exp Biol. 2004;207(Pt 14):2389–400. https://doi.org/10.1242/jeb.01036.
109. Parthasarathy R, Tan A, Bai H, Palli SR. Transcription factor broad suppresses precocious development of adult structures during larval–pupal metamorphosis in the red flour beetle, *Tribolium castaneum*. Mech Dev. 2008;125(3-4):299–313. https://doi.org/10.1016/j.mod.2007.11.001.
110. Wu Z-N, Chen X, Du Y-J, Zhou J-J, ZhuGe Q-C. Molecular identification and characterization of the Orco orthologue of *Spodoptera litura*. Insect Sci. 2013;20(2):175–82. https://doi.org/10.1111/j.1744-7917.2011.01483.x.
111. Engsontia P, Sanderson AP, Cobb M, Walden KKO, Robertson HM, Brown S. The red flour beetle's large nose: an expanded odorant receptor gene

family in *Tribolium castaneum*. Insect Biochem Mol Biol. 2008;38(4):387–97. https://doi.org/10.1016/j.ibmb.2007.10.005.
112. Utz S, Schachtner J. Development of A-type allatostatin immunoreactivity in antennal lobe neurons of the sphinx moth Manduca sexta. Cell Tissue Res. 2005;320(1):149–62. https://doi.org/10.1007/s00441-004-1059-3.
113. Utz S, Huetteroth W, Vömel M, Schachtner J. Mas-allatotropin in the developing antennal lobe of the sphinx moth *Manduca sexta*: distribution, time course, developmental regulation, and colocalization with other neuropeptides. Dev Neurobiol. 2008;68(1):123–42. https://doi.org/10.1002/dneu.20579.
114. Homberg U. Distribution of neurotransmitters in the insect brain. Stuttgart: G. Fischer; 1994.
115. Homberg U, Hildebrand JG. Postembryonic development of γ-aminobutyric acid-like Immunoreactivity in the brain of the sphinx moth Manduca sexta. J Comp Neurol. 1994;339(1):132–49. https://doi.org/10.1002/cne.903390112.
116. Sokoloff A. The genetics of *Tribolium* and related species. New York; London: Academic Press; 1966.
117. Berghammer AJ, Bucher G, Maderspacher F, Klingler M. A system to efficiently maintain embryonic lethal mutations in the flour beetle *Tribolium castaneum*. Dev Genes Evol. 1999;209(6):382–9. https://doi.org/10.1007/s004270050268.
118. Ho FK. Optic Organs of *Tribolium confusum* and *T. castaneum* and Their Usefulness in Age Determination (Coleoptera: Tenebrionidae). Ann Entomol Soc Am. 1961;54:921–5. https://doi.org/10.1093/aesa/54.6.921.
119. Friedrich M, Rambold I, Melzer RR. The early stages of ommatidial development in the flour beetle *Tribolium castaneum* (Coleoptera; Tenebrionidae). Dev Genes Evol. 1996;206(2):136–46. https://doi.org/10.1007/s004270050039.
120. Heuer CM, Kollmann M, Binzer M, Schachtner J. Neuropeptides in insect mushroom bodies. Arthropod Struct Dev. 2012;41(3):199–226. https://doi.org/10.1016/j.asd.2012.02.005.
121. Mowiol embedding medium. Cold Spring Harb Protoc. 2010;2010:pdb.rec12110-pdb.rec12110.
122. Chehrehasa F, Meedeniya ACB, Dwyer P, Abrahamsen G, Mackay-Sim A. EdU, a new thymidine analogue for labelling proliferating cells in the nervous system. J Neurosci Methods. 2009;177(1):122–30. https://doi.org/10.1016/j.jneumeth.2008.10.006.
123. Salic A, Mitchison TJ. A chemical method for fast and sensitive detection of DNA synthesis in vivo. Proc Natl Acad Sci U S A. 2008;105(7):2415–20. https://doi.org/10.1073/pnas.0712168105.
124. Vandekerckhove J, Deboben A, Nassal M, Wieland T. The phalloidin binding site of F-actin. EMBO J. 1985;4(11):2815–8. https://doi.org/10.1002/j.1460-2075.1985.tb04008.x.
125. Vitzthum H, Homberg U, Agricola H. Distribution of Dip-allatostatin I-like immunoreactivity in the brain of the locust Schistocerca gregaria with detailed analysis of immunostaining in the central complex. J Comp Neurol. 1996;369(3):419–37. https://doi.org/10.1002/(SICI)1096-9861(19960603)369:3<419::AID-CNE7>3.0.CO;2-8.
126. Klagges BR, Heimbeck G, Godenschwege TA, Hofbauer A, Pflugfelder GO, Reifegerste R, et al. Invertebrate synapsins: a single gene codes for several isoforms in *Drosophila*. J Neurosci. 1996;16(10):3154–65. https://doi.org/10.1523/JNEUROSCI.16-10-03154.1996.
127. Pasch E, Muenz TS, Rössler W. CaMKII is differentially localized in synaptic regions of kenyon cells within the mushroom bodies of the honeybee brain. J Comp Neurol. 2011;519(18):3700–12. https://doi.org/10.1002/cne.22683.
128. Oertel WH, Schmechel DE, Tappaz ML, Kopin IJ. Production of a specific antiserum to rat brain glutamic acid decarboxylase by injection of an antigen-antibody complex. Neuroscience. 1981;6(12):2689–700. https://doi.org/10.1016/0306-4522(81)90113-5.
129. Trebels B, Dippel S, Goetz B, Graebner M, Hofmann C, Hofmann F, et al. Metamorphic development of the olfactory system in the red flour beetle (Tribolium castaneum, HERBST) - Dataset Staging; 2020. https://doi.org/10.17192/FDR/42.
130. Trebels B, Dippel S, Goetz B, Graebner M, Hofmann C, Hofmann F, et al. Metamorphic development of the olfactory system in the red flour beetle (Tribolium castaneum, HERBST) – Dataset Orco RNAi; 2020. https://doi.org/10.17192/FDR/35.
131. Trebels B, Dippel S, Goetz B, Graebner M, Hofmann C, Hofmann F, et al. Metamorphic development of the olfactory system in the red flour beetle (Tribolium castaneum, HERBST) - Dataset Antennal OSNs; 2020. https://doi.org/10.17192/FDR/37.
132. Trebels B, Dippel S, Goetz B, Graebner M, Hofmann C, Hofmann F, et al. Metamorphic development of the olfactory system in the red flour beetle (Tribolium castaneum, HERBST) – Dataset AL Local Neurons; 2020. https://doi.org/10.17192/FDR/40.
133. Trebels B, Dippel S, Goetz B, Graebner M, Hofmann C, Hofmann F, et al. Metamorphic development of the olfactory system in the red flour beetle (Tribolium castaneum, HERBST) - Dataset Antennal CSNs; 2020. https://doi.org/10.17192/FDR/38.
134. Trebels B, Dippel S, Goetz B, Graebner M, Hofmann C, Hofmann F, et al. Metamorphic development of the olfactory system in the red flour beetle (Tribolium castaneum, HERBST) – Dataset Apis mellifera supplemental experiments; 2020. https://doi.org/10.17192/FDR/39.
135. Trebels B, Dippel S, Goetz B, Graebner M, Hofmann C, Hofmann F, et al. Metamorphic development of the olfactory system in the red flour beetle (Tribolium castaneum, HERBST) - Datast AL Glomeruli; 2020. https://doi.org/10.17192/FDR/41.
136. Trebels B, Dippel S, Goetz B, Graebner M, Hofmann C, Hofmann F, et al. Metamorphic development of the olfactory system in the red flour beetle (Tribolium castaneum, HERBST) – Dataset GOC Glomeruli; 2020. https://doi.org/10.17192/FDR/36.
137. Trebels B, Dippel S, Goetz B, Graebner M, Hofmann C, Hofmann F, et al. Metamorphic development of the olfactory system in the red flour beetle (Tribolium castaneum, HERBST) - Dataset GAD Western Blot Raw Images; 2020. https://doi.org/10.17192/FDR/34.

Publisher's Note

5

The palpal olfactory pathway

An update on the palpal olfactory system of red flour beetles (Tribolium castaneum, Herbst)

Bjoern Trebels [1, #], Stefan Dippel [1, #, §], Janet Anders [1], Clara Ernst [1], Brigitte Goetz [1], Tim Keyser [1], Karl Heinz Rexer [2], Ernst A. Wimmer [3], Joachim Schachtner [1, 4]

(1) Department of Biology, Animal Physiology, Philipps-University Marburg, Karl-von-Frisch-Str. 8, 35032 Marburg, Germany.
(2) Department of Biology, Biodiversity of plants, Philipps-University Marburg, Karl-von-Frisch-Str. 8, 35032 Marburg, Germany.
(3) Department of Developmental Biology, Georg-August-University Göttingen, Johann-Friedrich-Blumenbach-Institute for Zoology and Anthropology, GZMB, Ernst-Caspari-Haus, Justus-von-Liebig-Weg 11, Göttingen, 37077, Germany
(4) Clausthal University of Technology, Adolph-Roemer-Str. 2a, 38678 Clausthal-Zellerfeld, Germany

# Equal contribution
§ Present address: Institute for General Zoology and Developmental Biology, AG Zoology with Emphasis on Molecular Developmental Biology of Animals, Justus-Liebig-University Giessen, Heinrich-Buff-Ring 38, 35392 Giessen, Germany.

5.1 Abstract

Background: The current picture of the olfactory pathway in holometabolous insects declares the paired antennal lobes as the sole primary processing centers, which receive input from the olfactory sensory neurons of the antennae and palps. In hemimetabolous insects, on the other hand, olfactory cues of the antennae and palps are processed separately. Recent findings in *Tribolium castaneum* showed that the beetle's olfactory system is organized differently. Primary processing of the palpal and antennal olfactory input occurs separately from each other. While the antennal olfactory sensory neurons project into the antennal lobes, those of the palps project into the paired glomerular lobes and the unpaired gnathal olfactory center.
Results: The current study, provides an update on the palpal olfactory pathway by combining scanning electron micrographs with confocal imaging of immunohistochemical staining and reporter expression in the EF-1-B-dsRed and Orco-Gal4 lines. We identified the sensilla types housing the dendrites of the palpal olfactory sensory neurons and extend the anatomical characterization of the gnathal olfactory center by 3D reconstructions. Further, we exemplary investigated the distribution of several neuromediators in the gnathal olfactory center and the glomerular lobes that are commonly identified in the antennal lobes.
Conclusions: Our analysis expands the picture of the palpal olfactory pathway in *T. castaneum*. The similarities in the neuromediator repertoire between antennal lobes, glomerular lobes, and gnathal olfactory center underline the role of the latter two as primary olfactory processing centers and suggest that the repertoire of neuromediators does not correlate with the complexity of the processing centers, rather might be a requirement for finetuning, processing, and primary evaluation of incoming information.

5.2 Background

To find hosts, conspecifics and mates, oviposition sites, and food sources insects, often depend on their chemical senses [1–12]. The olfactory and gustatory systems are precisely tuned to discriminate between chemical cues. They translate perceived information based on composition, concentration, and spatial and temporal distribution, into innate and learned behavior.
Chemosensation starts with the perception of the semiochemicals at the chemosensory sensilla of the antennae and palps. The sensilla house the chemosensory neurons (CSNs) that divide into olfactory sensory neurons (OSNs) and gustatory sensory neurons (GSNs).
The OSNs present the olfactory receptors, either odorant receptors (ORs) or ionotropic glutamate-like receptors (IRs), on their membranes [13–17]. Via their axons, the OSNs relay the perceived olfactory information to the respective primary processing centers. The antennal OSNs project into the antennal lobes, while the destination of the palpal OSNs differs among species. In hemimetabolous insects, the palpal OSNs project into the glomerular lobes (LGs) [18]. The current picture of olfaction in holometabolous insects declares the ALs as primary processing centers for antennal and palpal olfactory input [19–23]. However, at least in the red flour beetle, the palpal OSNs do not project into the ALs but into the paired LGs and the unpaired, glomerularly organized gnathal olfactory center (GOC; Fig. 5.1).
Within the ALs, the olfactory information perceived by the OSNs is processed by a network of local interneurons (LNs) that interconnect the olfactory glomeruli. Olfactory representations by the LNs are mainly shaped by the inhibitory transmitter gamma amino-butyric acid (GABA) or the excitatory transmitter acetylcholine [24–37], but also by numerous neuropeptides [18, 38–40].
Based on the available data on the anatomy of *T. castaneum's* olfactory system [14] and the transmitter repertoire of the ALs [38], the current study provides insight into the separate palpal olfactory pathway. It especially focuses on the anatomical and biochemical characterization of the unpaired GOC, but also the paired LGs. We utilized confocal imaging of transgenic lines labeling CSNs and OSNs in combination with (immuno)-histochemistry to visualize the chemosensory neurons within the palps, as wells their central projections. Further, we employed scanning electron microscopy to visualize and identify the chemosensory sensilla of the palps.

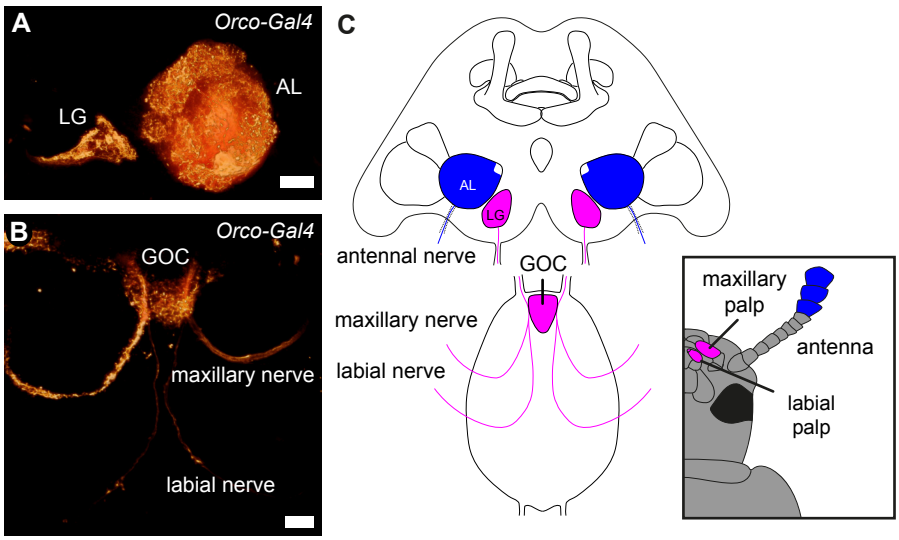

Fig. 5.1: Primary olfactory pathways in the red flour beetle *Tribolium castaneum*.
Volume Rendering of the reporter signal in the OSN-labeling partial Orco-GAL4 line **A** of the glomerular lobes (LG), antennal lobes (AL), and **B** the gnathal olfactory center (GOC) with its sensory inputs. **C** Schematic of the primary processing centers and their sensory inputs. Antennal OSNs (blue) project into the ALs, while the palpal OSNs (magenta) project into the GOC and LGs. Scale bars 20 µm (A), 10µm (B).

5.3 Results

The labial and maxillary palps and their olfactory sensory neurons

In *T. castaneum*, the labial and maxillary palps are olfactory sensory appendages. Their sensory input is processed in the paired LGs and the unpaired GOC (Fig. 5.1; see also [14]). In both, the maxillary and labial palps, soma, dendrites, and axons of the OSN are labeled in the Orco-GAL4 line (Fig. 5.2 A, D). The OSN dendrites innervate sensilla at the palpal tips. We approved the presence of ORCO by specific antibody staining against Orco in the CSN labeling EF-1-B-DsRed line (Fig. 5.2 B-B', E-E'). Scanning electron microscopy was used to determine the sensilla types on the palpal tips. On both palp types, the maxillary and labial palps, (Fig. 5.2 C, F), we found the same three types of sensilla and classified them according to [41] as basiconic sensilla (magenta), blunt basiconic sensilla (green), and styloconic sensilla (yellow). Based on exemplary manual counting in SEM images, we estimate that the tip of the maxillary palp houses roughly 90 sensilla divided into about 20 (n = 2; #1: 22, #2: 16) basiconic, 60 (n = 2; #1: 63, #2: 57) blunt basiconic, and 10 (n = 2; #1: 13, #2: 8) styloconic sensilla. The labial palp's tip houses roughly 85 sensilla divided into about 25 (n = 2; #1: 26, #2: 21) basiconic, 50 (n = 2; #1: 58, #2: 42) blunt basiconic, and 10 (n = 2; #1: 9, #2: 11) styloconic sensilla.

High-resolution confocal images of the maxillary and labial palps in the Orco-GAL4 line were used to determine which sensilla type house OSN dendrites. We find that the styloconic (sSty; Supplemental Figure S1 A-A'). Further, the basiconic (sBas) and/or blunt basiconic (sBBas)

sensilla also house OSN dendrites (Supplemental Figure S1 B-B'). A differentiation between basiconic and blunt basiconic sensilla in the confocal images was not possible due to resolution limits in imaging the cuticular autofluorescence.

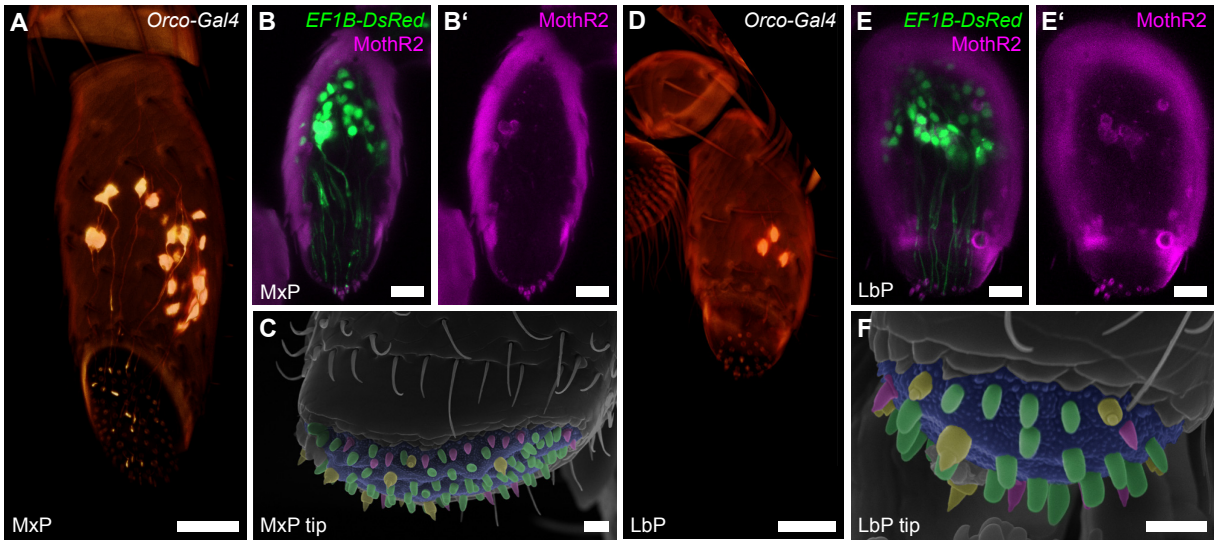

Fig. 5.2: OSNs of the maxillary and labial palps
A, D Volume rendering of the reporter signal in the Orco-GAL4xUAS-DsRed line in maxillary palps (MxP) and labial palps (LbP). **B, E** Orco immunostaining (magenta) and reporter signal (green) on palpal cryosections in the CSN-labeling EF-1-B-DsRed line within the maxillary (MxP) and labial palps (LbP). **C, F** Scanning electron micrographs of the tips of the maxillary (MxP) and labial (LbP) palps and their sensilla: basiconic sensilla (sBas) – magenta, blunt basiconic sensilla (sBBas) – green, and styloconic sensilla (sSty) – yellow. Scale bars 20µm (A, D), 10µm (B-B', E-E'), 5µm (C, F).

Anatomy of the gnathal olfactory center

Manual 3D-reconstructions of the GOC (Fig. 5.3 A) based on the fluorescent reporter signal in the EF-1-B-DsRed line and fluorescent staining of f-actin and synapsin (Fig. 5.3 C) were used to analyze the glomerular organization of the GOC. On average, we identified about 30 glomeruli (mean = 30.33, SD = 4.72, n = 9) of varying shape and size, which was confirmed by two exemplary 3D reconstructions after applying the expansion microscopy (ExM) protocol [42]. In both cases, 31 glomeruli could be identified.

While most glomeruli cannot be correlated between specimens, we usually find about 4 stacked and easily identifiable wedge-like glomeruli in comparable positions across specimens (Fig. 5.3 B).

Local neurons as revealed by GAD immunostaining

In *Drosophila melanogaster* [26] and other insects [18, 43], the vast majority of the local neurons (LN) of the AL use the inhibitory transmitter GABA, which is synthesized by the glutamic acid decarboxylase (GAD). As previously published, GAD immunostaining revealed that the AL LNs located in a cluster lateral to the ALs (Fig. 5.4 A; see also [44]), which compares to cluster CL7 in *Tenebrio molitor* [45]. Although the glomerular lobes display faint GAD immunoreactivity,

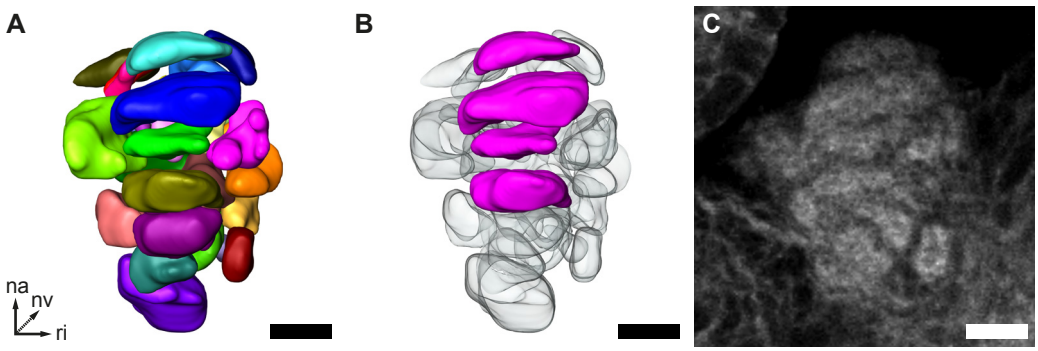

Fig. 5.3: GOC anatamoy
A Representative 3D-reconstruction of the GOC **B** Wedge-like glomeruli (magenta) in the same GOC shown in (A). These glomeruli are recognizable across specimens. **C** Single optical slice of the phalloidin staining of the GOC reconstructed in (A) and (B). Scale bars 10 µm.

we did not detect corresponding somas in the near vicinity (Fig. 5.4 B). Within the GOC, we find GAD immunoreactive fibers throughout the neuropil volume (Fig. 5.4 C). N-anterior to the GOC, we identified six nearby GAD immunoreactive somas (Fig. 5.4 Ca, Cb, Cc marked with asterisks), of which four (n = 2) could be confirmed to extend their neurites into the GOC (Fig. 5.4 Cb, Cc).

Neuropeptides

Several neuropeptides have been identified in the AL of the red flour beetle [38]. We exemplarily compared the distribution of allatotropin (AT), tachykinin-related peptides (TKRP), and myoinhibitory peptides (MIPs) across the three primary olfactory processing centers.

Similar to the AL (Fig. 5.5 A; see also [38]) immunohistochemical staining of AT revealed a sparkly pattern within the LG (Fig. 5.5 B). In contrast, immunostaining of AT in the GOC revealed a denser pattern with visible glomerular substructures in its n-anterior part (Fig. 5.5 C). In all three neuropils, staining is distributed over the total neuropil volume.

The general distribution of TKRP as visualized by the Lom-TK-II antiserum in the AL (Fig. 5.5; see also [38]), and the GOC (Fig. 5.5 F) revealed distinguishable glomeruli. While the staining is distributed within the whole AL, within the GOC, a portion at the n-posterior end is not stained (Fig. 5.5 F”). Within the LG (Fig. 5.5 E), dense spots are distinguishable all over the neuropil volume. Similar to TKRPs, MIPs are found broadly distributed all over the AL volume (Fig. 5.5 G; see also [38]). Within the GOC, only a few glomeruli across the neuropil volume are labeled (Fig. 5.5 I). In the LG (Fig. 5.5 H), dense spots are distinguishable all over the neuropil volume.

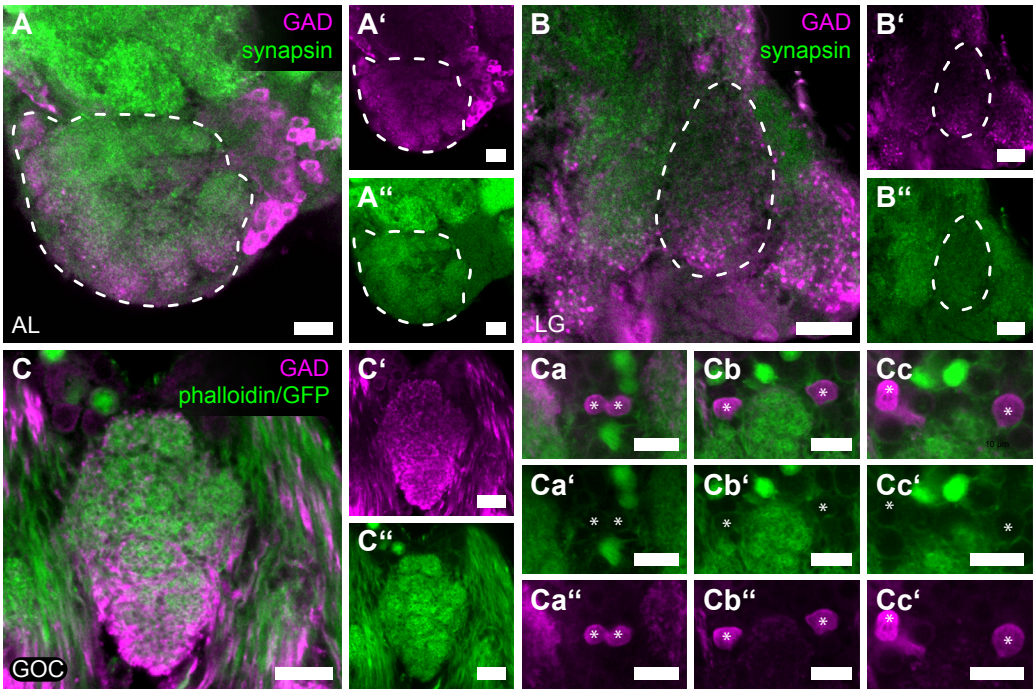

Fig. 5.4: GAD immunoreactivity in the primary olfactory processing centers.
Representative optical slices displaying GAD immunostaining (magenta) in the **A** AL, **B** LG, and **C** GOC. **A** GAD immunoreactive somas are located lateral to the glomeruli and enter the neuropile via a single tract. **B** GAD-ir fibers are distributed within the whole volume of the LG, while somas could not be detected in the near vicinity **C** GAD-ir fibers cover the complete GOC. **Ca, Cb, Cc** GAD-ir soma (asterisks) n-anterior near the GOC. Of those, at least 4 (Cb, Cc) extend fibers into the GOC volume. Scale bars 10 µm. In (A) the staining was obtained using the GADsheep antisera in (B and C) using the GADrabbit antisera. The general neuroanatomy is depicted in green. In (A, B) via synapsin immunostaining and in (C - Cc) via phalloidin staining and 3XP3-eGFP reporter signal in the EF-1-B-DsRed line.

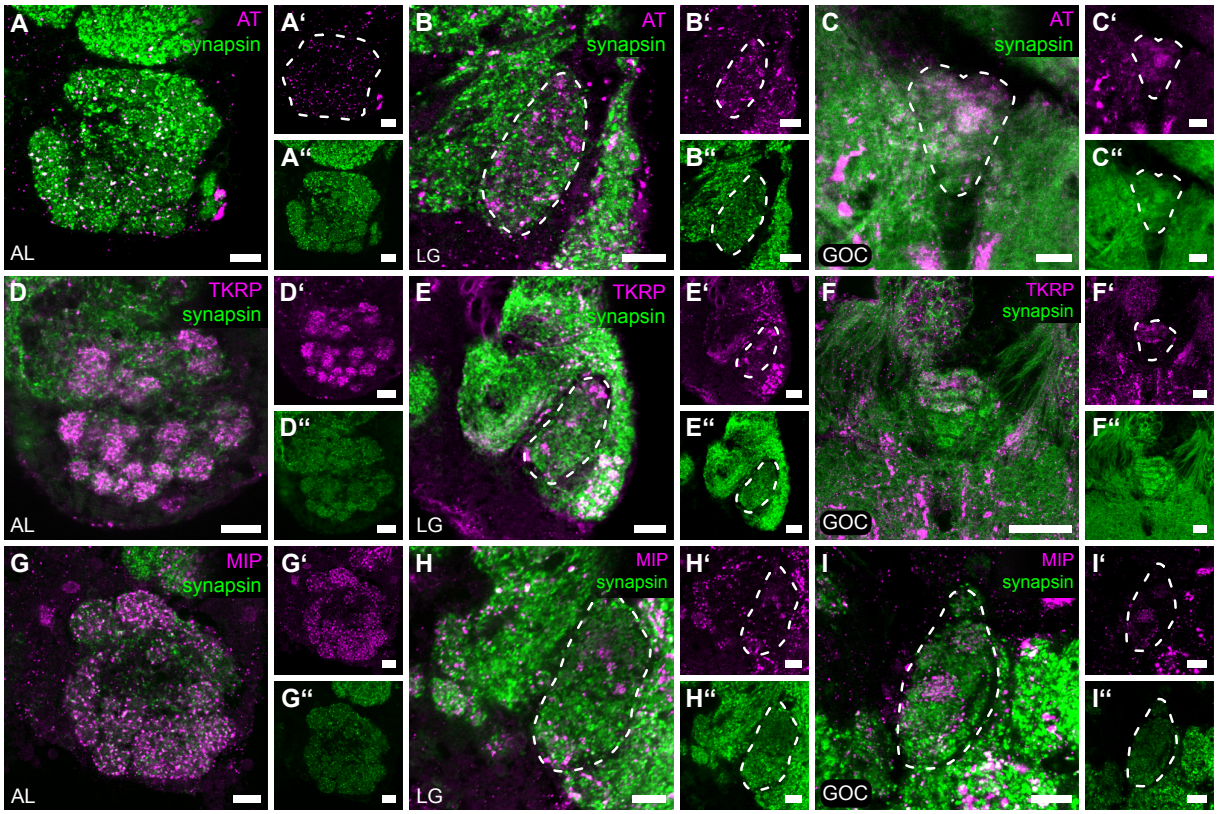

Fig. 5.5: Neuropeptides in the primary olfactory processing centers.
Representative optical slices displaying neuropeptide immunostaining (magenta) in the antennal lobes (AL), glomerular lobes (LG), and gnathal olfactory center (GOC). **A-C** Allatotropin [AT] immunostaining shows a sparkly pattern in the AL and LGs (A, B) and a denser pattern in the GOC (C). **D-F** Immunostaining of Tachykinin related peptides [TKRP] reveals identifiable glomeruli in the complete AL and the n-anterior portion GOC (D, F), and dense spots, likely resembling microglomeruli in the LGs (E) **G-I** While immunostaining against Myoinhibitory peptides [MIP] visualizes identifiable glomeruli in the total AL (G) and dense spots across the complete LG (H), only a few glomeruli of the GOC are stained (I). Scale bars 10µm. The general neuroanatomy (green) is visualized via synapsin immunostaining.

Serotonin

Each AL is innervated by a neuron expressing the biogenic amine serotonin (5-HT), whose soma is located lateral to the respective AL (Fig. 5.6 A, D). These neurons share the gross morphology with similar neurons found in other insects [45–48]. Within the ALs, the innervation covers most glomeruli with varicose ramifications, except for a few glomeruli located n-anterolateral (Fig. 5.6 A, asterisks).

Within the LG, 5-HT immunoreactivity is found laterally in the n-posterior portion of the neuropil, where varicose ramifications can be observed, while the n-anterior half is not innervated (Fig. 5.6 B asterisk). The GOC is presumably innervated by two neurons, located in the n-anterior cell cluster. Their neurites extend towards the GOC and unfortunately, the staining faded in all preparations so that we could not confirm them entering the GOC. The overall innervation pattern of the GOC glomeruli is similar to the AL, as the glomeruli are encapsulated by Serotonin immunoreactive fibers. As in the AL, we find that few n-anterior located glomeruli are not innervated (Fig. 5.6 C asterisk).

5.4 Discussion

In the red flour beetle *T. castaneum*, the antennae and palps are major olfactory sensory organs [14]. The antennal olfactory pathway and the transmitter repertoire of the antennal lobe were already described [14, 38, 49]. In the current study, we extended the few available data on the palpal olfactory pathway and the corresponding primary processing centers. [14].

The palps as olfactory sensory organs

The maxillary and labial palps of *T. castaneum* both house a reasonable number of OSNs and thus are major olfactory appendages [14]. The OSN somas are located within the distal segment of the maxillary and labial palps, while their dendrites project into the sensilla of the palpal tips. Based on SEM, we identified the same three sensilla types at the tips of the maxillary and labial palps: basiconic, blunt basiconic, and styloconic sensilla. High-resolution confocal stacks of the reporter signal in the Orco-Gal4 line and immunohistochemical staining against Orco revealed that the styloconic sensilla, as well as the basiconic sensilla and/or blunt basiconic house OSN dendrites. This contrasts findings in the vinegar fly *D. melanogaster* where the basiconic sensilla are the sole olfactory sensilla type [50].

The semiochemicals detected by the palpal OSNs of *T. castaneum* remain unknown. However, given the exposed position of the sensilla, those OSNs are most likely involved in short-range attraction as the palpal OSNs in flies [51] or food evaluation like the proboscis OSNs in *Manduca sexta* [52]. This also fits the palpation behavior preceding food uptake observed in *Locusta migratoria* [53].

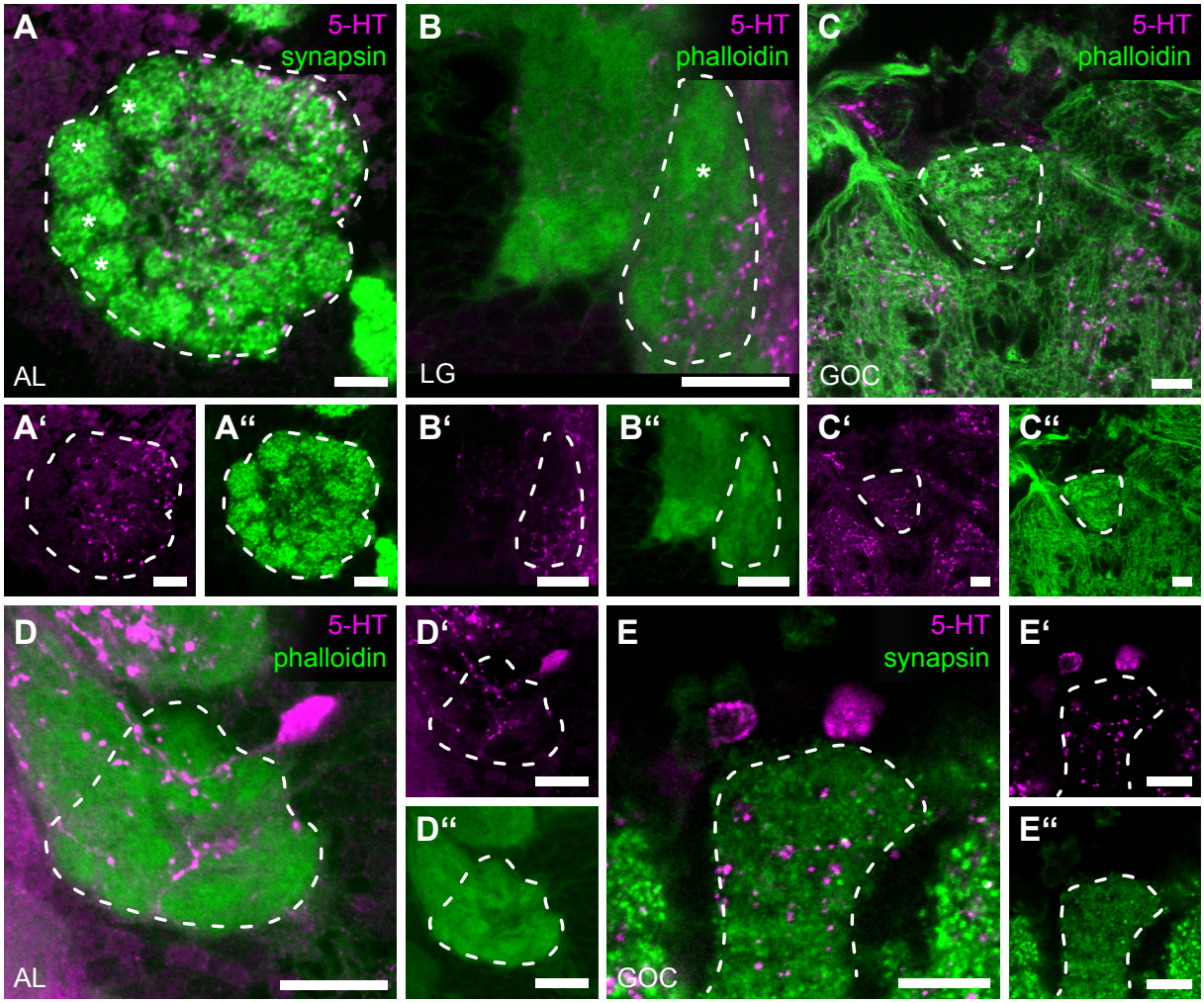

Fig. 5.6: Serotonin (5-HT) immunoreactivity.
Representative optical slices displaying Serotonin (5-HT) immunostaining in the antennal lobes (AL), glomerular lobes (LG), and the gnathal olfactory center (GOC) **A** In the AL immunoreactive fibers cover most but not all glomeruli; asterisks indicate non-innervated glomeruli, **B** Also in the LGs immunoreactive fibers cover only part of the neuropil; asterisk indicates the position of the non-innervated area. **C** As in AL and LG, the GOC is only partially innervated by immunoreactive fibers; asterisk indicates the position of non-innervated glomeruli. **D** Single Serotonin-immunoreactive neuron innervating the ipsilateral AL. **E** Serotonin immunoreactive neurons innervate the GOC. Scale bars 10 µm. The general neuroanatomy (green) is either depicted via synapsin immunostaining (A, E) or phalloidin staining (B-D).

Anatomy of the gnathal olfactory center

We tested several ubiquitous neuronal markers to provide a clear picture of the anatomy: reporter expression in the neuron labeling EF 1 B DsRed line, synapsin immunohistochemistry, and f-actin staining using phalloidin. While all three techniques were suitable to visualize the gross anatomy of the GOC, none was sufficient alone to determine the boundaries of all glomeruli. The best results were accomplished by using the phalloidin staining in combination with one of the other two, with the transgenic line providing better results compared to the synapsin staining. Based on these combinations, we performed exemplary manual 3D-reconstructions from confocal image stacks to visualize the number, shape, and position of the GOC glomeruli. Due to the small size of the GOC and typically hard to define borders between single glomeruli, we also used the technique of expansion microscopy (ExM) [42] to obtain higher spatial resolutions and to emphasize the glomeruli borders (Supplemental Fig. S2). As many fluorochromes used in immunohistochemistry are not suitable for ExM [54–56] and, like most proteins, phalloidin is degraded through the process, we could only rely on the DsRed reporter signal of the EF-1-B-DsRed line. However, even with the improvement of the spatial resolution, we did get more obviously pronounced glomeruli boundaries.

Our results show that with about 30, the glomeruli number is at the lower margin of the previously suggested range of 30 to 40 glomeruli [14]. The number of identified GOC glomeruli corresponds well with the 28 ORs found to be significantly enriched in the mouthparts compared to the body - as identified by RNA sequencing [14].

Neuromediator repertoires

The AL, LG, and GOC are all considered primary olfactory processing centers [14]. We, therefore, asked whether we find a similar set of neuromediators and similar distribution patterns within the neuropils of the different primary olfactory processing centers. The neuronal network of the ALs deploys a variety of neuromediators that are used during the processing of odor information [57]. This includes classical transmitters like GABA, neuropeptides, such as AT, TKRPs, MIPs, but also biogenic amines like serotonin, which we selected for an exemplary comparison between the three olfactory processing centers of the red flour beetle.

GABA has been described as the major inhibitory transmitter of the AL local neurons [26, 45, 58–62]. Neuropeptides are frequently considered to be co-transmitters at synaptic sites [63]. In vertebrates, they are mainly believed to function as neuromodulators [63]. In the ALs of *T. castaneum* and many other insect species neuropeptides are predominantly localized in LN and the number of identified neuropeptides in ALs of different insect species via mass spectrometry ranges between 20 and about 40 [38–40]. These include Allatotropin (AT), Tachykine related peptides (TKRPs), and Myoinhibitory peptides (MIPs).

Serotonin is generally assumed to play a modulatory function in various contexts [64–66] and in the AL, Serotonin immunoreactive fibers form a conserved pattern across insect species [48, 67–73].

In short, we found all tested neuromediators in the ALs, LGs, and GOC with different distribution patterns (Fig. 5.4, Fig. 5.5, Fig. 5.6, Fig. 5.7).

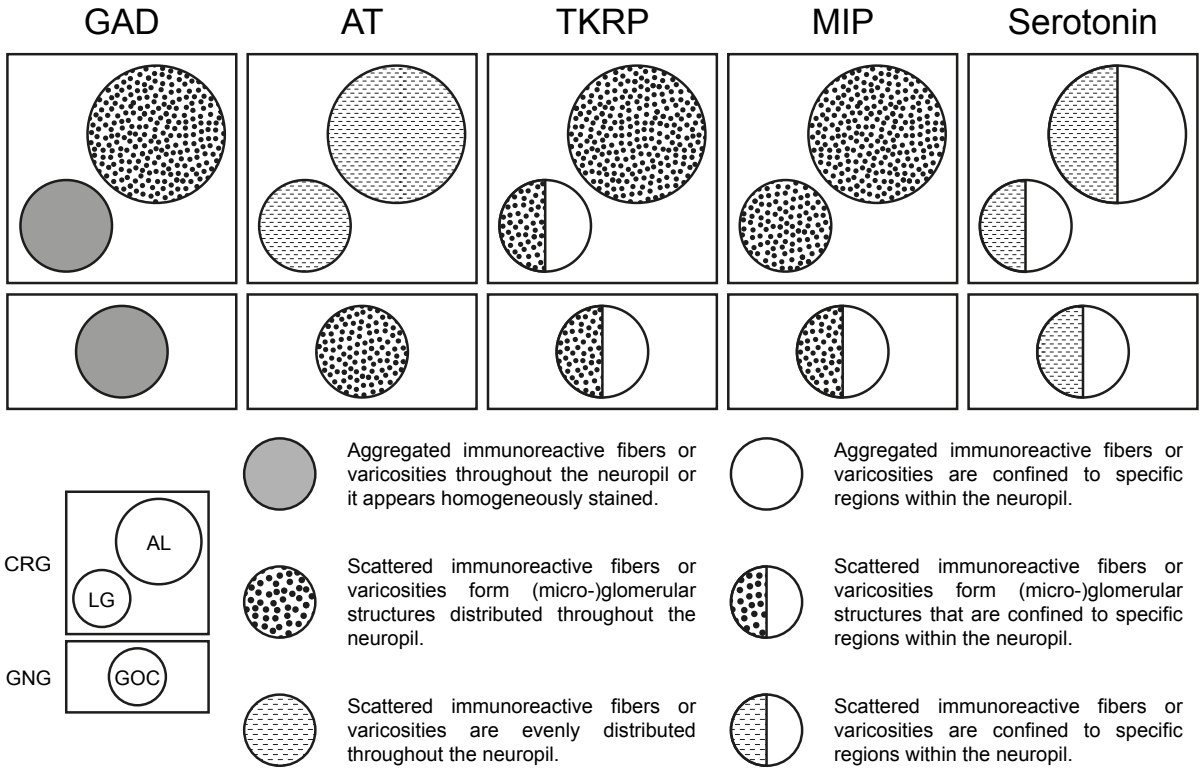

Fig. 5.7: Distribution of the tested neuromediators GAD, AT, TKRP, MIP, and Serotonin within the primary olfactory processing centers of *T. castaneum*.

GAD

The distribution of GAD immunoreactivity in the ALs resembles the findings of GABA immunoreactivity in other hemi- and holometabolous insect species [45, 58–61], with GABA containing fibers of AL local neurons innervating all glomeruli (Fig. 5.4 A, Fig. 5.7; see also [44]). The antennal lobe of *T. castaneum* is innervated by about 165 GAD-ir LNs [44], which is considerably more than the about 100 local neurons found in the lateral AL cluster in *D. melanogaster* [24] and more than the about 125 GABA-ir neurons found in the cluster CL7 in *T. castaneum*'s close relative *T. molitor* [45].

GABA is considered the major transmitter of local interneurons in the ALs [18]. Therefore, we expected suchlike for the LGs and the GOC and indeed both neuropils showed homogeneous innervation by GAD immunoreactive fibers (Fig. 5.4 B, C; Fig. 5.7) – indicating that GABA is also a major transmitter in the LGs and the GOC.

For the GOC, the source of the GAD-ir fibers is provided via at least four GAD-ir cell bodies in the near vicinity (Fig. 5.4 Cb, Cc). For the LG, we could not detect the somas responsible for the innervating GAD-ir fibers in the near vicinity. As the used antiserum typically nicely stains cell bodies, the innervation very likely stems from other brain areas.

Neuropeptides

The distribution of the three neuropeptide families investigated in this study in the ALs of *T. castaneum* has been described earlier and serves as a reference [38]. Naively and given the fact that the LGs and the GOC are primary olfactory processing centers, like the ALs, one could expect a similar distribution of the three analyzed neuropeptide families. While that is indeed true for the sole deployment of the investigated neuropeptides in the LGs and the GOC, their distribution patterns are different.

For MIP and TKRP, a clear glomerular pattern is visible in the GOC, as evident in the ALs, and, in both cases, dense spots were revealed in the LGs. Those might resemble microglomerular structures. However, in both cases only a part of the GOC and with TKRP also only a part of the LGs is innervated by respectively immunoreactive fibers. In the case of AT, a sparkly distribution, very similar to that in the ALs, is found in the LGs. In the GOC that staining pattern appears denser with visible glomerulization. The fact that portions of the LGs and the GOC are note marked in immunostaining against TKRPs and MIPs could mean are not subject to local modulation by those two neuropeptides.

The occurrence of all three neuropeptide families in the LGs and the GOC despite their presumably less complex network is somehow remarkable. It seems as if the repertoire does not correlate with complexity, but that the diverse repertoire might be involved in finetuning, processing, and primary evaluation of incoming information. LGs are not described in other holometabolous insect species as they are supposed to be fused with the ALs [19] and therefore no data about neuropeptide localization is available. Further, only a few, superficial data from hemimetabolous insects concerning neuropeptides in the LGs exist. As in the red flour beetle, AT is distributed over the total volume of the LG in *Schistocerca gregaria* [74]. MIPs in turn are described to be present in LGs of the madeira cockroach *Rhyparobia maderae* [75], as are TKRPs [76].

Only a few studies on the role of neuropeptides in olfactory signaling are available. For example, small neuropeptide F (sNPF) in the ALs is involved in increasing food searching behavior in hungry *D. melanogaster* [30], while MIPs in the AL are involved in the same

behavior in mated female flies [77]. Further, studies in the fly showed that TKRPs in the ALs can modify odor sensitivity [78, 79] and seemingly play a role in regulating food attraction [80]. Given the potential role of MIPs and TRKPs in food searching behavior, it is not surprising to find them in the primary processing center for palpal olfaction – with palpal OSNs likely being involved in short-range attraction and food evaluation as laid out above.

Serotonin

The staining pattern of the serotonin-ir fibers in the ALs of *T. castaneum* arises from one neuron per hemisphere, located lateral to the ALs. These neurons share their gross morphology with specific serotonin-immunoreactive neurons described in various other insect species, while their arborization patterns show a high variability [18, 45–48]. In the ALs of *T. castaneum*, the innervation pattern resembles a meshwork of varicosities distributed over the boundaries of most, but not all, glomeruli. The partial innervation of the GOC is presumably provided via two serotonin-ir cell bodies in the near vicinity. For the LGs, we did not detect a serotonin-positive cell body as a source of the partial innervation. Like our findings for GABA, we suggest that the source of the serotonin-ir fibers in the LG stems from other brain areas.

As not all glomeruli of the ALs and the GOC are covered by serotonin-ir varicosities, this suggests that certain glomeruli and the corresponding odor processing are not subject to serotonin modulation, which seemingly also applies to the AL glomeruli in *D. melanogaster* [46, 81].

The role of Serotonin in the olfactory system seems to be heterogeneous but in general, modulates odor-evoked responsiveness and/or sensitivity [82]. For example, Serotonin was shown to increase the responsiveness to olfactory signals in *M. sexta* [83–85] and *D. melanogaster* [86, 87].

5.5 Materials and Methods

Animals

All experiments were performed using red flour beetles (*Tribolium castaneum*, Herbst 1797; Insecta, Coleoptera) of the wild-type strain "San Bernadino" [88], the transgenic CSN-labeling EF1-B-DsRed line (elongation factor1-alpha regulatory region-DsRedExpress; kindly provided by Michalis Averof, Institut de Genomique Fonctionnelle de Lyon, France) [14, 89], or the OSN-labeling partial Orco-Gal4 line [14]. The beetles were bred under constant darkness at about 30°C (wildtype) or 28°C (transgenes) and 40-50% relative humidity on organic whole grain wheat flour supplemented with 5% dried yeast powder and 0.05% Fumagilin-B (Medivet Pharmaceuticals Ltd., High River, Alberta, Canada) to prevent sporozoan infections [90].

Histochemical staining

Dissection and staining were performed as previously published [14, 38]. Blocking was performed in either 5% normal goat serum or normal donkey Serum (both Jackson Immuno Research, Westgrove, PA, USA). For concentrations and details on markers and antibodies see Table 5.1. Following staining ganglia were mounted either aqueous in the Mowiol [91] or after dehydration in an ascending ethanol series (50%, 70%, 90%, 95%, 100%, 100%; 3 minutes each) and cleared with methyl salicylate (Merck, Gernsheim, Germany) in Permount mounting medium (Fisher Scientific, Pittsburgh, PA) between two coverslips using a layer of two reinforcing rings as spacers to prevent squeezing.

Tab. 5.1: Overview of used antibodies and markers

Name	Abbreviation	Host species	Dilution	Vendor/Donor (catalog #, batch #, RRID #)	Reference	Specificity in T. castaneum
Drosophila melanogaster Synapsin I (SYNORF1)	Synapsin	Mouse	1:50	E. Bucher, University of Würzburg, Germany (n/a, n/a, AB_2313617)	[92]	[93]
Locusta migratoria Tachykinin II	TKRP		1:20,000	Jena Bioscience, Jena, Germany (CLK-AZ118-1; Kli009-030; n/a)	[94]	[38]
Rattus norvegicusglutamate decarboxylase (sheep)	GAD_{sheep}	Sheep	1:5,000	W. Oertel, Laboratory of Clinical Science, Mansfield, MA, USA (n/a; n/a;n/a)	[95]	[44]
Rattus norvegicusglutamate decarboxylase (rabbit)	GAD_{rabbit}	Rabbit	1:1,000	Sigma-Adrich; now Merck KGaA, Darmstadt, Germany (G5163; 113M4772; AB_477019)		[44]
Periplaneta americana myoinhibitory peptide I	MIP	Rabbit	1:5,000	M. Eckert, University of Jena, Germany (#; #; AB_2314803)	[96]	[38]
Manduca sexta allatotropin	AT	Rabbit	1:5,000	J. Veenstra, University of Bordeaux, France (#; #; AB_2313973)	[97]	[38]
5-Hydroxy-Tryptamine (serotonin)	5-HT	Rabbit	1:20,000	Immunostar (200800; 924005; AB_572263)		
Red fluorescent protein	DsRed	Chicken	1:3,000	Rockland Immunochemicals INC, Limerick, PA, USA (600-901-379, 26274, AB_10704808)		
Cy3 coupled goat anti-chicken	GACh-Cy3	Goat	1:300	Jackson ImmunoResearch; Westgrove, PA, USA (103-165-155, 93117, AB_2337386)		
Cy3 coupled goat anti-rabbit	GAR-Cy3	Goat	1:300	Jackson ImmunoResearch; Westgrove, PA, USA (111-165-144, n/a, AB_2338006)		
Cy5 coupled goat anti-mouse	GAM-Cy5	Goat	1:300	Jackson ImmunoResearch; Westgrove, PA, USA (115-175-146, n/a, AB_2338713)		
Cy2 coupled donkey anti-sheep	DAS-Cy2	Donkey	1:300	Jackson ImmunoResearch; Westgrove, PA, USA (713-225-147, n/a, AB_2340735)		
4',6-diamidin-2-phenylindol	DAPI		1:20,000	Sigma Aldrich, Steinheim, Germany (D9542, n/a, 28718-90-3)	[98]	
Alexa Flour 488 coupled phalloidine	Phalloidin		1:200	Thermo Fischer Scientific, Rockford, IL, USA (A12379; n/a; n/a)	[99]	
Alexa Flour 405 coupled phalloidine	Phalloidin		1:500	Abcam, Cambridge, UK (ab176752; n/a; n/a)	[99]	

Expansion microscopy (ExM)

For ExM we adapted the protocol for intact thick tissues [42]. Following incubation with the secondary antisera ganglia were equilibrated in 2-(N-morpholino)ethanesulfonic acid buffered saline [42] for 30 min. Afterward, ganglia were treated according to the protocol. Gelation chambers were build using cover glasses.

Image acquisition and analysis

Fluorescent preparations were imaged utilizing a confocal laser scanning microscope (TCS SP2 or TCS SP5, Leica Microsystems, Wetzlar, Germany) and analyzed with Amira graphics software (FEI SAS a part of Thermo Fisher Scientific, Merignac Cedex, France). Further image

processing (global level adjustments, contrast, and brightness optimization) was performed in Photoshop CC (Adobe Systems, San Jose, CA, USA), while final figure arrangements were made in Illustrator CC (Adobe Systems).

Scanning electron microscopy

Cold anesthetized adult beetles were decapitated and the heads were fixed overnight in 4% formaldehyde in 0.01M PBS at 4°C and afterward washed in PBS. Washed samples were then dehydrated in an ascending acetone series (30, 50, 3x 100%). Finally, acetone was allowed to evaporate overnight. After being sputtered with gold (Balzers Union Sputter Coater, Balzers, Lichtenstein; Quorum Technologies Ltd, Ringmer, UK), specimens were examined using an SEM (S-530, Hitachi High-Technologies Europe GmbH, Krefeld, Germany). Micrographs were taken using a digital image acquisition unit (DISS 5, point electronic, Halle Germany).

Authors contributions

B.T. conceived and designed the study, acquired, analyzed, and interpreted the data; and drafted and revised the article; J.A., C.E., B.G., T.K., and K-H.R. acquired and analyzed the data; S.D., E.A.W., and J.S. conceived and designed the study; analyzed and interpreted the data; and drafted and revised the article. All authors read and approved the final manuscript.

Data availability

All data generated or analyzed during this study are available from the corresponding authors upon request.

Ethics approval and consent to participate

All experiments involving animals were performed in compliance with the guidelines of the European Union (Directive 2010/63/EU). All experiments were on insects, therefore approval of the study by an ethics committee was unnecessary.

Acknowledgments

We thank Jürgen Krieger for providing the cross-reactive Orco antiserum, Gregor Bucher and Michaelis Averof for sharing transgenic beetle lines, and Martina Kern for technical expertise. Parts of this study were funded within the Deutsche Forschungsgemeinschaft SPP 1392: SCHA 678/13-1 (J.S.) and WI 1797/4-1 (E.A.W.). The funders had no role in the study design, data collection, interpretation, or the decision to submit the work for publication.

5.6 References

[1] Dicke, M. "Behavioural and Community Ecology of Plants That Cry for Help". In: *Plant Cell Environ.* 32.6 (2009), pp. 654–665. ISSN: 01407791, 13653040. DOI: 10.1111/j.1365-3040.2008.01913.x.

[2] Laska, M. "Olfactory Discrimination Ability and Odor Structure: Activity Relationships in Honeybees". In: *Chem. Senses* 24.4 (1999), pp. 429–438. ISSN: 1464-3553. DOI: 10.1093/chemse/24.4.429.

[3] Linz, J., Baschwitz, A., Strutz, A., Dweck, H. K. M., Sachse, S., Hansson, B. S., and Stensmyr, M. C. "Host Plant-Driven Sensory Specialization in *Drosophila Erecta*". In: *Proc. Biol. Sci.* 280.1760 (2013), p. 20130626. ISSN: 1471-2954. DOI: 10.1098/rspb.2013.0626.

[4] Liu, M., Yu, H., and Li, G. "Oviposition Deterrents from Eggs of the Cotton Bollworm, *Helicoverpa Armigera* (Lepidoptera: Noctuidae): Chemical Identification and Analysis by Electroantennogram". In: *J. Insect Physiol.* 54.4 (2008), pp. 656–662. ISSN: 00221910. DOI: 10.1016/j.jinsphys.2008.01.002.

[5] Paczkowski, S., Paczkowska, M., Dippel, S., Flematti, G., and Schütz, S. "Volatile Combustion Products of Wood Attract *Acanthocnemus Nigricans* (Coleoptera: Acanthocnemidae)". In: *J. Insect. Behav.* 27.2 (2014), pp. 228–238. ISSN: 0892-7553. DOI: 10.1007/s10905-013-9430-4.

[6] Stensmyr, M. C., Dweck, H. K. M., Farhan, A., et al. "A Conserved Dedicated Olfactory Circuit for Detecting Harmful Microbes in Drosophila". In: *Cell* 151.6 (2012), pp. 1345–1357. ISSN: 1097-4172. DOI: 10.1016/j.cell.2012.09.046.

[7] Sun, Y.-L., Huang, L.-Q., Pelosi, P., and Wang, C.-Z. "Expression in Antennae and Reproductive Organs Suggests a Dual Role of an Odorant-Binding Protein in Two Sibling *Helicoverpa* Species". In: *PLoS ONE* 7.1 (2012), e30040. ISSN: 1932-6203. DOI: 10.1371/journal.pone.0030040.

[8] Visser, J. H. "Host Odor Perception in Phytophagous Insects". In: *Annu. Rev. Entomol.* 31.1 (1986), pp. 121–144. ISSN: 0066-4170, 1545-4487. DOI: 10.1146/annurev.en.31.010186.001005.

[9] Weiss, L. A., Dahanukar, A., Kwon, J. Y., Banerjee, D., and Carlson, J. R. "The Molecular and Cellular Basis of Bitter Taste in Drosophila". In: *Neuron* 69.2 (2011), pp. 258–272. ISSN: 1097-4199. DOI: 10.1016/j.neuron.2011.01.001.

[10] Weissteiner, S., Huetteroth, W., Kollmann, M., Weißbecker, B., Romani, R., Schachtner, J., Schütz, S., and Marion-Poll, F. "Cockchafer Larvae Smell Host Root Scents in Soil". In: *PLoS ONE* 7.10 (2012), e45827. ISSN: 1932-6203. DOI: 10.1371/journal.pone.0045827.

[11] Whiteman, N. and Pierce, N. "Delicious Poison: Genetics of Drosophila Host Plant Preference". In: *Trends Ecol. Evol.* 23.9 (2008), pp. 473–478. ISSN: 01695347. DOI: 10.1016/j.tree.2008.05.010.

[12] Yang, C.-H., Belawat, P., Hafen, E., Jan, L. Y., and Jan, Y.-N. "Drosophila Egg-Laying Site Selection as a System to Study Simple Decision-Making Processes". In: *Science* 319.5870 (2008), pp. 1679–1683. ISSN: 0036-8075. DOI: 10.1126/science.1151842.

[13] Benton, R., Vannice, K. S., Gomez-Diaz, C., and Vosshall, L. B. "Variant Ionotropic Glutamate Receptors as Chemosensory Receptors in Drosophila". In: *Cell* 136.1 (2009), pp. 149–162. ISSN: 1097-4172. DOI: 10.1016/j.cell.2008.12.001.

[14] Dippel, S., Kollmann, M., Oberhofer, G., et al. "Morphological and Transcriptomic Analysis of a Beetle Chemosensory System Reveals a Gnathal Olfactory Center". In: *BMC Biol.* 14.1 (2016), p. 90. ISSN: 1741-7007. DOI: 10.1186/s12915-016-0304-z.

[15] Missbach, C., Dweck, H. K., Vogel, H., Vilcinskas, A., Stensmyr, M. C., Hansson, B. S., and Grosse-Wilde, E. "Evolution of Insect Olfactory Receptors". In: *eLife* 3 (2014), e02115. ISSN: 2050-084X. DOI: 10.7554/eLife.02115.

[16] Sato, K., Pellegrino, M., Nakagawa, T., Nakagawa, T., Vosshall, L. B., and Touhara, K. "Insect Olfactory Receptors Are Heteromeric Ligand-Gated Ion Channels". In: *Nature* 452.7190 (2008), pp. 1002–1006. ISSN: 0028-0836. DOI: 10.1038/nature06850.

[17] Wicher, D., Schäfer, R., Bauernfeind, R., Stensmyr, M. C., Heller, R., Heinemann, S. H., and Hansson, B. S. "Drosophila Odorant Receptors Are Both Ligand-Gated and Cyclic-Nucleotide-Activated Cation Channels". In: *Nature* 452.7190 (2008), pp. 1007–1011. ISSN: 0028-0836. DOI: 10.1038/nature06861.

[18] Schachtner, J., Schmidt, M., and Homberg, U. "Organization and Evolutionary Trends of Primary Olfactory Brain Centers in Tetraconata (Crustacea+Hexapoda)". In: *Arthropod. Struct. Dev.* 34.3 (2005), pp. 257–299. ISSN: 14678039. DOI: 10.1016/j.asd.2005.04.003.

[19] Anton, S. and Homberg, U. "Antennal Lobe Structure". In: *Insect Olfaction*. Ed. by Hansson, B. S. 1999, pp. 97–124.

[20] Lin, T., Li, C., Liu, J., Smith, B. H., Lei, H., and Zeng, X. "Glomerular Organization in the Antennal Lobe of the Oriental Fruit Fly Bactrocera Dorsalis". In: *Front. Neuroanat.* 12 (2018), p. 71. ISSN: 1662-5129. DOI: 10.3389/fnana.2018.00071.

[21] Riabinina, O., Task, D., Marr, E., Lin, C.-C., Alford, R., O'Brochta, D. A., and Potter, C. J. "Organization of Olfactory Centres in the Malaria Mosquito Anopheles Gambiae". In: *Nat. Commun.* 7 (2016), p. 13010. ISSN: 2041-1723. DOI: 10.1038/ncomms13010.

[22] Szyszka, P. and Galizia, C. G. "Olfaction in Insects". In: *Handbook of Olfaction and Gustation*. Ed. by Doty, R. L. 3. ed. Hoboken, NJ: Wiley, 2015, pp. 531–546. ISBN: 978-1-118-13922-6.

[23] Vosshall, L. B. "Olfaction in Drosophila". In: *Curr. Opin. Neurobiol.* 10.4 (2000), pp. 498–503. ISSN: 0959-4388. DOI: 10.1016/S0959-4388(00)00111-2.

[24] Chou, Y.-H., Spletter, M. L., Yaksi, E., Leong, J. C. S., Wilson, R. I., and Luo, L. "Diversity and Wiring Variability of Olfactory Local Interneurons in the *Drosophila* Antennal Lobe". In: *Nat. Neurosci.* 13.4 (2010), pp. 439–449. ISSN: 1546-1726. DOI: 10.1038/nn.2489.

[25] Nagel, K. I., Hong, E. J., and Wilson, R. I. "Synaptic and Circuit Mechanisms Promoting Broadband Transmission of Olfactory Stimulus Dynamics". In: *Nat. Neurosci.* 18.1 (2015), pp. 56–65. ISSN: 1097-6256, 1546-1726. DOI: 10.1038/nn.3895.

[26] Okada, R., Awasaki, T., and Ito, K. "Gamma-Aminobutyric Acid (GABA)-Mediated Neural Connections in the *Drosophila* Antennal Lobe". In: *J. Comp. Neurol.* 514.1 (2009), pp. 74–91. ISSN: 0021-9967. DOI: 10.1002/cne.21971.

[27] Olsen, S. R., Bhandawat, V., and Wilson, R. I. "Excitatory Interactions between Olfactory Processing Channels in the *Drosophila* Antennal Lobe". In: *Neuron* 54.1 (2007), pp. 89–103. ISSN: 08966273. DOI: 10.1016/j.neuron.2007.03.010.

[28] Olsen, S. R., Bhandawat, V., and Wilson, R. I. "Divisive Normalization in Olfactory Population Codes". In: *Neuron* 66.2 (2010), pp. 287–299. ISSN: 08966273. DOI: 10.1016/j.neuron.2010.04.009.

[29] Olsen, S. R. and Wilson, R. I. "Lateral Presynaptic Inhibition Mediates Gain Control in an Olfactory Circuit". In: *Nature* 452.7190 (2008), pp. 956–960. ISSN: 0028-0836. DOI: 10.1038/nature06864.

[30] Root, C. M. "Propagation and Modulation of Activity in Early Olfactory Processing and Its Relevance to Odor-Driven Behavior". PhD thesis. San Diego: University of California, San Diego, 2010. URL: https://escholarship.org/uc/item/20q9w0st.

[31] Sachse, S. and Galizia, C. G. "Role of Inhibition for Temporal and Spatial Odor Representation in Olfactory Output Neurons: A Calcium Imaging Study". In: *J Neurophysiol* 87.2 (2002), pp. 1106–1117. ISSN: 0022-3077. DOI: 10.1152/jn.00325.2001.

[32] Shang, Y., Claridge-Chang, A., Sjulson, L., Pypaert, M., and Miesenböck, G. "Excitatory Local Circuits and Their Implications for Olfactory Processing in the Fly Antennal Lobe". In: *Cell* 128.3 (2007), pp. 601–612. ISSN: 00928674. DOI: 10.1016/j.cell.2006.12.034.

[33] Silbering, A. F. and Galizia, C. G. "Processing of Odor Mixtures in the *Drosophila* Antennal Lobe Reveals Both Global Inhibition and Glomerulus-Specific Interactions". In: *J. Neurosci.* 27.44 (2007), pp. 11966–11977. ISSN: 0270-6474, 1529-2401. DOI: 10.1523/JNEUROSCI.3099-07.2007.

[34] Stopfer, M., Bhagavan, S., Smith, B. H., and Laurent, G. "Impaired Odour Discrimination on Desynchronization of Odour-Encoding Neural Assemblies". In: *Nature* 390.6655 (1997), pp. 70–74. ISSN: 0028-0836, 1476-4687. DOI: 10.1038/36335.

[35] Tanaka, N. K., Ito, K., and Stopfer, M. "Odor-Evoked Neural Oscillations in *Drosophila* Are Mediated by Widely Branching Interneurons". In: *J. Neurosci.* 29.26 (2009), pp. 8595–8603. ISSN: 0270-6474, 1529-2401. DOI: 10.1523/JNEUROSCI.1455-09.2009.

[36] Wilson, R. I. "Early Olfactory Processing in *Drosophila* : Mechanisms and Principles". In: *Annu. Rev. Neurosci.* 36.1 (2013), pp. 217–241. ISSN: 0147-006X, 1545-4126. DOI: 10.1146/annurev-neuro-062111-150533.

[37] Wilson, R. I. and Laurent, G. "Role of GABAergic Inhibition in Shaping Odor-Evoked Spatiotemporal Patterns in the *Drosophila* Antennal Lobe". In: *J Neurosci* 25.40 (2005), pp. 9069–9079. ISSN: 1529-2401. DOI: 10.1523/JNEUROSCI.2070-05.2005.

[38] Binzer, M., Heuer, C. M., Kollmann, M., Kahnt, J., Hauser, F., Grimmelikhuijzen, C. J. P., and Schachtner, J. "Neuropeptidome of *Tribolium Castaneum* Antennal Lobes and Mushroom Bodies". In: *J. Comp. Neurol.* 522.2 (2014), pp. 337–357. ISSN: 0021-9967. DOI: 10.1002/cne.23399.

[39] Carlsson, M. A., Diesner, M., Schachtner, J., and Nässel, D. R. "Multiple Neuropeptides in the *Drosophila* Antennal Lobe Suggest Complex Modulatory Circuits". In: *J. Comp. Neurol.* 518.16 (2010), pp. 3359–3380. ISSN: 0021-9967. DOI: 10.1002/cne.22405.

[40] Siju, K. P., Reifenrath, A., Scheiblich, H., Neupert, S., Predel, R., Hansson, B. S., Schachtner, J., and Ignell, R. "Neuropeptides in the Antennal Lobe of the Yellow Fever Mosquito, *Aedes Aegypti*". In: *J. Comp. Neurol.* 522.3 (2014), pp. 592–608. ISSN: 0021-9967. DOI: 10.1002/cne.23434.

[41] Roth, L. M. and Willis, E. R. "Hygroreceptors in Coleoptera". In: *J. Exp. Zool.* 117.3 (1951), pp. 451–487. DOI: 10.1002/jez.1401170305.

[42] Asano, S. M., Gao, R., Wassie, A. T., Tillberg, P. W., Chen, F., and Boyden, E. S. "Expansion Microscopy: Protocols for Imaging Proteins and RNA in Cells and Tissues". In: *Current Protocols in Cell Biology* 80.1 (2018), e56. ISSN: 19342500. DOI: 10.1002/cpcb.56.

[43] Kay, L. M. and Stopfer, M. "Information Processing in the Olfactory Systems of Insects and Vertebrates". In: *Semin. Cell Dev. Biol.* 17.4 (2006), pp. 433–442. ISSN: 1084-9521. DOI: 10.1016/j.semcdb.2006.04.012.

[44] Trebels, B., Dippel, S., Goetz, B., et al. "Metamorphic Development of the Olfactory System in the Red Flour Beetle (Tribolium Castaneum, Herbst)". In: *BMC Biol* 19.1 (2021), p. 155. ISSN: 1741-7007. DOI: 10.1186/s12915-021-01055-8.

[45] Wegerhoff, R. "GABA and Serotonin Immunoreactivity during Postembryonic Brain Development in the Beetle *Tenebrio Molitor*". In: *Microsc. Res. Tech.* 45.3 (1999), pp. 154–164. ISSN: 1059-910X. DOI: 10.1002/(SICI)1097-0029(19990501)45:3<154::AID-JEMT3>3.0.CO;2-5.

[46] Coates, K. E., Majot, A. T., Zhang, X., Michael, C. T., Spitzer, S. L., Gaudry, Q., and Dacks, A. M. "Identified Serotonergic Modulatory Neurons Have Heterogeneous Synaptic Connectivity within the Olfactory System of Drosophila". In: *J. Neurosci.* 37.31 (2017), pp. 7318–7331. ISSN: 0270-6474. DOI: 10.1523/JNEUROSCI.0192-17.2017.

[47] Dacks, A. M., Christensen, T. A., and Hildebrand, J. G. "Phylogeny of a Serotonin-Immunoreactive Neuron in the Primary Olfactory Center of the Insect Brain". In: *J. Comp. Neurol.* 498.6 (2006), pp. 727–746. ISSN: 0021-9967. DOI: 10.1002/cne.21076.

[48] Kent, K. S., Hoskins, S. G., and Hildebrand, J. G. "A Novel Serotonin-Immunoreactive Neuron in the Antennal Lobe of the Sphinx Moth Manduca Sexta Persists throughout Postembryonic Life". In: *J. Neurobiol.* 18.5 (1987), pp. 451–465. ISSN: 1097-4695. DOI: 10.1002/neu.480180506.

[49] Dreyer, D., Vitt, H., Dippel, S., Goetz, B., El Jundi, B., Kollmann, M., Huetteroth, W., and Schachtner, J. "3D Standard Brain of the Red Flour Beetle *Tribolium Castaneum:* A Tool to Study Metamorphic Development and Adult Plasticity". In: *Front Syst Neurosci* 4 (2010), p. 3. ISSN: 1662-5137. DOI: 10.3389/neuro.06.003.2010.

[50] Bruyne, M., Clyne, P. J., and Carlson, J. R. "Odor Coding in a Model Olfactory Organ". In: *J. Neurosci.* 19.11 (1999), pp. 4520–4532. ISSN: 0270-6474. DOI: 10.1523/JNEUROSCI.19-11-04520.1999.

[51] Dweck, H. K., Ebrahim, S. A., Khallaf, M. A., et al. "Olfactory Channels Associated with the Drosophila Maxillary Palp Mediate Short- and Long-Range Attraction". In: *eLife* 5 (2016). Ed. by Scott, K., e14925. ISSN: 2050-084X. DOI: 10.7554/elife.14925.

[52] Haverkamp, A., Yon, F., Keesey, I. W., Mißbach, C., Koenig, C., Hansson, B. S., Baldwin, I. T., Knaden, M., and Kessler, D. "Hawkmoths Evaluate Scenting Flowers with the Tip of Their Proboscis". In: *eLife* 5 (2016). Ed. by Dicke, M., e15039. ISSN: 2050-084X. DOI: 10.7554/elife.15039.

[53] Blaney, W. M. and Duckett, A. M. "The Significance of Palpation by the Maxillary Palps of Locusta Migratoria (L): An Electrophysiological and Behavioural Study". In: *J. Exp. Biol.* 63.3 (1975), pp. 701–712. ISSN: 0022-0949, 1477-9145. URL: https://jeb.biologists.org/content/63/3/701 (visited on 11/19/2019).

[54] Chozinski, T. J., Halpern, A. R., Okawa, H., Kim, H.-J., Tremel, G. J., Wong, R. O. L., and Vaughan, J. C. "Expansion Microscopy with Conventional Antibodies and Fluorescent Proteins". In: *Nat. Methods* 13.6 (2016), pp. 485–488. ISSN: 1548-7105. DOI: 10.1038/nmeth.3833.

[55] Karagiannis, E. D. and Boyden, E. S. "Expansion Microscopy: Development and Neuroscience Applications". In: *Curr. Opin. Neurobiol.* 50 (2018), pp. 56–63. ISSN: 1873-6882. DOI: 10.1016/j.conb.2017.12.012.

[56] Tillberg, P. W., Chen, F., Piatkevich, K. D., et al. "Protein-Retention Expansion Microscopy of Cells and Tissues Labeled Using Standard Fluorescent Proteins and Antibodies". In: *Nat. Biotechnol.* 34.9 (2016), pp. 987–992. ISSN: 1546-1696. DOI: 10.1038/nbt.3625.

[57] Homberg, U. and Müller, U. "Neuroactive Substances in the Antennal Lobe". In: *Insect Olfaction*. Ed. by Hansson, B. S. Berlin, Heidelberg: Springer, 1999, pp. 181–206. ISBN: 978-3-662-07911-9.

[58] Distler, P. "GABA-immunohistochemistry as a Label for Identifying Types of Local Interneurons and Their Synaptic Contacts in the Antennal Lobes of the American Cockroach". In: *Histochemistry* 93.6 (1990), pp. 617–626. ISSN: 1432-119X. DOI: 10.1007/bf00272204.

[59] Hoskins, S. G., Homberg, U., Kingan, T. G., Christensen, T. A., and Hildebrand, J. G. "Immunocytochemistry of GABA in the Antennal Lobes of the Sphinx Moth *Manduca Sexta*". In: *Cell Tissue Res.* 244.2 (1986), pp. 243–252. ISSN: 1432-0878. DOI: 10.1007/bf00219199.

[60] Leitch, B. et Laurent, G. « GABAergic synapses in the antennal lobe and mushroom body of the locust olfactory system ». In : *J. Comp. Neurol.* 372.4 (1996), p. 487-514. ISSN : 1096-9861. DOI : 10.1002/(sici)1096-9861(19960902)372:4<487::aid-cne1>3.0.co;2-0.

[61] Schäfer, S. and Bicker, G. "Distribution of GABA-like Immunoreactivity in the Brain of the Honeybee". In: *J. Comp. Neurol.* 246.3 (1986), pp. 287–300. ISSN: 1096-9861. DOI: 10.1002/cne.902460302.

[62] Seidel, C. and Bicker, G. "Colocalization of NADPH-diaphorase and GABA-immunoreactivity in the Olfactory and Visual System of the Locust". In: *Brain Res.* 769.2 (1997), pp. 273–280. ISSN: 0006-8993. DOI: 10.1016/s0006-8993(97)00716-6.

[63] Nässel, D. R. and Zandawala, M. "Recent Advances in Neuropeptide Signaling in Drosophila, from Genes to Physiology and Behavior". In: *Prog. Neurobiol.* 179 (2019), p. 101607. ISSN: 03010082. DOI: 10.1016/j.pneurobio.2019.02.003.

[64] Erber, J., Kloppenburg, P., and Scheidler, A. "Neuromodulation by Serotonin and Octopamine in the Honeybee: Behaviour, Neuroanatomy and Electrophysiology". In: *Experientia* 49.12 (1993), pp. 1073–1083. ISSN: 1420-9071. DOI: 10.1007/bf01929916.

[65] Mercer, A. R., Hayashi, J. H., and Hildebrand, J. G. "Modulatory Effects of 5-Hydroxytryptamine on Voltage-Activated Currents in Cultured Antennal Lobe Neurones of the Sphinx Moth Manduca Sexta." In: *J. Exp. Biol.* 198.3 (1995), pp. 613–627. ISSN: 0022-0949, 1477-9145. URL: http://jeb.biologists.org/content/198/3/613 (visited on 03/08/2019).

[66] Mercer, A. R., Kloppenburg, P., and Hildebrand, J. G. "Serotonin-Induced Changes in the Excitability of Cultured Antennal-Lobe Neurons of the Sphinx Moth Manduca Sexta". In: *J Comp Physiol A* 178.1 (1996), pp. 21–31. ISSN: 1432-1351. DOI: 10.1007/bf00189587.

[67] Breidbach, O. "Serotonin-Immunoreactive Brain Interneurons Persist during Metamorphosis of an Insect: A Developmental Study of the Brain of Tenebrio Molitor L. (Coleoptera)". In: *Cell Tissue Res* 259.2 (1990), pp. 345–360. ISSN: 1432-0878. DOI: 10.1007/bf00318458.

[68] Nässel, D. R. "Serotonin and Serotonin-Immunoreactive Neurons in the Nervous System of Insects". In: *Progress in Neurobiology* 30.1 (1988), pp. 1–85. ISSN: 0301-0082. DOI: 10.1016/0301-0082(88)90002-0.

[69] Rehder, V., Bicker, G., and Hammer, M. "Serotonin-Immunoreactive Neurons in the Antennal Lobes and Suboesophageal Ganglion of the Honeybee". In: *Cell Tissue Res.* 247.1 (1987), pp. 59–66. ISSN: 1432-0878. DOI: 10.1007/bf00216547.

[70] Salecker, I. and Distler, P. "Serotonin-Immunoreactive Neurons in the Antennal Lobes of the American Cockroach Periplaneta Americana: Light- and Electron-Microscopic Observations". In: *Histochemistry* 94.5 (1990), pp. 463–473. ISSN: 1432-119X. DOI: 10.1007/bf00272608.

[71] Schürmann, F. W. and Klemm, N. "Serotonin-Immunoreactive Neurons in the Brain of the Honeybee". In: *J. Comp. Neurol.* 225.4 (1984), pp. 570–580. ISSN: 1096-9861. DOI: 10.1002/cne.902250407.

[72] Strambi, C., Bennis, N., Renucci, M., Charpin, P., Augier, R., Strambi, A., Cymborowski, B., and Puizillout, J. J. "Serotonin-Immunoreactive Neurons in the Cerebral Complex of Acheta Domesticus: Experimental Study in Normal and Drug Treated Insects". In: *Zool. Jahrb. Abt. Für Allg. Zool. Physiol. TiereZoologische Jahrb. Abt. Für Allg. Zool. Physiol. Tiere* 93.3 (1989), pp. 353–374.

[73] Tyrer, N. M., Turner, J. D., and Altman, J. S. "Identifiable Neurons in the Locust Central Nervous System That React with Antibodies to Serotonin". In: *J. Comp. Neurol.* 227.3 (1984), pp. 313–330. ISSN: 1096-9861. DOI: 10.1002/cne.902270303.

[74] Homberg, U., Brandl, C., Clynen, E., Schoofs, L., and Veenstra, J. A. "Mas-Allatotropin/Lom-AG-myotropin I Immunostaining in the Brain of the Locust, Schistocerca Gregaria". In: *Cell Tissue Res* 318.2 (2004), pp. 439–457. ISSN: 1432-0878. DOI: 10.1007/s00441-004-0913-7.

[75] Schulze, J., Neupert, S., Schmidt, L., Predel, R., Lamkemeyer, T., Homberg, U., and Stengl, M. "Myoinhibitory Peptides in the Brain of the Cockroach Leucophaea Maderae and Colocalization with Pigment-Dispersing Factor in Circadian Pacemaker Cells". In: *J. Comp. Neurol.* 520.5 (2012), pp. 1078–1097. ISSN: 1096-9861. DOI: 10.1002/cne.22785.

[76] Muren, J. E., Lundquist, C. T., and Nässel, D. R. "Abundant Distribution of Locustatachykinin-like Peptide in the Nervous System and Intestine of the Cockroach Leucophaea Maderae". In: *Philosophical Transactions of the Royal Society of London. Series B: Biological Sciences* 348.1326 (1995), pp. 423–444. DOI: 10.1098/rstb.1995.0079.

[77] Hussain, A., Üçpunar, H. K., Zhang, M., Loschek, L. F., and Grunwald Kadow, I. C. "Neuropeptides Modulate Female Chemosensory Processing upon Mating in Drosophila". In: *PLoS Biol* 14.5 (2016). Ed. by Hassan, B. A., e1002455. ISSN: 1545-7885. DOI: 10.1371/journal.pbio.1002455.

[78] Winther, A. M., Acebes, A., and Ferrús, A. "Tachykinin-Related Peptides Modulate Odor Perception and Locomotor Activity in Drosophila". In: *Molecular and Cellular Neuroscience* 31.3 (2006), pp. 399–406. ISSN: 10447431. DOI: 10.1016/j.mcn.2005.10.010.

[79] Winther, A. M. and Ignell, R. "Local Peptidergic Signaling in the Antennal Lobe Shapes Olfactory Behavior". In: *Fly* 4.2 (2010), pp. 167–171. ISSN: 1933-6934, 1933-6942. DOI: 10.4161/fly.4.2.11467.

[80] Ko, K. I., Root, C. M., Lindsay, S. A., Zaninovich, O. A., Shepherd, A. K., Wasserman, S. A., Kim, S. M., and Wang, J. W. "Starvation Promotes Concerted Modulation of Appetitive Olfactory Behavior via Parallel Neuromodulatory Circuits". In: *eLife* 4 (2015). Ed. by Ramaswami, M., e08298. ISSN: 2050-084X. DOI: 10.7554/elife.08298.

[81] Singh, A. P., Das, R. N., Rao, G., Aggarwal, A., Diegelmann, S., Evers, J. F., Karandikar, H., Landgraf, M., Rodrigues, V., and VijayRaghavan, K. "Sensory Neuron-Derived Eph Regulates Glomerular Arbors and Modulatory Function of a Central Serotonergic Neuron". In: *PLoS Genet* 9.4 (2013). Ed. by Desplan, C., e1003452. ISSN: 1553-7404. DOI: 10.1371/journal.pgen.1003452.

[82] Lizbinski, K. M. and Dacks, A. M. "Intrinsic and Extrinsic Neuromodulation of Olfactory Processing". In: *Front. Cell. Neurosci.* 11 (2018), p. 424. ISSN: 1662-5102. DOI: 10.3389/fncel.2017.00424.

[83] Dacks, A. M., Christensen, T. A., and Hildebrand, J. G. "Modulation of Olfactory Information Processing in the Antennal Lobe of *Manduca Sexta* by Serotonin". In: *Journal of Neurophysiology* 99.5 (2008), pp. 2077–2085. ISSN: 0022-3077, 1522-1598. DOI: 10.1152/jn.01372.2007.

[84] Kloppenburg, P., Ferns, D., and Mercer, A. R. "Serotonin Enhances Central Olfactory Neuron Responses to Female Sex Pheromone in the Male Sphinx Moth Manduca Sexta". In: *J. Neurosci.* 19.19 (1999), pp. 8172–8181. ISSN: 1529-2401.

[85] Kloppenburg, P. and Mercer, A. R. "Serotonin Modulation of Moth Central Olfactory Neurons". In: *Annu. Rev. Entomol.* 53.1 (2008), pp. 179–190. ISSN: 0066-4170, 1545-4487. DOI: 10.1146/annurev.ento.53.103106.093408.

[86] Dacks, A. M., Green, D. S., Root, C. M., Nighorn, A. J., and Wang, J. W. "Serotonin Modulates Olfactory Processing in the Antennal Lobe of Drosophila". In: *J Neurogenet* 23.4 (2009), pp. 366–377. ISSN: 1563-5260. DOI: 10.3109/01677060903085722.

[87] Zhang, X. and Gaudry, Q. "Functional Integration of a Serotonergic Neuron in the Drosophila Antennal Lobe". In: *Elife* 5 (2016), e16836. ISSN: 2050-084X. DOI: 10.7554/elife.16836.

[88] Sokoloff, A. *The Genetics of* Tribolium *and Related Species*. Vol. Supplement 1. Advances in Genetics. New York; London: Academic Press, 1966. 232 pp.

[89] Posnien, N., Koniszewski, N. D. B., and Bucher, G. "Insect Tc-six4 Marks a Unit with Similarity to Vertebrate Placodes". In: *Dev. Biol.* 350.1 (2011), pp. 208–216. ISSN: 1095-564X. DOI: 10.1016/j.ydbio.2010.10.024.

[90] Berghammer, A. J., Bucher, G., Maderspacher, F., and Klingler, M. "A System to Efficiently Maintain Embryonic Lethal Mutations in the Flour Beetle *Tribolium Castaneum*". In: *Dev. Genes Evol.* 209.6 (1999), pp. 382–389. ISSN: 1432-041X. DOI: 10.1007/s004270050268.

[91] "Mowiol Embedding Medium". In: *Cold Spring Harb. Protoc.* 2010.1 (2010), pdb.rec12110–pdb.rec12110. ISSN: 1559-6095. DOI: 10.1101/pdb.rec12110.

[92] Klagges, B. R., Heimbeck, G., Godenschwege, T. A., Hofbauer, A., Pflugfelder, G. O., Reifegerste, R., Reisch, D., Schaupp, M., Buchner, S., and Buchner, E. "Invertebrate Synapsins: A Single Gene Codes for Several Isoforms in *Drosophila*". In: *J. Neurosci.* 16.10 (1996), pp. 3154–3165. ISSN: 0270-6474. DOI: 10.1523/JNEUROSCI.16-10-03154.1996.

[93] Utz, S., Huetteroth, W., Vömel, M., and Schachtner, J. "Mas-Allatotropin in the Developing Antennal Lobe of the Sphinx Moth *Manduca Sexta*: Distribution, Time Course, Developmental Regulation, and Colocalization with Other Neuropeptides". In: *Dev. Neurobiol.* 68.1 (2008), pp. 123–142. ISSN: 1932-846X. DOI: 10.1002/dneu.20579.

[94] Veenstra, J. A., Lau, G. W., Agricola, H. J., and D. H. Petzel. "Immunohistological Localization of Regulatory Peptides in the Midgut of the Female Mosquito *Aedes Aegypti*". In: *Histochem. Cell Biol.* 104.5 (1995), pp. 337–347. ISSN: 0948-6143.

[95] Oertel, W. H., Schmechel, D. E., Tappaz, M. L., and Kopin, I. J. "Production of a Specific Antiserum to Rat Brain Glutamic Acid Decarboxylase by Injection of an Antigen-Antibody Complex". In: *Neuroscience* 6.12 (1981), pp. 2689–2700. ISSN: 0306-4522. DOI: 10.1016/0306-4522(81)90113-5.

[96] Predel, R., Rapus, J., and Eckert, M. "Myoinhibitory Neuropeptides in the American Cockroach". In: *Peptides* 22.2 (2001), pp. 199–208. ISSN: 0196-9781. DOI: 10.1016/s0196-9781(00)00383-1.

[97] Veenstra, J. A. and Hagedorn, H. H. "Sensitive Enzyme Immunoassay for Manduca Allatotropin and the Existence of an Allatotropin-Immunoreactive Peptide in Periplaneta Americana". In: *Arch. Insect. Biochem. Physiol.* 23.3 (1993), pp. 99–109. ISSN: 1520-6327. DOI: 10.1002/arch.940230302.

[98] Tanious, F. A., Veal, J. M., Buczak, H., Ratmeyer, L. S., and Wilson, W. D. "DAPI (4',6-Diamidino-2-Phenylindole) Binds Differently to DNA and RNA: Minor-Groove Binding at AT Sites and Intercalation at AU Sites". In: *Biochemistry* 31.12 (1992), pp. 3103–3112. ISSN: 0006-2960. DOI: 10.1021/bi00127a010.

[99] Vandekerckhove, J., Deboben, A., Nassal, M., and Wieland, T. "The Phalloidin Binding Site of F-actin". In: *EMBO J.* 4.11 (1985), pp. 2815–2818. ISSN: 0261-4189. DOI: 10.1002/j.1460-2075.1985.tb04008.x.

Part III

Appendix

A | Supplemental information

The following pages contain the supplemental figures, tables, and methods of chapter 3. The original supplemental information is available online at https://www.nature.com/articles/s41598-020-57639-x).

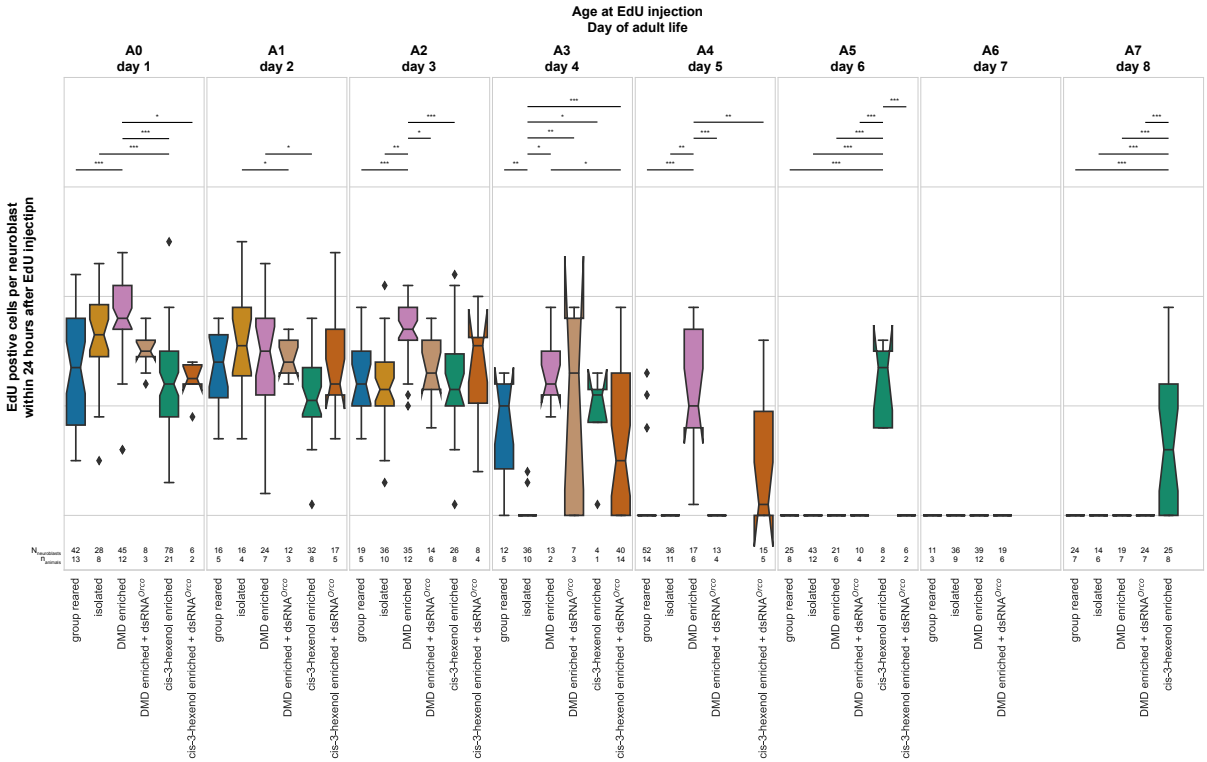

Fig. S1: Number of adult born Kenyon cells under different conditions. Box plots with whiskers representing the 5-95% percentile of new-born cells per neuroblast within 24 hours after EdU injection during the first week after adult eclosion based on [N] analysed neuroblasts originating from [n] beetles. Notches indicate the 95% confidence interval of the median. The bar represents the 25-75 percentile, the line the median, and the diamonds data points outside the 5-95% range. Horizontal lines at 0 indicate presence of neuroblasts, but no occurring neurogenesis. asterisks: statistical significance levels (Holm-corrected) of difference in median as calculated by Dunn's multiple comparison test (* pcorr<0.05, ** pcorr<0.01, *** pcorr<0.001).

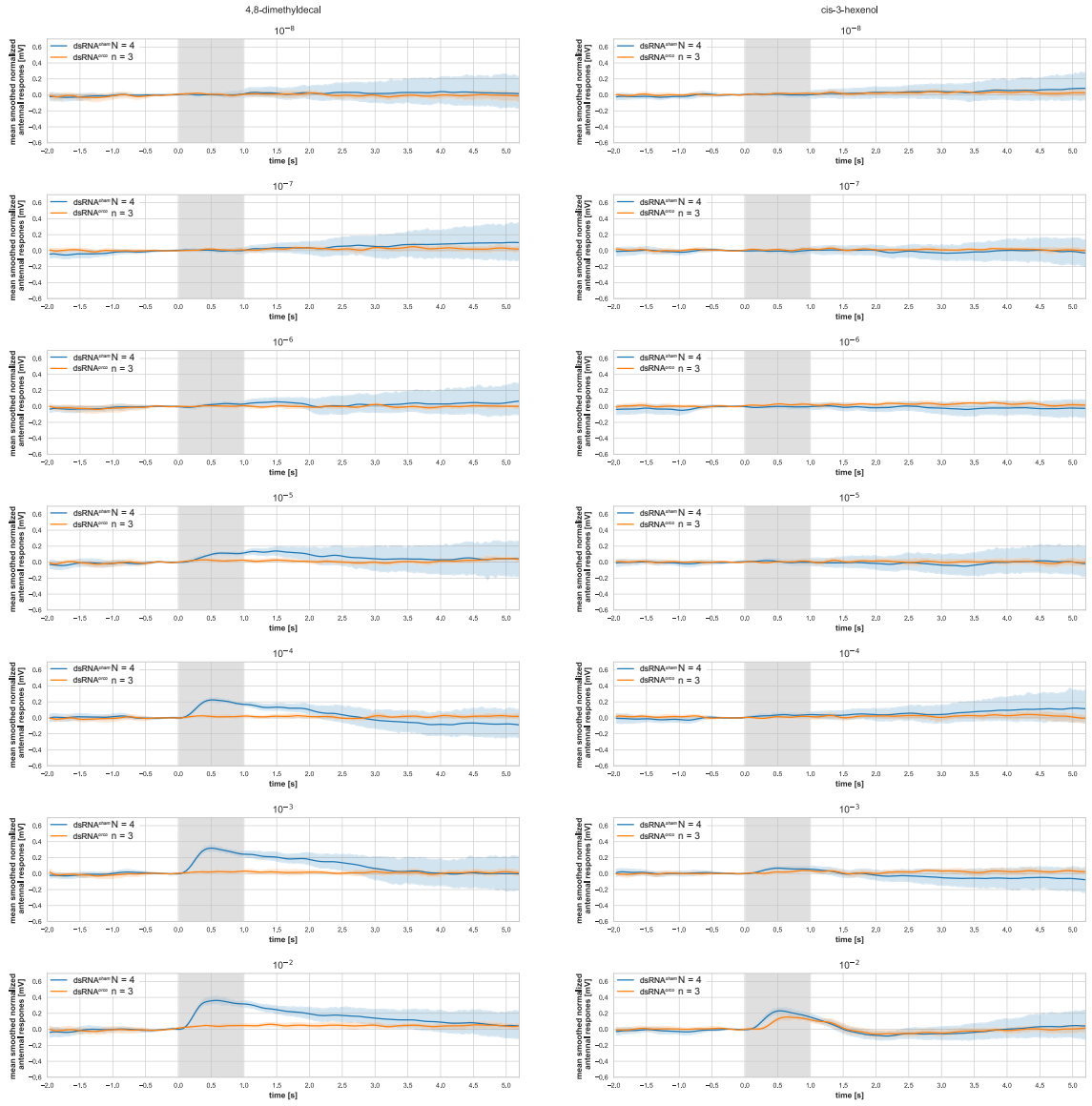

Fig. S2: EAG responses to 4,8-dimethyldecanal and cis-3-hexenol. Line plots of the mean EAG response after robust LOESS smoothing and normilization (substraction of the response to silicone oil, which was used as solvent) to 4,8-dimethyldecanal (DMD) and cis-3-hexenol. Sample sizes are given in the respective subplots. [N] represents the number of animals, while [n] represents the number of replicated per animal. Corespondigly colored shaded areas represent he confidence interval of the mean equivalent to the standard error calculated by bootstrap analysis. Odour stimuli were present for 1 s (grey box) and stimulus onset was set to t = 0.

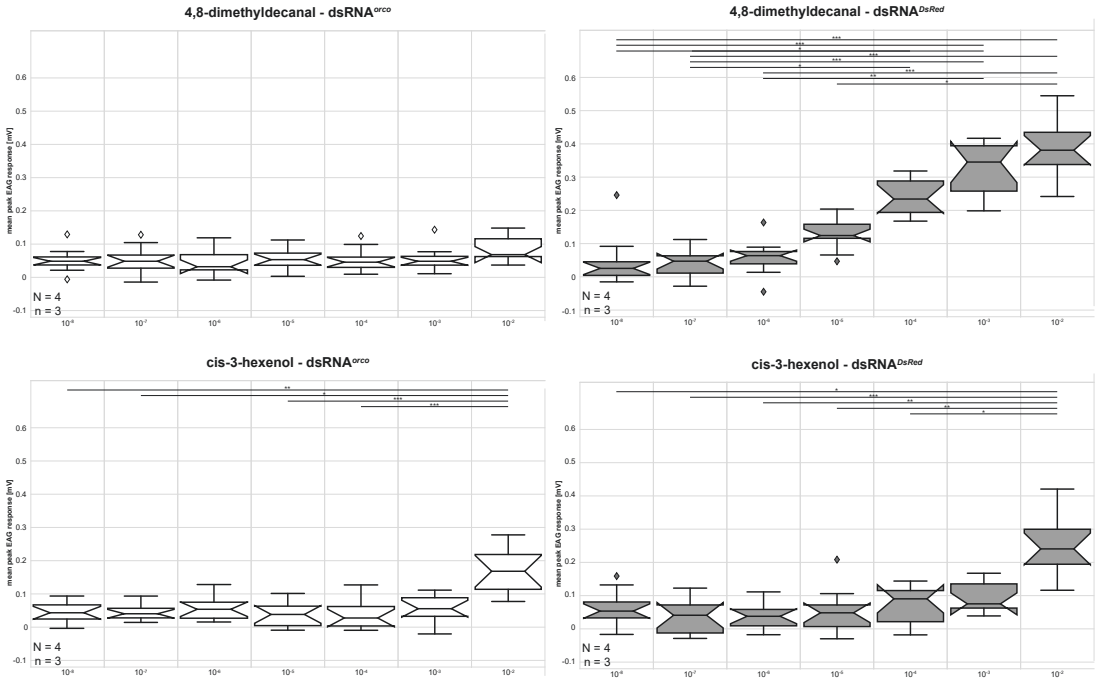

Fig. S3: Peak EAG responses to 4,8-dimethyldecanal and cis-3-hexenol. Box plots with whiskers representing the 5-95% percentile of the peak EAG response after robust LOESS smoothing and normalization (subtraction of the response to silicone oil, which was used as solvent) to 4,8-dimethyldecanal (DMD) and cis-3-hexenol. Sample sizes are given in the respective subplots. [N] represents the number of animals, while [n] represents the number of replicated per animal. Notches indicate the 95% confidence interval of the median. The bar represents the 25-75 percentile, the line represents the median and the diamonds represent data points outside the 5-95% range. Statistical analysis between the different odour dilutions per dsRNA and odour was performed by Kruskal Wallis test followed by posthocanalysis with Dunn's multiple comparison test. asterisks: statistical significance levels (Holm-corrected) of difference in median (* pcorr<0.05, ** pcorr<0.01, *** pcorr<0.001).

Note: This figure shows the same data as the figure in the original supplements to the publication, but has been rearranged for layout reasons.

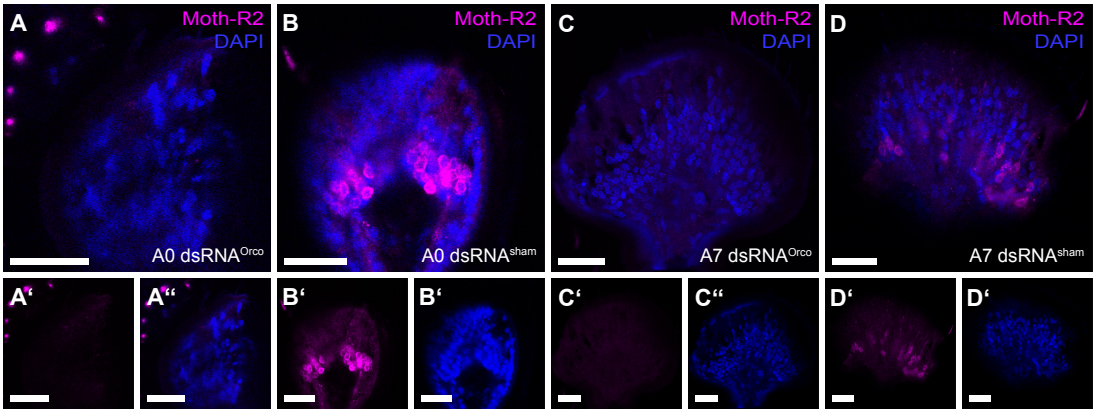

Fig. S4: Verification of the Orco knockdown. Representative optical sections from antennal cryo-sections of freshly eclosed (A0) and seven days old (A7) beetles of the San Bernadino strain after dsRNA^{Orco} or of the black strain after dsRNA^{Sham} treatment respectively. Depicted in blue cell nuclei stained with DAPI and in magenta Orco expressing OSNs with the Moth-R2 antiserum. There is no detectable staining in the antenna after Orco knockdown, whereas in the antenna of the sham treated beetles, the odorant receptor neurons (OSNs) are clearly labelled by the antiserum. Scalebars 20µm.

Note: This figure shows the same data as the figure in the original supplements to the publication, but has been rearranged for layout reasons.

Tab. S1: Comparison of cell numbers per age between of both sexes. The number of neuroblasts "N" originating from "n" animals is given for both sexes for each age of EdU injection (A0 – A7) and experimental groups. Numbers of newborn cells per neuroplasts in males and females were compared by Kruskal-Wallis test. Rounded test results (p-values) are given for each age and experimental group if data from both sexes was obtained.

		A0 | day 1	A1 | day 2	A2 | day 3	A3 | day 4	A4 | day 5	A5 | day 6	A6 | day 7	A7 | day 8
group-reared	$n_{animals\text{-}male}$	7	3	3	3	10	3	2	3
	$N_{neuroblasts\text{-}male}$	20	10	11	7	36	10	8	10
	$n_{animals\text{-}female}$	6	2	2	2	4	5	1	4
	$N_{neuroblasts\text{-}female}$	22	6	8	5	16	15	3	14
	p	0.3063	0.7000	0.1038	0.8059	0.2309	10.000	10.000	10.000
isolated	$n_{animals\text{-}male}$	5	3	5	6	6	6	5	1
	$N_{neuroblasts\text{-}male}$	16	12	17	22	18	21	20	2
	$n_{animals\text{-}female}$	3	1	5	4	5	6	4	5
	$N_{neuroblasts\text{-}female}$	12	4	19	14	18	22	16	12
	p	0.4980	0.1450	0.0004	0.2526	10.000	10.000	10.000	10.000
cis-3-hexenol enriched	$n_{animals\text{-}male}$	9	5	4	1	0	2	0	5
	$N_{neuroblasts\text{-}male}$	35	20	13	4	0	8	0	15
	$n_{animals\text{-}female}$	12	3	4	0	0	0	0	3
	$N_{neuroblasts\text{-}female}$	43	12	13	0	0	0	0	10
	p	0.4682	0.2903	0.0925	#	#	#	#	0.2701
cis-3-hexenol enriched + dsRNA^{Orco}	$n_{animals\text{-}male}$	1	3	2	4	4	1	0	0
	$N_{neuroblasts\text{-}male}$	4	12	5	9	11	2	0	0
	$n_{animals\text{-}female}$	1	2	2	10	1	1	0	0
	$N_{neuroblasts\text{-}female}$	2	5	3	31	4	4	0	0
	p	0.2333	0.0801	0.3682	0.2599	0.0024	1.000	#	#
4,8-dimethyldecanal enriched	$n_{animals\text{-}male}$	5	5	5	4	2	6	8	4
	$N_{neuroblasts\text{-}male}$	19	19	16	7	6	21	25	11
	$n_{animals\text{-}female}$	7	2	7	2	4	0	6	3
	$N_{neuroblasts\text{-}female}$	26	5	19	6	11	0	14	8
	p	0.0951	0.4750	0.5694	0.0698	0.5767	#	1.000	1.000
4,8-dimethyldecanal enriched + dsRNA^{Orco}	$n_{animals\text{-}male}$	0	0	2	0	1	3	3	3
	$N_{neuroblasts\text{-}male}$	0	0	5	0	3	6	8	10
	$n_{animals\text{-}female}$	3	3	4	2	3	1	3	4
	$N_{neuroblasts\text{-}female}$	8	12	9	7	10	4	11	14
	p	#	#	0.7862	#	10.000	10.000	10.000	10.000

Tab. S2: Comparison of the different experimental group within one age. Numbers of newborn cells per neuroplasts over the different injection times (A0 to A7) within one experimental group were compared by Kruskal Wallis test with posthoc analysis using Dunns' multiple comparison test. Rounded test results (p-values) are given for each age and experimental group. The results were used to indicate significances in Supplemental Fig. S1.

		A0 | day 1	A1 | day 2	A2 | day 3	A3 | day 4	A4 | day 5	A5 | day 6	A6 | day 7	A7 | day 8
isolated	**A0 | day 1**	-1	1	1	4.84E-17	3.23E-18	1.38E-19	3.23E-18	4.67E-11
	A1 | day 2	1	-1	1	3.38E-11	5.73E-12	1.45E-12	5.73E-12	3.18E-08
	A2 | day 3	1	1	-1	8.67E-13	7.15E-14	4.55E-15	7.15E-14	5.04E-08
	A3 | day 4	4.84E-17	3.38E-11	8.67E-13	-1	1	1	1	1
	A4 | day 5	3.23E-18	5.73E-12	7.15E-14	1	-1	1	1	1
	A5 | day 6	1.38E-19	1.45E-12	4.55E-15	1	1	-1	1	1
	A6 | day 7	3.23E-18	5.73E-12	7.15E-14	1	1	1	-1	1
	A7 | day 8	4.67E-11	3.18E-08	5.04E-08	1	1	1	1	-1
group-reared	**A0 | day 1**	-1	1	1	0.612922288	8.36E-18	2.47E-13	1.42E-07	5.18E-13
	A1 | day 2	1	-1	1	0.754034011	4.93E-10	7.16E-09	4.84E-06	9.47E-09
	A2 | day 3	1	1	-1	1	1.34E-09	2.35E-08	1.68E-05	3.13E-08
	A3 | day 4	0.612922288	0.754034011	1	-1	0.002167139	0.002585399	0.020484094	0.00266697
	A4 | day 5	8.36E-18	4.93E-10	1.34E-09	0.002167139	-1	1	1	1
	A5 | day 6	2.47E-13	7.16E-09	2.35E-08	0.002585399	1	-1	1	1
	A6 | day 7	1.42E-07	4.84E-06	1.68E-05	0.020484094	1	1	-1	1
	A7 | day 8	5.18E-13	9.47E-09	3.13E-08	0.00266697	1	1	1	-1
4,8-dimethyldecanal enriched	**A0 | day 1**	-1	0.358547436	1	0.138862716	0.01976019	4.03E-14	1.66E-20	3.37E-13
	A1 | day 2	0.358547436	-1	1	1	1	2.77E-06	2.69E-08	5.67E-06
	A2 | day 3	1	1	-1	0.493493138	0.147034108	5.61E-11	2.51E-15	2.53E-10
	A3 | day 4	0.138862716	1	0.493493138	-1	1	0.003417715	0.000754315	0.004009721
	A4 | day 5	0.01976019	1	0.147034108	1	-1	0.003568221	0.000648657	0.004329133
	A5 | day 6	4.03E-14	2.77E-06	5.61E-11	0.003417715	0.003568221	-1	1	1
	A6 | day 7	1.66E-20	2.69E-08	2.51E-15	0.000754315	0.000648657	1	-1	1
	A7 | day 8	3.37E-13	5.67E-06	2.53E-10	0.004009721	0.004329133	1	1	-1
4,8-dimethyldecanal enriched + dsRNA^{orco}	**A0 | day 1**	-1	1	1	1	5.84E-05	0.000160087	1.42E-05	6.34E-06
	A1 | day 2	1	-1	1	1	1.66E-05	7.10E-05	2.04E-06	5.73E-07
	A2 | day 3	1	1	-1	1	2.01E-05	9.28E-05	2.10E-06	5.59E-07
	A3 | day 4	1	1	1	-1	0.046742403	0.068143552	0.027902765	0.021774952
	A4 | day 5	5.84E-05	1.66E-05	2.01E-05	0.046742403	-1	1	1	1
	A5 | day 6	0.000160087	7.10E-05	9.28E-05	0.068143552	1	-1	1	1
	A6 | day 7	1.42E-05	2.04E-06	2.10E-06	0.027902765	1	1	-1	1
	A7 | day 8	6.34E-06	5.73E-07	5.59E-07	0.021774952	1	1	1	-1
group cis-3-hexenol enriched	**A0 | day 1**	-1	1	1	1	1	1		0.001154556
	A1 | day 2	1	-1	1	1	1	1		0.052875925
	A2 | day 3	1	1	-1	1	1	1		0.011720653
	A3 | day 4	1	1	1	-1	1	1		1
	A4 | day 5	1	1	1	1	-1	1		1
	A5 | day 6	1	1	1	1	1	-1		0.19770883
	A7 | day 8	0.001154556	0.052875925	0.011720653	1	1	0.19770883		-1
cis-3-hexenol enriched + dsRNA^{orco}	**A0 | day 1**	-1	1	1	0.320239746	0.20983734	0.016002824		
	A1 | day 2	1	-1	1	0.004877305	0.006037926	0.000309038		
	A2 | day 3	1	1	-1	0.047997981	0.034154525	0.001755258		
	A3 | day 4	0.320239746	0.004877305	0.047997981	-1	1	0.187388262		
	A4 | day 5	0.20983734	0.006037926	0.034154525	1	-1	0.510586405		
	A5 | day 6	0.016002824	0.000309038	0.001755258	0.187388262	0.510586405	-1		

Tab. S3: Comparison of the different ages within one experimental group. Numbers of newborn cells per neuroplasts within one experimental group over the different injection times (A0 to A7) were compared by Kruskal Wallis test with posthoc analysis using Dunns' multiple comparison test. Rounded test results (p-values) are given for each age and experimental group. The results were used to indicate signifacances in Fig. 1

		group-reared	isolated	4,8-dimethyldecanal enriched	4,8-dimethyldecanal enriched + dsRNA^{orco}	cis-3-hexenol enriched	cis-3-hexenol enriched + dsRNA^{orco}
A0 | day 1	**group-reared**	-1	0.117102147	0.000138692	1	0.590386995	1
	isolated	0.117102147	-1	1	1	1	0.316598998
	4,8-dimethyldecanal enriched	0.000138692	1	-1	0.590386995	6.36E-11	0.036444773
	4,8-dimethyldecanal enriched + dsRNA^{orco}	1	1	0.590386995	-1	0.699818698	1
	cis-3-hexenol enriched	0.590386995	0.000133143	6.36E-11	0.699818698	-1	1
	cis-3-hexenol enriched + dsRNA^{orco}	1	0.316598998	0.036444773	1	1	-1
A1 | day 2	**group-reared**	-1	1	1	1	0.841516063	1
	isolated	1	-1	1	1	0.020427712	1
	4,8-dimethyldecanal enriched	1	1	-1	1	0.023768744	1
	4,8-dimethyldecanal enriched + dsRNA^{orco}	1	1	1	-1	0.326369485	1
	cis-3-hexenol enriched	0.841516063	0.020427712	0.023768744	0.326369485	-1	0.841516063
	cis-3-hexenol enriched + dsRNA^{orco}	1	1	1	1	0.841516063	-1
A2 | day 3	**group-reared**	-1	1	0.000115535	1	1	1
	isolated	1	-1	2.24E-07	1	1	1
	4,8-dimethyldecanal enriched	0.000115535	2.24E-07	-1	0.042322766	2.62E-05	0.334101551
	4,8-dimethyldecanal enriched + dsRNA^{orco}	1	1	0.042322766	-1	1	1
	cis-3-hexenol enriched	1	1	2.62E-05	1	-1	1
	cis-3-hexenol enriched + dsRNA^{orco}	1	1	0.334101551	1	1	-1
A3 | day 4	**group-reared**	-1	0.00113321	0.650642434	1	1	1
	isolated	0.00113321	-1	5.57E-09	0.008941583	0.031009534	4.13E-05
	4,8-dimethyldecanal enriched	0.650642434	5.57E-09	-1	1	1	0.031009534
	4,8-dimethyldecanal enriched + dsRNA^{orco}	1	0.008941583	1	-1	1	1
	cis-3-hexenol enriched	1	0.031009534	1	1	-1	1
	cis-3-hexenol enriched + dsRNA^{orco}	1	4.13E-05	0.031009534	1	1	-1
A4 | day 5	**group-reared**	-1	1	8.44E-16	1		0.000970773
	isolated	1	-1	5.94E-16	1		0.000355396
	4,8-dimethyldecanal enriched	8.44E-16	5.94E-16	-1	1.88E-10		0.002964403
	4,8-dimethyldecanal enriched + dsRNA^{orco}	1	1	1.88E-10	-1		0.004061159
	cis-3-hexenol enriched + dsRNA^{orco}	0.000970773	0.000355396	0.002964403	0.004061159		-1
A5 | day 6	**group-reared**	-1	1	1	1	1.85E-20	1
	isolated	1	-1	1	1	1.10E-22	1
	4,8-dimethyldecanal enriched	1	1	-1	1	1.32E-19	1
	4,8-dimethyldecanal enriched + dsRNA^{orco}	1	1	1	-1	3.51E-15	1
	cis-3-hexenol enriched	1.85E-20	1.10E-22	1.32E-19	1.32E-19	-1	7.59E-12
	cis-3-hexenol enriched + dsRNA^{orco}	1	1	1	1	7.59E-12	-1
A6 | day 7	**group-reared**	-1	1	1	1		
	isolated	1	-1	1	1		
	4,8-dimethyldecanal enriched	1	1	-1	1		
	4,8-dimethyldecanal enriched + dsRNA^{orco}	1	1	1	-1		
A7 | day 8	**group-reared**	-1				9.38E-08	
	isolated		-1			6.20E-06	
	4,8-dimethyldecanal enriched			-1		5.60E-07	
	4,8-dimethyldecanal enriched + dsRNA^{orco}				-1	9.38E-08	
	cis-3-hexenol enriched	9.38E-08	6.20E-06	5.60E-07	9.38E-08	-1	

Supplemetary method S1: Python script for cell number analysis

```
#load modules
import pandas as pd
import matplotlib.pyplot as plt
import seaborn as sns
import scipy.stats as ss
import scikit_posthocs as sp

#global variables
groups = ['group reared', 'isolated', '4,8-dimethyldecanal enriched', '4,8-dimethyldecanal enriched + dsRNA[Orco]', 'cis-3-hexenol enriched', 'cis-3-hexenol enriched + dsRNA[Orco]']
group_labels = ['group reared', 'isolated', 'DMD enriched', 'DMD enriched + dsRNA$^{Orco}$', 'cis-3-hexenol enriched', 'cis-3-hexenol enriched + dsRNA$^{Orco}$']
ages = ['A0', 'A1', 'A2', 'A3', 'A4', 'A5', 'A6', 'A7']
age_labels = ['A0\nday 1', 'A1\nday 2', 'A2\nday 3', 'A3\nday 4', 'A4\nday 5', 'A5\nday 6', 'A6\nday 7', 'A7\nday 8']
sexes = ['male', 'female']


#open datafile
print('--------------------')
print('Loading data')
data = pd.read_excel('data.xlsx', na_values=['NA'])

#filter rows with missing/unusable neuroblasts
data = data[data['NB_state']=='present'].copy()

#separate experimental groups
data_groups = {}
for i in groups:
    data_groups[i] = data[data['group']==i].copy()
print('Done')
print('--------------------')

#get oberservations
print('--------------------')
print('get observations')
for i in groups:
    data_l = data_groups[i].copy()
    N_animals = data_l.groupby('age')['specimen'].nunique()
    n_neuroblasts = data_l.groupby('age')['specimen'].count()
    output_as = "statistics/observations_" + i + '.xlsx'
    with pd.ExcelWriter(output_as) as writer:
        N_animals.to_excel(writer, sheet_name='animals')
        n_neuroblasts.to_excel(writer, sheet_name='neuroblasts')

print('Done')
print('--------------------')

#do statistics
print('--------------------')
print('Performing statistical tests')
# per group
```

```
print('- per group')
for i in data_groups:
#select data
    data_group = data_groups[i]
    #do statistics
    data_kw = [data_group.loc[ids, 'cells'].values for ids in data_group.groupby('age').groups.values()]
    check = data_group.cells.nunique()
    if check > 1:
        H, p = ss.kruskal(*data_kw)
        outputkw = pd.DataFrame(data={'type': ['test statistics (H)', 'p-Value'], 'value': [H, p]})
        if p < 0.05:
            output = sp.posthoc_dunn(data_group, val_col='cells', group_col='age', p_adjust = 'holm')
            output_as = "statistics/per_group_" + i + '.xlsx'
            with pd.ExcelWriter(output_as) as writer:
                outputkw.to_excel(writer, sheet_name='Kruskals Walis')
                if p < 0.05:
                    output.to_excel(writer, sheet_name='Dunn\'s Posthoc')
#do statistics per age
print('- per age')
for i in range(len(ages)):
    data_ages = data[data['age']==ages[i]]
    #do statistics
    data_kw = [data_ages.loc[ids, 'cells'].values for ids in data_ages.groupby('group').groups.values()]
    check = data_ages.cells.nunique()
    if check > 1:
        H, p = ss.kruskal(*data_kw)
        outputkw = pd.DataFrame(data={'type': ['test statistics (H)', 'p-Value'], 'value': [H, p]})
        if p < 0.05:
            output = sp.posthoc_dunn(data_ages, val_col='cells', group_col='group', p_adjust = 'holm')
        output_as = "statistics/per_age_" + ages[i] + '.xlsx'
        with pd.ExcelWriter(output_as) as writer:
            outputkw.to_excel(writer, sheet_name='Kruskals Walis')
            if p < 0.05:
                output.to_excel(writer, sheet_name='Dunn\'s Posthoc')


#overall
print('- overall')

data_combined = data.copy()
data_combined['all_stat_groups'] = data_combined['age'] + '_' + data_combined['group']
#do statistics
data_kw = [data_combined.loc[ids, 'cells'].values for ids in data_combined.groupby('all_stat_groups').groups.values()]
check = data_combined.cells.nunique()
if check > 1:
    H, p = ss.kruskal(*data_kw)
```

```
        outputkw = pd.DataFrame(data={'type': ['test statistics (H)', 'p-Value'], 'value': [H, p]})
97      if p < 0.05:
            output = sp.posthoc_dunn(data_combined, val_col='cells', group_col='all_stat_groups', p_adjust = 'holm')
99          output_as = "statistics/overall.xlsx"
        with pd.ExcelWriter(output_as) as writer:
101         outputkw.to_excel(writer, sheet_name='Kruskals Walis')
            if p < 0.05:
103             output.to_excel(writer, sheet_name='Dunn\'s Posthoc')

105 print('Done')
    print('--------------------')
107
    print('--------------------')
109 print('Start plotting data')

111 #make pointplot
    print('- pointplot')
113 sns.set_style('whitegrid')
    fig, axes = plt.subplots(6,1, figsize=(10,15), dpi=300, sharex=False, sharey=True)
115 plt.subplots_adjust(left  = 0.08    , right = 0.99, bottom = 0.05, top = 0.95, hspace=0.55, wspace = 0)
    for i in range(len(groups)):
117     data_group_name = groups[i]
        print(' --' + data_group_name)
119     data_group = data_groups[data_group_name].copy()
        sns.pointplot(data=data_group, x='age', y='cells', join=False, linestyles=["--"], capsize=.1, errwidth=.5, scale = 0.9, color="black", ax=axes[i])
121     axes[i].set_title(group_labels[i], weight='bold', size='larger')
    fig.savefig('figures/pointplot.png')
123 fig.savefig('figures/pointplot.pdf')
    plt.close()
125

127 print('- boxplot ages')
    my_pal = {'group reared': "#0173b2", 'isolated': "#de8f05", 'cis-3-hexenol enriched': "#029e73", 'cis-3-hexenol enriched + dsRNA[Orco]': "#d55e00", '4,8-dimethyldecanal enriched': "#cc78bc", '4,8-dimethyldecanal enriched + dsRNA[Orco]': "#ca9161"} #colorblind
129 fig, axes = plt.subplots(1,len(ages), sharey=True, figsize=(15,10), dpi=300)
    plt.subplots_adjust(left  = 0.05, right = 0.99, bottom = 0.3, top = 0.95, hspace=0.2, wspace = 0.02)
131 for i in range(len(ages)):
        axes[i].set_ylim(-4.99,42.99)
133     print(' --' + ages[i])
        data_ages = data[data['age']==ages[i]]
135     sns.boxplot(data=data_ages, x='group', y='cells', ax=axes[i], notch=True, palette=my_pal, order=groups)
        if i == 0:
137         axes[i].set_ylabel('adult born Kenyon cells per neuroblast\nwithin 24 hours after EdU injection', weight='bold', size='medium')
```

```
        else:
139         axes[i].set_ylabel('')
        axes[i].set_title(age_labels[i], weight='bold', size='medium')
141     xlabels = axes[i].get_xticklabels()
        axes[i].set_xticklabels(group_labels, rotation='vertical')
143     axes[i].set_xlabel('')

145 fig.savefig('figures/boxplot_ages.png')
    fig.savefig('figures/boxplot_ages.pdf')
147 plt.close()

149 #Scheirer-Ray-Hare-Test (Implementation from jpinzonc on guithub)
    data['rank'] = data.cells.sort_values().rank(numeric_only = float)
151

153 rows = data.groupby(['group'], as_index = False).agg({'rank':['count', '
        mean', 'var']}).rename(columns={'rank':'row'})
    rows.columns = ['_'.join(col) for col in rows.columns]
155 rows.columns = rows.columns.str.replace(r'_$',"")
    rows['row_mean_rows'] = rows.row_mean.mean()
157 rows['sqdev'] = (rows.row_mean - rows.row_mean_rows)**2

159 cols = data.groupby(['age'], as_index = False).agg({'rank':['count', 'mean'
        , 'var']}).rename(columns={'rank':'col'})
    cols.columns = ['_'.join(col) for col in cols.columns]
161 cols.columns = cols.columns.str.replace(r'_$',"")
    cols['col_mean_cols'] = cols.col_mean.mean()
163 cols['sqdev'] = (cols.col_mean - cols.col_mean_cols)**2

165 data_sum = data.groupby(['group', 'age'], as_index = False).agg({'rank':['
        count', 'mean', 'var']})
    data_sum.columns = ['_'.join(col) for col in data_sum.columns]
167 data_sum.columns = data_sum.columns.str.replace(r'_$',"")

169 nobs_row = rows.row_count.mean()
    nobs_total = rows.row_count.sum()
171 nobs_col = cols.col_count.mean()

173 Columns_SS = cols.sqdev.sum()*nobs_col
    Rows_SS = rows.sqdev.sum()*nobs_row
175 Within_SS = data_sum.rank_var.sum()*(data_sum.rank_count.min()-1)
    MS = data['rank'].var()
177 TOTAL_SS = MS * (nobs_total-1)
    Inter_SS = TOTAL_SS - Within_SS - Rows_SS - Columns_SS
179
    H_rows = Rows_SS/MS
181 H_cols = Columns_SS/MS
    H_int = Inter_SS/MS
183
    df_rows = len(rows)-1
185 df_cols = len(cols)-1
    df_int = df_rows*df_cols
187 df_total = len(data)-1
    df_within = df_total - df_int - df_cols - df_rows
189
```

```
p_rows = round(1-ss.chi2.cdf(H_rows, df_rows),4)
p_cols = round(1-ss.chi2.cdf(H_cols, df_cols),4)
p_inter = round(1-ss.chi2.cdf(H_int, df_int),4)

results = pd.DataFrame(columns=['var','df','H','p'])
results = results.append([{'var':'Group','df':df_rows,'H':H_rows,'p':p_rows}],ignore_index=True,sort=False)
results = results.append([{'var':'Age','df':df_cols,'H':H_cols,'p':p_cols}],ignore_index=True,sort=False)
results = results.append([{'var':'Group:Age','df':df_int,'H':H_int,'p':p_inter}],ignore_index=True,sort=False)

print(results)

print('Done')
print('--------------------')
```

Supplemetary method S2: Python script for EAG analysis

```
# load modules
import numpy as np
import pandas as pd
import matplotlib.pyplot as plt
import seaborn as sns
import matplotlib
import matplotlib.patches as patches
from matplotlib.ticker import (MultipleLocator, FormatStrFormatter, AutoMinorLocator)
import os
import scipy.stats as ss
import scikit_posthocs as sp
from localreg import *
#import data from structured excel sheets (xlsx only) [mv]:[stimulus][subsessions]; replicates as sheets; one file per animal
#input excel-files must be placed in the folder "excel_data" and have the following filename structure: "dsRNA_odorant_animal" and the sheets must have following names for the 3 replicates: a, b, c (see example.xlsx)

#global variables to be edited to relfect the data
########################################
dsRNAs = ['dsRed', 'orco'] #order is also used for boxplplots of peak responses
dsRNA_names = ['dsRNA$^{DsRed}$','dsRNA$^{Orco}$'] # needs ot be in the same order as dsRNAs
odorants = ['dmd', 'hexenol']
animals = ['female_1', 'female_2', 'female_3', 'female_3', 'female_4', 'female_5']
replicates = ['a', 'b', 'c']
subsessions = ['DMD', 'silicone oil','10^-8','10^-7','10^-6','10^-5','10^-4','10^-3','10^-2']
subsessions_to_plot = ['10^-8','10^-7','10^-6','10^-5','10^-4','10^-3','10^-2']
subsessions_to_plot_names = ['10$^{-8}$','10$^{-7}$','10$^{-6}$','10$^{-5}$','10$^{-4}$','10$^{-3}$','10$^{-2}$'] # nice names for plotting, need to be in the same order as subsessions_to_plot
```

```
odorant_names = ['4,8-dimethyldecanal', 'cis-3-hexenol'] # needs ot be in the same order as odorants
exclude = ['dsRed_dmd_female_2', 'dsRed_hexenol_female_2', 'orco_dmd_female_1', 'orco_hexenol_female_1'] # enter filename (without extension) of animals datasets to exclude
datapoints_to_use = 300 # equals to sampling frequence x desired time in sec after stimulus onset + 50 <-- 2 seconds before stimulus onset

#do not change from here
########################################
#check if all necessary output folders exist and create them if not
if not os.path.exists('csv'):
    os.makedirs('csv')
if not os.path.exists('csv_g'):
    os.makedirs('csv_g')
if not os.path.exists('figures'):
    os.makedirs('figures')
if not os.path.exists('statistics'):
    os.makedirs('statistics')

#load data from excel files (filter for files to exclude) into dataframe list and save the subessions to csv
sessions = {}
print('Start importing data from excel')
print('----------------------')
for i in dsRNAs:
    for j in odorants:
        for k in animals:
            for l in replicates:
                for m in subsessions:
                    filename = i + '_' + j + '_' + k
                    session_name = i + '_' + j + '_' + k + '_' + l + '_' + m
                    print('Current file is: ' + filename + '.xlsx')
                    if (filename in exclude):
                        print('excluded from analysis due to bad raw data')
                    else:
                        print('Current sheet is: ' + l)
                        print('Current test odorant is: ' + j)
                        print('Current subsession is: ' + m)
                        print('loading data')
                        data_in = pd.read_excel('excel_data/' + filename + '.xlsx', index_col=None, na_values=['NA'], sheet_name=l)
                        data_in.dropna(inplace=True)
                        data_in = data_in.head(datapoints_to_use)
                        #select only time, stimulus and subsession column
                        excol = ['t', 'stimulus', m]
                        data_in = data_in.filter(items=excol)
                        data_in.rename(columns = {m:'mV'}, inplace=True)
                        #add dsRNA, animal, odorant, replicat and subsession
                        data_in['dsRNA'] = i
                        data_in['animal'] = k
                        data_in['odor'] = j
                        data_in['replicat'] = l
```

```
                        data_in['subsession'] = m
                        data_in["stimulus"] = pd.to_numeric(data_in["
    stimulus"], downcast='integer')
                        #invert mV for nicer display
                        data_in['mV'] = data_in['mV'] * (-1)
                        sessions[session_name] = data_in.copy()
                        print('writing csv')
                        sessions[session_name].to_csv('csv/' + session_name
     + '.csv', sep=';', index=None, header=True, decimal='.') #csv with "."
    as decimal seprator
                        sessions[session_name].to_csv('csv_g/' +
    session_name + '.csv', sep=';', index=None, header=True, decimal=',') #
    csv with "," as decimal seprator
                    print('done')
                    print('----------------------')

#create new file for supplements containing everthing
print('combine datasets of the same conditions for supplements')
print('----------------------')
sessions_combined = pd.DataFrame()
for i in sessions:
    print('Current session is: ' + i)
    sessions_combined = sessions_combined.append(sessions[i])
#save to csv
sessions_combined.to_csv('csv/EAG_data_analyzed_raw.csv', sep=';', index=
    None, header=True, decimal='.') #csv with "." as decimal seprator
sessions_combined.to_csv('csv_g/EAG_data_analyzed_raw.csv', sep=';', index=
    None, header=True, decimal=',') #csv with "," as decimal seprator
print('done')
print('----------------------')

#smooth the raw data using robust LOESS method to count for unwanted spikes
     in the transient voltage train
print('Smooth the data')
print('----------------------')
sessions_smoothed = {}
for i in sessions:
    print('Current smoothing: ' + i)
    session_l = sessions[i].copy()
    x = session_l['t'].to_numpy()
    y = session_l['mV'].to_numpy()
    smoothed = localreg(x, y, degree=2, kernel=tricube, width=0.3)
    session_l['mV'] = smoothed
    sessions_smoothed[i] = session_l
    print('----------------------')

#normalize the smoothed data by substracting the response to silicone oil
print('Normalize the data')
print('----------------------')
sessions_normalized = {}
for i in dsRNAs:
    for j in odorants:
        for k in animals:
            for l in replicates:
                for m in subsessions:
```

```
                    filename = i + '_' + j + '_' + k
                    if (filename in exclude):
                        print(filename + '.xlsx was excluded from analysis due to bad raw data')
                    else:
                        session_name = i + '_' + j + '_' + k + '_' + l + '_' + m
                        ref_name = i + '_' + j + '_' + k + '_' + l + '_silicone oil'
                        print('Current session is: ' + session_name)
                        session_local = sessions_smoothed[session_name].copy()
                        session_local_ref = sessions_smoothed[ref_name]
                        session_local['mV'] = session_local['mV'] - session_local_ref['mV']
                        sessions_normalized[session_name] = session_local.copy()
                        print('done')
                        print('----------------------')

#combine datasets of the same conditions for plotting
print('combine smoothed and nomrlaized datasets of the same conditions')
print('----------------------')
sessions_normalized_combined = pd.DataFrame()
for i in sessions_normalized:
    print('Current session is: ' + i)
    sessions_normalized_combined = sessions_normalized_combined.append(sessions_normalized[i])
print('done')
print('----------------------')

#plot line graphs with error bars for all desired subsessions
print('plot linegraphs of the mean eag responses over time')
print('----------------------')
fig_rows = len(subsessions_to_plot)
fig_cols = len(odorants)
sns.set_style('white', rc={"lines.linewidth": 0.7})
fig, axes = plt.subplots(fig_rows,fig_cols, figsize=(10,15), dpi=300, sharex=False, sharey=False)
plt.subplots_adjust(top=0.95, bottom=0.05, left=0.1, right=0.95, hspace=0.5, wspace = 0.2)
for i in range(len(odorants)):
    data_odorants = sessions_normalized_combined[sessions_normalized_combined['odor']==odorants[i]]
    print('Current odor is: ' + odorants[i])
    for j in range(len(subsessions_to_plot)):
        print('now plotting: ' + subsessions_to_plot[j])
        data_plot = data_odorants[data_odorants['subsession']==subsessions_to_plot[j]]
        data_plot = data_plot[data_plot['t']<=5]
        sns.lineplot(data=data_plot, x='t', y='mV', hue='dsRNA', ax=axes[j,i], palette='colorblind')
        #plot.despine()
        handles, labels = axes[j,i].get_legend_handles_labels()
```

```
            axes[j,i].legend(handles=handles[1:], labels=dsRNA_names,
        columnspacing=1, title="", loc="upper left", ncol=2, frameon=True,
        fontsize='smaller')
163         axes[j,i].set_xlim([-2,+5])
            axes[j,i].set_ylim([-0.58,0.58])
165         axes[j,i].set_title(odorant_names[i] + ' ' +
        subsessions_to_plot_names[j], weight='bold', size='medium')
            axes[j,i].set_xlabel('time [s]', weight='bold', size='small')
167         axes[j,i].set_ylabel('mean EAG response [mV]', weight='bold', size=
        'small')
            axes[j,i].tick_params(labelsize='x-small')
169         axes[j,i].minorticks_on()
            # Customize the major grid
171         axes[j,i].grid(which='major', linestyle='-', linewidth='0.5', color
        ='black')
            # Customize the minor grid
173         axes[j,i].grid(which='minor', linestyle=':', linewidth='0.5', color
        ='grey')
            a=[0,-1]
175         b=[0,1]
            c=[1,-1]
177         d=[1,1]
            width = c[0] - a[0]
179         height = d[1] - a[1]
            axes[j,i].add_patch(patches.Rectangle((0, -1), width, height,
        facecolor="silver",zorder=0))
181 #save figure as png for quick evaluation and pdf for further external
        processing
    fig.savefig('figures/lineplot.png')
183 fig.savefig('figures/lineplot.pdf')
    plt.close()
185 print('done')
    print('----------------------')
187
    #get the peak responsed during stimulus presentation from the smoothed
        normlized data
189 print('get peak responses during stimulus presentation')
    print('----------------------')
191 max_mVs = pd.DataFrame()
    for i in sessions_normalized:
193     data_l = sessions_normalized[i].copy()
        #filter values during stimulus presentation
195     data_l = data_l[data_l['stimulus'] == 1]
        peak = data_l.loc[data_l['mV'].idxmax()]
197     #copy data
        max_mVs = max_mVs.append(peak)
199 #save to csv
    max_mVs.to_csv('csv/max_mVs.csv', sep=';', index=None, header=True, decimal
        ='.') #csv with "." as decimal seprator
201 max_mVs.to_csv('csv_g/max_mVs.csv', sep=';', index=None, header=True,
        decimal=',') #csv with "," as decimal seprator
    print('done')
203 print('----------------------')

205 #make boxplots of peak responses
```

```
print('plot boxplots of the peak eag respondes during stimulus presentation')
print('----------------------')
sns.set_style('whitegrid')
fig_cols = len(subsessions_to_plot)
fig_rows = len(odorants)
fig, axes = plt.subplots(fig_rows,fig_cols, figsize=(15,10), dpi=300, sharex=False, sharey=True)
plt.subplots_adjust(left = 0.06, right = 0.99, bottom = 0.05, top = 0.9, hspace=0.2, wspace = 0)
for i in range(len(odorants)):
    data_odorants = max_mVs[max_mVs['odor']==odorants[i]]
    print('Current odor is: ' + odorants[i])
    for j in range(len(subsessions_to_plot)):
        print('now plotting: ' + subsessions_to_plot[j])
        data_plot = data_odorants[data_odorants['subsession']==subsessions_to_plot[j]]
        sns.boxplot(data=data_plot, x='dsRNA', y='mV', ax=axes[i,j], notch=True, palette='colorblind', order=dsRNAs)
        axes[i,j].set_ylim(-0.12,0.7)
        axes[i,j].set_ylabel('')
        axes[i,0].set_ylabel('peak EAG response [mV] to \n' + odorant_names[i], weight='bold', size='large')
        axes[i,j].set_xticklabels(dsRNA_names)
        axes[i,j].set_xlabel('')
        axes[i,j].set_title(subsessions_to_plot_names[j], weight='bold', size='large')
#save figure as png for quick evaluation and pdf for further external processing
fig.savefig('figures/boxplot.png')
fig.savefig('figures/boxplot.pdf')
plt.close()
print('done')
print('----------------------')

#compare the peak EAG responses of the dsRNA treatments within the odor/subsession groups
print('compare the peak eag responses during stimulus presentation between dsRNAs for the concentrations')
print('----------------------')
for i in range(len(odorants)):
    data_odorants = max_mVs[max_mVs['odor']==odorants[i]]
    print('Current odor is: ' + odorants[i])
    for j in range(len(subsessions_to_plot)):
        print('now comapring: ' + subsessions_to_plot[j])
        data_session = data_odorants[data_odorants['subsession']==subsessions_to_plot[j]]
        data_kw = [data_session.loc[ids, 'mV'].values for ids in data_session.groupby('dsRNA').groups.values()]
        H, p = ss.kruskal(*data_kw)
        outputkw = pd.DataFrame(data={'type': ['test statistics (H)', 'p-Value'], 'value': [H, p]})
        if p < 0.05:
            output = sp.posthoc_dunn(data_session, val_col='mV', group_col='dsRNA', p_adjust = 'holm', sort='true')
```

```
247             with pd.ExcelWriter('statistics/peak_responses_between_dsRNAs_' +
        odorants[i] + '_' + subsessions_to_plot[j] + '.xlsx') as writer:
                outputkw.to_excel(writer, sheet_name='Kruskals Walis')
249             if p <0.05:
                    output.to_excel(writer, sheet_name='Dunn\'s Posthoc')
251 print('done')
    print('----------------------')
```

A.1 Metamorphic development of the olfactory system in the red flour beetle (*Tribolium castaneum*, Herbst)

The following pages contain the supplemental figures and tables of chapter 4. The original supplemental files (including the videos S3 and S4) are availabe online at https://bmcbiol.biomedcentral.com/articles/10.1186/s12915-021-01055-8).

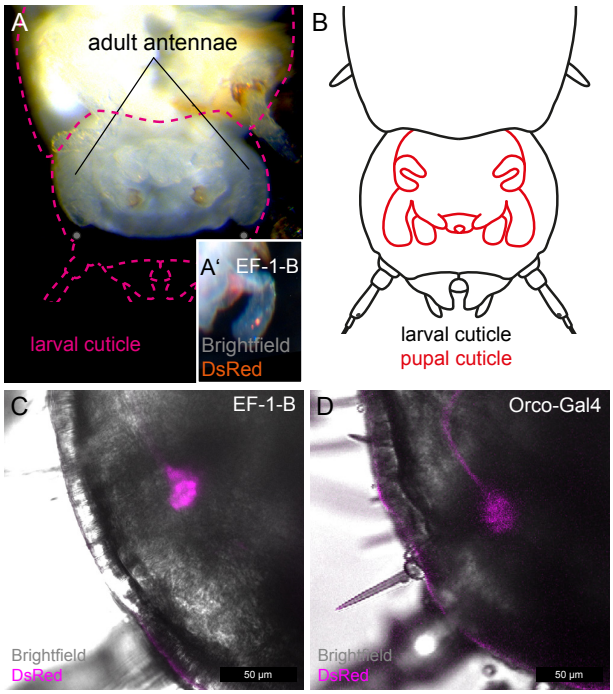

Fig. S1: Localization of the adult appendages and sensory neurons in the head capsule of the prepupa.
(A-A') Stereo microscopic image in ventral view of a prepupa with the opened larval head capsule, showing the location of the adult appendages within the prepupal head capsule, as well as the location of the CSNs in the adult antennae. (B) Schematic drawing of the location of the adult head within the prepupal head capsule in dorsal view. (C, D) Confocal image of the DsRed reporter signal (magenta) of the EF-1-B-line (C) and Orco-Gal4xUAS-DsRed-line (D), showing the position of the CSNs / OSNs cell cluster in the intact head capsule of prepupae. Scale bars 50 µm.

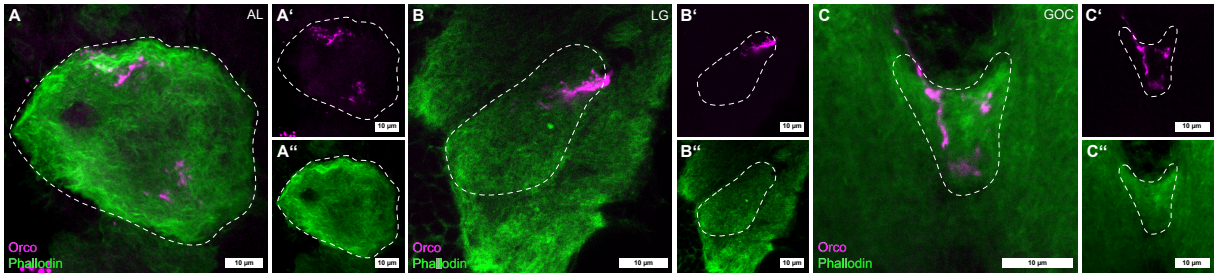

Fig. S2: OSN in primary processing centers at P0%.
Representative optical slices showing the DsRed reporter signal (magenta) of the Orco-GAL4 line, indicating OSN, counterstained with phalloidin (green) to visualize the general neuroarchitecture. All scale bars 10 µm.
Note: This figure shows the same data as the figure in the original supplements to the publication, but has been rearranged for layout reasons.

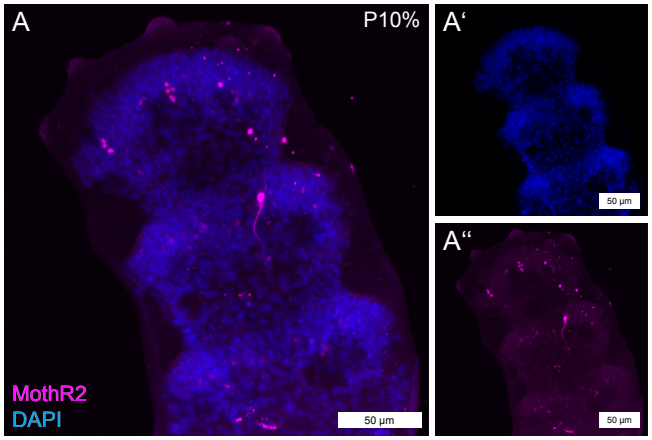

Fig. S5: Orco in the antennae before glomeruli formation.
Confocal maximum projection of 50µm slice a P10% antenna showing OSNs labeled by immunohistochemistry using the crossreactive Moth-R2 antiserum. Scale bars 50µm

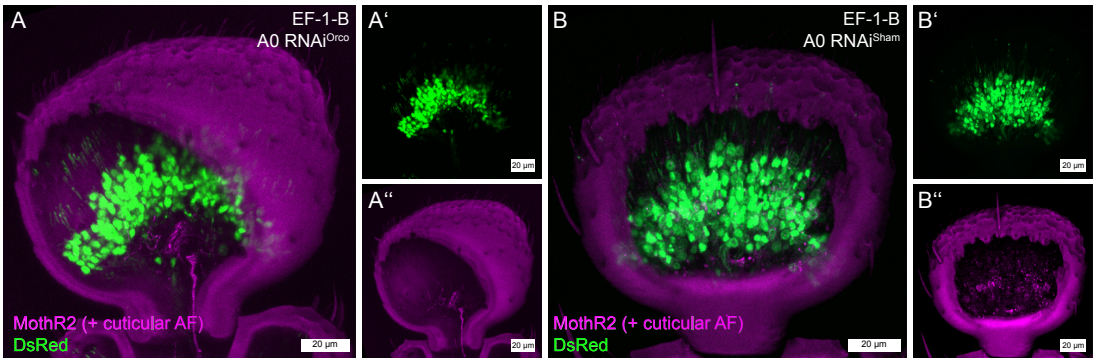

Fig. S6: Immunohistochemical Orco knock-down verification.
Representative maximum projections of 50 µm cry-sections of the antennae of freshly eclosed (A0) beetles of the CSN-labeling EF-1-B-DsRed line after (A) RNAi^{Orco} and (B) RNAi^{Sham} injection. (A – A”, B – B”) The DsRed reporter signal is depicted in green, while Orco immunostaining is depicted in magenta. This channel also includes the autofluorescence of the antennal cuticle. In both treatment groups, the gross CSN distribution is very similar, while Orco cannot be detected in the RNAi^{Orco} group (A). Scale bars 20 µm.

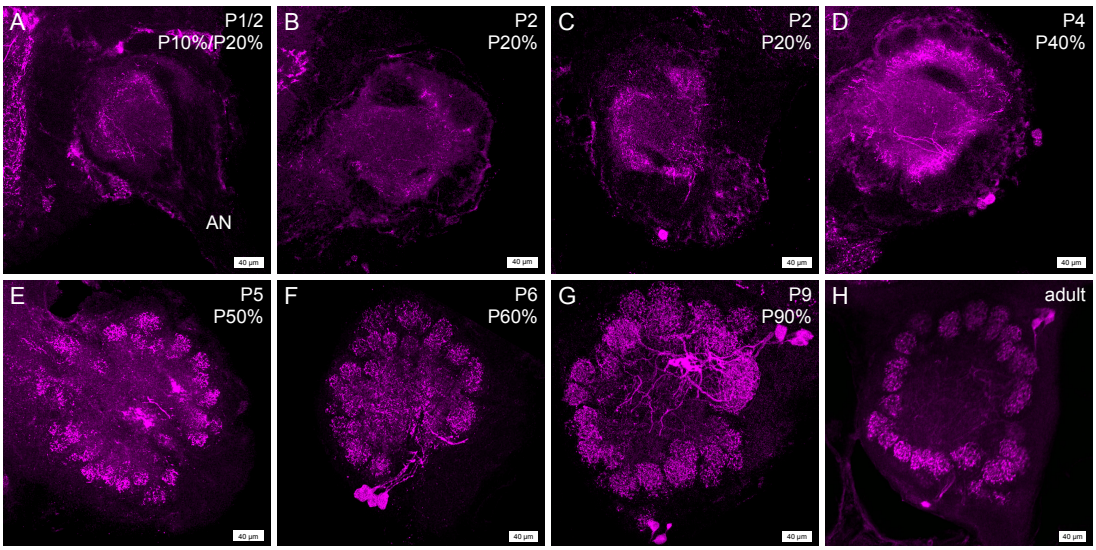

Fig. S7: Development of AST-A immunoreactivity in the AL of *Apis mellifera*.
Representative optical slices of AST-A immunoreactivity in the AL of *A. mellifera* workers at different developmental stages. (A) In the AL of P10% pupae, AST-A fibers are restricted to the lateral portion of the AL. (B, C) At P20% AST-A fibers penetrate the AL. (D) At P40% immunoreactive fibers locate in most of the forming glomeruli. (E-H) From P50% AST-A immunoreactivity shows clearly distinguishable glomeruli, which grow until adult eclosion. Scale bars 40µm.

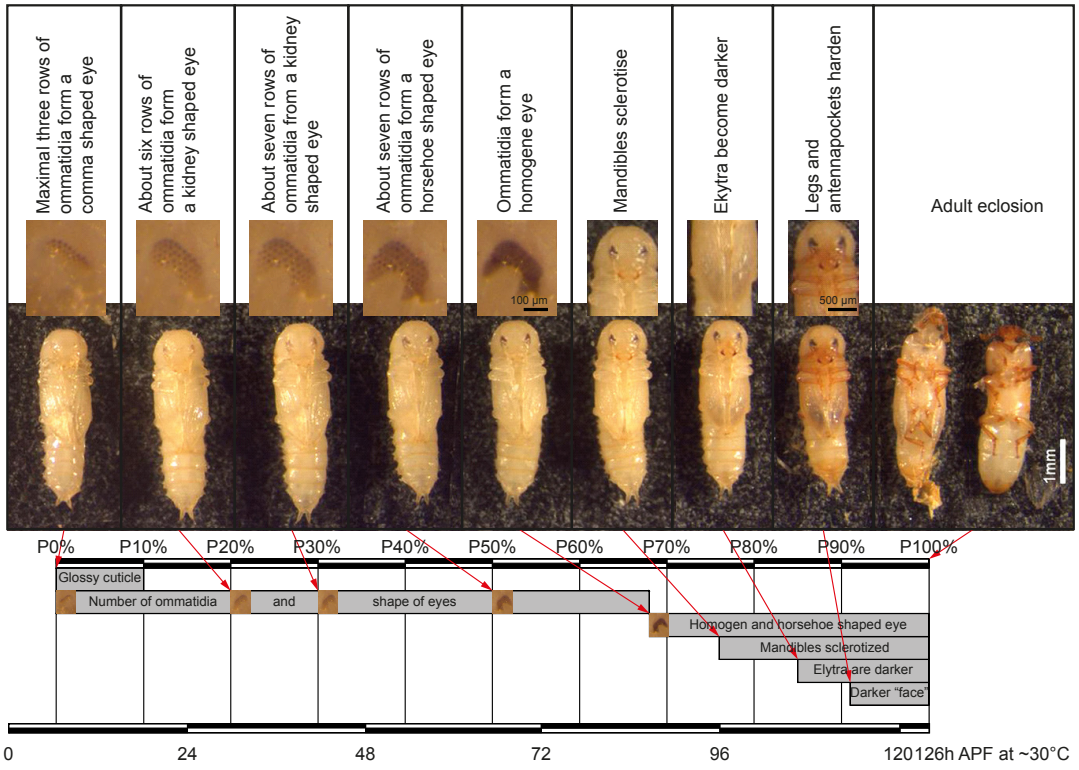

Fig. S8: Staging of wild-type beetles during metamorphosis.
The comparison of time-lapse recordings of nine pupae led to an averaged time for the metamorphosis of 126 h (5,25 d) at 30°C with a deviation of 5,3 h. The development of the eyes [118,119], as well as the sclerotization of mandibles, elytra, and legs, served as external markers, in a time-dependent context. The fresh eclosed pupae are brighter and glossy with a maximum of three rows of ommatidia. After about 20% (25 h after pupa formation (APF)), about six rows of ommatidia are visible and form a kidney-shaped eye. At 30% (40 h APF) the formation of the seventh row is in progress and the distance between the ommatidia shrinks. At about 50% all ommatidia are visible and outgrowth to the sides of the antennal pocket, thus the eyes look horseshoe-shaped. After 68% (86 h APF; SD 2,6 h) the outlines of ommatidia are resolved and the eye appears homogeneous. Besides the eye, at 76% (96 h APF, SD 3,6 h) the majority of mandibles are amber followed by the coloration of the elytra at 85% (106 h APF, SD 2,9 h) and sclerotization of the legs and antennae at 91% (114 h APF, SD 3.3). Finally, the imago eclosed after 126 h (SD 5.3 h).

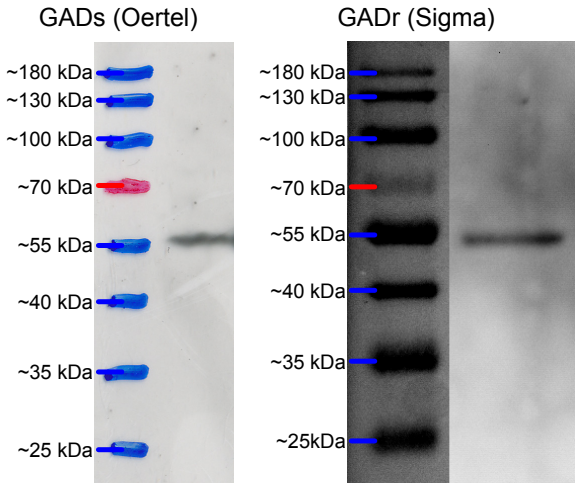

Fig. S9: Specificity of the used antisera against GAD.
Western blot analysis on *Tribolium castaneum* brain tissue shows a single band of about 55 kDa for both antibodies which corresponds to the predicted size of Tcas-GAD (UniProt ID: D6WRJ1) of about 58 kDa.

A.2 An update on the palpal olfactory pathway of the red flour beetle *Tribolium castaneum*, Herbst

This page contains the supplemental figures of chapter 5.

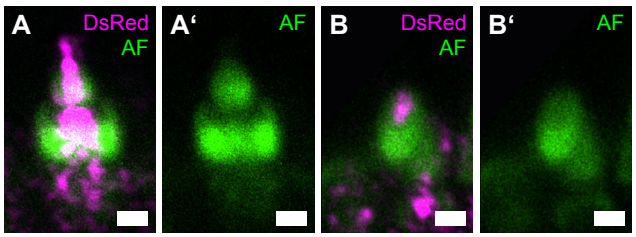

Fig. S1: Optical slices from confocal image stacks of the DsRed reporter signal and cuticular autofluorescence (AF) in the Orco-Gal4xUAS-DsRed line showing **A-A‘** styloconic sensilla and **B-B‘** basiconic/blunt basiconic sensilla (differentiation not possible due to resolution limits in imaging cuticular autofluorescence). All scale bars 2µm.

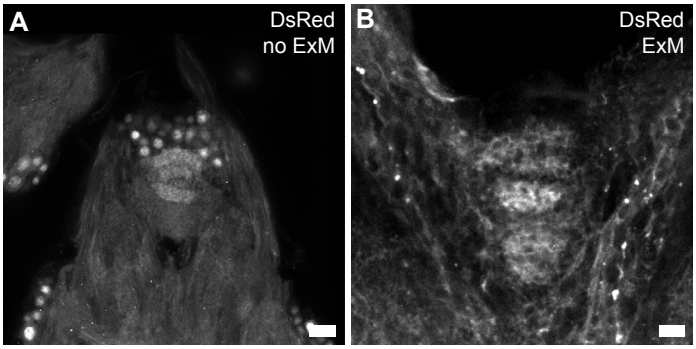

Fig. S2: Comparison of an unexpanded and an expanded GOC.
A Single optical slice of the n-dorsal part of a representative GOC as depicted by the DsRed reporter signal in the neuron labeling EF-1-B-DsRed line **B** Single optical slice of the n-dorsal part of a representative GOC as depicted by the DsRed reporter signal in the neuron labeling EF-1-B-DsRed line after application of the ExM protocol. Scale bars 10µm.

B | Additional publications

While they are not offically part of this dissertation, work on the following articles was conducted during my time as doctoral candidate.

Comparison of navigation-related brain regions in migratory versus non-migratory noctuid moths

Liv de Vries, Keram Pfeiffer, *Bjoern Trebels*, Andrea K. Adden, Ken Green, Eric Warrent, and Stanley Heinze

Published in **Frontiers in Behavioral Neuroscience**, **11**, 158 (2017)
DOI: 10.3389/fnbeh.2017.00158

My contribution:
Development of standardization routines and performation of brain atlas generation in cooperation with Prof. Dr. Keram Pfeiffer.

Mutually exclusive expression of closely related odorant-binding proteins 9A and 9B in the antenna of the red flour beetle *Tribolium castaneum*

Alice Montino, Karthi Balakrishnan, Stefan Dippel, *Bjoern Trebels*, Piotr Neumann, and Ernst A. Wimmer
Published in **Biolmolecules**, **2021**, 11(10), 1502
DOI: 10.3390/biom11101502

My contribution:
Development of the Python scripts for the statistical analysis of the EAG data and execution of the statistical analysis including the generation of graphical representations.

C | Curriculum vitæ

The content of this page was removed as it contains personal information.

The content of this page was removed as it contains personal information.

Danksagung

Jetzt am Ende meiner Dissertation möchte ich mich bei allen bedanken, die mich auf meinem Weg zur Promotion begleitet haben. Seit gewiss euch allen gilt mein Dank. Dennoch möchte einige besonders hervorheben:

Meinem Betreuer Prof. Dr. Joachim Schachtner gilt mein größter Dank. Er hat mir mit der Vergabe des Promotionsthemas erst die Möglichkeit zur Promotion gegeben. Ich danke ihm für seine wissenschaftliche Förderung und sein Vertrauen, dass mir den Raum zur Entwicklung gegeben hat.

Bei Prof. Dr. Uwe Homberg möchte für die Bereitschaft zur für die Übernahme der Zweitkorrektur danken, aber auch für seine jederzeitige Gesprächsbereitschaft und Unterstützung danken.

Prof. Dr. Monika Hassel und Prof. Dr. Christian Helker danke ich herzlich für die Bereitschaft Teil der Prüfungskommission zu sein.

Ich danke allen Mitgliedern der Arbeitsgruppen der Neurobiologie in Marburg (Homberg, Schachtner, Pfeiffer), die mich während der Promotion und teilweise auch schon davor begleitet haben für die jederzeit gute Arbeitsatmosphäre, unzählige mehr oder weniger geistreiche Gespräche, Abende, ... - Ihr alle habt zum gelingen de Projektes beigetragen.
Besonders hervorheben möchte ich an dieser Stelle Stefan Dippel - Danke für die vielen Diskussionen und kurzen Auszeiten vom Laboralltag!
Mein besonderer Dank gilt zudem unserer technischen Assistentin Martina Kern - der Seele des Labors! Sie hat das reibungslose Arbeiten im Labor erst möglich gemacht und Stand immer mit Rat und Tat zur Seite.

Zuletzt gilt mein besonderer Dank meiner Familie die mich stets auf meinem Weg unterstützte. Ohne euch wäre ich heute sicherlich nicht an diesem Punkt und würde diese Zeilen schreiben.